2015

An Experimental Approach to Assess the Impact of Post Processing Variables on the Mechanical Characteristics of 3D Printed (Powder Binding Process) Parts

David Impens
University of Windsor

An Experimental Approach to Assess the Impact of Post Processing Variables on the Mechanical Characteristics of 3D Printed (Powder Binding Process) Parts

By

David Impens

A Thesis
Submitted to the Faculty of Graduate Studies
through the Department of **Mechanical, Automotive, and Materials Engineering**
in Partial Fulfillment of the Requirements for
the Degree of **Master of Applied Science**
at the University of Windsor

Windsor, Ontario, Canada

2015

An Experimental Approach to Assess the Impact of Post Processing Variables on the Mechanical Characteristics of 3D Printed (Powder Binding Process) Parts

by

David Impens

APPROVED BY:

____

Dr. J. Cort
Faculty of Human Kinetics

____

Dr. M. Wang
Mechanical, Automotive, and Materials Engineering

____

Dr. Urbanic, Advisor
Mechanical, Automotive, and Materials Engineering

February 10 2015

DECLARATION OF CO-AUTHORSHIP / PREVIOUS PUBLICATION

I. Co-Authorship Declaration

I hereby declare that this thesis incorporates material that is result of joint research, as follows:

This thesis also incorporates the outcome of a joint research undertaken in collaboration with Professor Dr. Urbanic. In all cases, the key ideas, primary contributions, experimental designs, data analysis and interpretation, were performed by the author, and the contribution of co-authors was primarily through the provision of discussion, suggestions, and review that led to the successful completion of the present work.

I am aware of the University of Windsor Senate Policy on Authorship and I certify that I have properly acknowledged the contribution of other researchers to my thesis, and have obtained written permission from each of the co-author(s) to include the above material(s) in my thesis.

I certify that, with the above qualification, this thesis, and the research to which it refers, is the product of my own work.

II. Declaration of Previous Publication

This thesis includes 2 original papers that have been previously submitted for publication in peer reviewed journals, as follows:

Thesis Chapter	Publication title/full citation	Publication status*
Chapter(s) 1,2,3,4,5,9,10	Assessing the Impact of Post-Processing Variables on Tensile and Compression Characteristics for 3D Printed Components (Paper ID: 424, Invited Session Paper)	Submitted: INCOM 2015
Chapter(s) All	A Comprehensive Assessment on the Impact of Post-Processing Variables on Tensile, Compressive and Bending Characteristics for 3D Printed Components (# RPJ-02-2015-0018)	Submitted: Rapid Prototyping Journal

I certify that I have obtained a written permission from the copyright owners to include the above published materials in my thesis. I certify that the above material describes work completed during my registration as graduate student at the University of Windsor.

I declare that, to the best of my knowledge, my thesis does not infringe upon anyone's copyright nor violate any proprietary rights and that any ideas, techniques, quotations, or any other material from the work of other people included in my thesis, published or otherwise, are fully acknowledged in accordance with the standard referencing practices. Furthermore, to the extent that I have included copyrighted material that surpasses the bounds of fair dealing within the meaning of the Canada Copyright Act, I certify that I have obtained a written permission from the copyright owners to include such materials in my thesis.

I declare that this is a true copy of my thesis, including any final revisions, as approved by my thesis committee and the Graduate Studies office, and that this thesis has not been submitted for a higher degree to any other University or Institution.

ABSTRACT

The study is designed to provide a robust understanding of the mechanical characteristic of a 3D printed part for selected post processing conditions. The 'green' printed parts are generally very brittle and porous, therefore, infiltrates are introduced to alter the mechanical characteristics, which will introduce new opportunities for this technology.

Exploratory testing is performed to shape the choices for post processing with the infiltrates. Specimen geometry, specific for tensile, compression and flexural testing were rendered in CAD software and printed on the Z-printer 450 (Zp150 powder / Zb59 binder) with three different build orientations (horizontal/ angled /vertical).

Results show that infiltrates can significantly improve the mechanical characteristics and material-infiltrate performance varies per build orientation.

It is now understood that this material does not react similar to other materials and cannot be easily predicted. Additional physical testing should be performed and this complete test set should be conducted for new infiltrates.

DEDICATION

I dedicate my thesis to my family and friends. A special feeling of gratitude to my loving parents, Gerald and Barbara Impens, whose words of encouragement and humble pride have helped push me along this journey. My brother Michael, along with my parents, has assisted me greatly during my difficult times so that I could overcome them and focus on moving forward. They were always available for any assistance requested and even the assistance that I had too much pride to ask for.

I also dedicate this thesis to my niece and nephews. The unconditional love given by Brittany, Logan and Cameron, gave me the energy and drive to finish what was started.

I dedicate this work to my friends. Many have supported me through the process. Their level of understanding and reassurance has helped make this journey a little smoother and many were my biggest cheerleaders.

ACKNOWLEDGEMENTS

I wish to thank my committee members who were more than generous with their expertise and precious time. A special thanks to Dr. Jill Urbanic, my advisor, for her countless hours of reflecting, reading, encouraging, and most of all patience throughout the entire process. Thank you, Dr. Michael Wang and Dr. Joel Cort, for agreeing to serve on my committee and provide constructive assistance, while giving me insight on the process and expectations. I would like to acknowledge and thank the University of Windsor and the Government of Canada for allowing me to conduct my research and providing any assistance requested as well as financial assistance. Special thanks go to the university test lab and their personnel for the help they have provided throughout this project.

Finally I would like to thank the professors and fellow students that assisted me with this project. Their excitement and willingness to provide feedback made the completion of this research an enjoyable experience.

TABLE OF CONTENTS

LIST OF TABLES

LIST OF FIGURES

LIST OF EQUATIONS

LIST OF APPENDICES

CHAPTER 1

INTRODUCTION

1.1 Introduction to Rapid Prototyping

Technological advancements in manufacturing include the incorporation of rapid prototyping (RP) technology. Using RP, a 3D part is developed from layering 2D cross sections successively to create the final solid. Other terms for the process family include additive manufacturing (AM), and layered manufacturing. Since inception, this field of technology has grown quickly resulting in design improvements for multiple applications as undercuts, free form geometry, and blind features are manufactured "easily", especially compared to traditional machining processes. In addition to this, no fixturing or specialty tooling is required for RP processes. There are many different processes and materials that can be employed under the RP umbrella. With so many choices, designers and researchers now have the burden of choosing the right combination for their application. The desired part from an RP machine will need to exhibit specific qualities. Among the functional qualities, the most important is the desired mechanical characteristics (compressive, tensile, and/or flexural strength) of the resultant part. By understanding the material and processes, the usefulness of the part for the desired application can be confidently predicted. Below, Figure 1 is an illustration to help understand the many types of decision and factors that can affect the mechanical characteristics of an RP part.

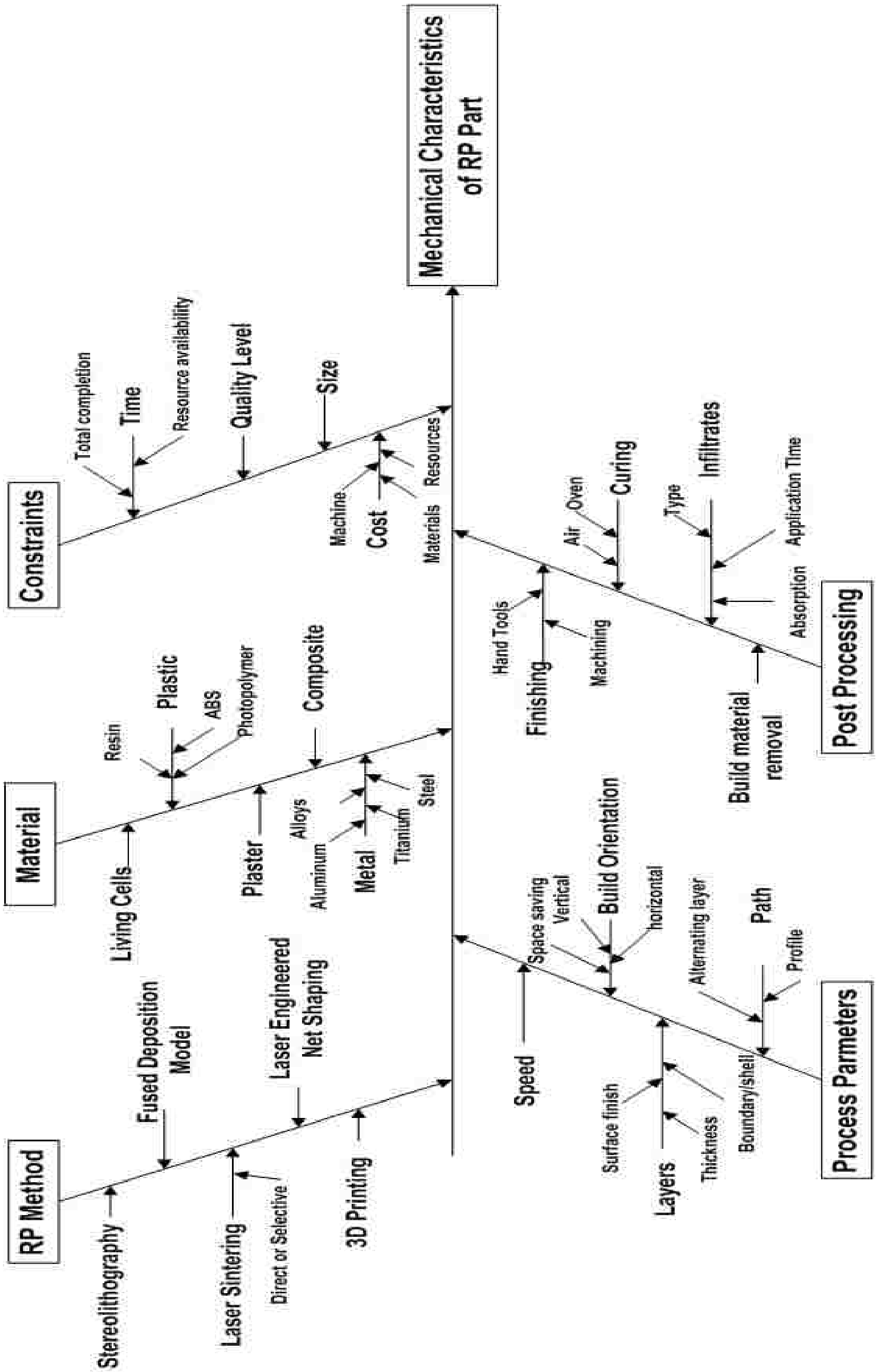

Figure 1 Fishbone Diagram illustrating Factors that can affect the Mechanical Characteristics of an RP Part

1.2 Rapid Prototype Technologies

Although there are many different machines used for rapid prototyping, RP technologies can be categorized into five main manufacturing processes: curing, sheet, dispensing, sintering and binding. Table 1 defines the main manufacturing processes used in RP.

Manufacturing Process	Definition
Curing Process	Where a photo-sensitive polymer is exposed to a light source in order to harden the polymer
Sheet Process	Where thin sheets of material are cut to shape and stacked on top of each other.
Dispensing Process	Where the material is melted and then deposited either as a hot filament or as individual hot droplets.
Sintering Process	Where a powdered material is sintered together using a heat source, typically a laser beam.
Binding Process	Where a liquid binder is deposited onto a bed of powder material to bind the particles together.

Table 1 5 Main Manufacturing Processes used in RP (Adapted from (Upcraft & Fletcher, 2003))

The manufacturing processes is not the only characteristics that makes them different compared to other forms of RP. Along with the manufacturing process, each RP technology has different materials and controllable parameters. Examples of the most common RP technologies are: Stereolithography (SLA), Laminated Object Manufacturing (LOM), Fused Deposition Modeling (FDM), Selective Laser Sintering (SLS), and 3DPrinting (3DP). The common RP's are summarized from authors Upcraft and Fletcher (2003).

1.2.1 Stereolithography

Stereolithography (SLA) can be dated back to the 1980's, making it one of the oldest RP technologies. Parts produced by SLA have a comparable surface finish to conventionally machined parts. The parts are commonly used in investment casting and as part masters in producing silicone moulds subsequently used in reaction or vacuum molding. The parts are produced within a vat of liquid polymer with a build platform that can be raised and lowered within the vat. When a part is being made, the platform's starting position is (0.050 – 0.250 mm) below the monomer liquid surface. An ultraviolet laser then traces of the cross section of one slice of the part, solidifying the liquid into a semi-solid polymer. The build platform lowers the width of the layer consistent with the starting height and the layers continue until the full part is produced. The parts will then need to be post processed by removing any support structures and places in an ultraviolet oven for final curing. This technology is able to produce complex geometry with good accuracy and surface finish from epoxy-based photo curable resins.

1.2.2 Laminated Object Manufacturing

Laminated object manufacturing (LOM) is the least expensive process to produce large parts with moderate geometrical complexity. Although non- paper can be used in this process (i.e. thin plastic sheets), LOM is usually described as turning paper back into wood. Parts made from this process are often durable wood patterns used in sand casting. The parts are produced by layers of material stacked up onto each other. For each layer, the material is stacked on to the base or previous layers with the adhesive coated side down. A heated roller is passed over the material to ensure that the layer is bonded with the previous one. Then a laser will cut though the layer, tracing the outline of the slice and to cross hatch the areas that are not included in the part geometry. After completion and removing the produced solid block of material, the crosshatched sections are broken away to reveal the final part geometry. Materials commonly used in this process include; paper, polyester/polyethylene-based material, ceramic coated paper and polycarbonate composite. Post processing is needed to improve the surface finish and to treat the material to avoid absorbing moisture.

1.2.3 Fused Deposition Modeling

Fused deposition modeling (FDM) was once known as a concept modeller. The parts are produced by extruding out filament from a heated nozzle. The nozzle, moving in the X-Y plane, deposits the filament onto the base to form the cross sectional slice of the part. The build platform is lowered and the next layer of filament is deposited. The filament is hot and bonds with the previous layered material. A second type of material is used to produce build up support material.

The support material is weaker and will need to be broken away from the part once the build is complete. There is a variety of build material available; ABS, elastomer and polycarbonate. Although the machine can be easily set up and used in many environments, the parts produced have poor strength in the vertical direction and the process is slow on parts with large masses.

1.2.4 Selective Laser Sintering

Selective laser sintering (SLS) can produce parts with complex geometry using a variety of different powdered material. Because metal powered is commonly used in this process, production tooling can be made directly. Parts are produced when a laser traces out the cross section of the layered slice on a layer of powder. The laser fuses the particles of the material (sinters) where is hits the powder. The un-sintered material deposited in the layers is used as support material for any subsequent layers with geometry that over hangs or with voids. The powder is layered on the build platform to start each cross sectional slice. The build platform is lowered, powder is layered and laser traces the cross sections until the part is complete. The build platform is raised and the non-sintered material is brushed off. Materials available for this technology include; carbon steel with polymer binder, nylon, polystyrene, polycarbonate, investment casting wax, ceramic coated with binder, zirconium sand coated with polymer and flexible elastomer. Along with the variety of material that can be used, parts often do not need additional support material or post curing, unless using ceramics. Unfortunately because of the process, the machines can take a long time to heat up and cool down. Also, being that powder material is used, the parts are porous and have can have a poor surface finish. If using these parts in investment casting, this would require the surface of these parts to be sealed.

1.2.5 3DPrinting

Three dimensional printing (3DP) was developed by the Massachusetts Institute of Technology. The parts that were made in this process were typically for ‘proof of concept’, as the parts were generally very brittle (Upcraft & Fletcher, 2003). The building of a 3D printed part is achieved by the layering of powder material and bonding them together. The build bed will have a layer of power layered on the surface by the feed roller. The printer head/binder cartridge will then dispense the binding material on the powder at the desired location dictated by the slice produced from the CAD representation of the part being built. Once that slice is complete, the build surface will then lower into the build chamber and the feed roller will push another layer of power on top of the bed. The print head will only deposit binder based on the parts geometry. There is no need for extra support material as the base powder acts as the support structure each time a new layer is feed through. Once the building is complete, the build chamber will then be raised and the full printed part will then be revealed. The excess build powder is brushed off and recycled for future use.

1.2.6 PolyJet

Along with the traditional categories of RP technologies are also hybrids. An example of a hybrid RP technology is the PolyJet process. The material that the polyjet uses is similar to that of SLA. The photopolymers are cured using UV light. The material is dispensed like a printer cartridge and similar to the application process of binder in 3DP. The liquid is dispensed on each layers cross-sectional slice and instantly solidified from the UV light with the machine. After each layer, the build platform is lowered and the process in repeated. Unlike the 3DP and SLA, there is no bed of material that can be used as support. Therefore, similar to the FDM process, support material is dispensed in the need areas by the printer head (Lipson & Kurma, 2013).

1.3 Motivation, Thesis Objectives, and Scope of Research

1.3.1 Motivation

There are many factors that can affect the mechanical characteristics of the RP part, and the contributing factors and their interactions are not well-understood. Each machine is configured for one technology type, and only certain materials and process parameters can be leveraged within that machine group. The remaining factors leave the designer with a limited range of achievable mechanical characteristics; however, there is limited baseline knowledge that can be leveraged by designers. Understanding and consequently expanding the range of properties could result in new application of the technology and parts.

1.3.2 Thesis Objectives

The objectives for this thesis are to develop a better understanding of the different factors that can influence the mechanical properties and decisions for design of an RP part, specifically using a 3D printer. The hypothesis is that the infiltrate will improve the tensile, compressive and flexural properties of the material in the similar ranking as previous studies. The results of the different infiltrates will also incorporate a range of strengths that will reflect the 3 build orientation conditions. The knowledge obtained from this comprehensive study can be used to understand how the different variables and decisions affect the final part and process. Thus, the designer could be able to more confidently predict the mechanical characteristics of the part through the use of infiltrates and the use of an intermediary value for build orientations. The introduction of a multiple infiltrate technique will also help bridge the ranges and demonstrate the ability to predict with closer tolerances. The analysis and knowledge of mechanical quality ranges will also help the designer tailor the variables to build a part with specific qualities while considering resource usage. Below, in Figure 2, is a fishbone diagram illustrating some of the factors that affect the mechanical properties of 3D printed parts.

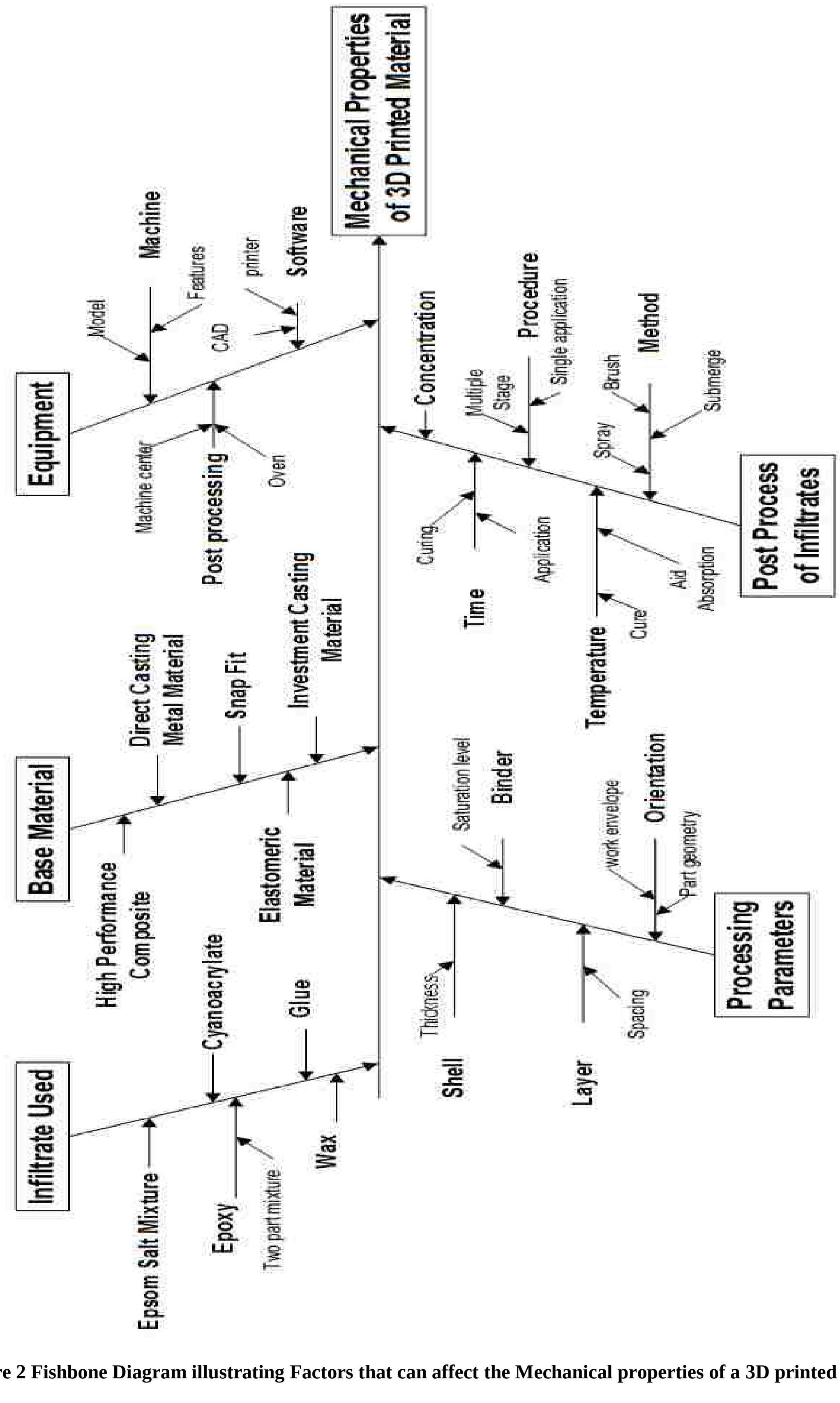

Figure 2 Fishbone Diagram illustrating Factors that can affect the Mechanical properties of a 3D printed Part

1.3.3 Scope of Research

There are many factors that can influence the mechanical properties of a 3D printed part, and selected elements are illustrated in the Ishikawa diagram (Figure 3(a) and (b)). However, there is limited published research correlating the tensile, compressive, and bending characteristics with respect to various infiltrate options. Therefore, the goal of this research is to perform a comprehensive study with respect to assessing the impact of selected post-processing variables on these mechanical characteristics. The experimental work is performed on a Z-Printer 450 machine using the ZP 150 powder, and the ZP 59 binder type.

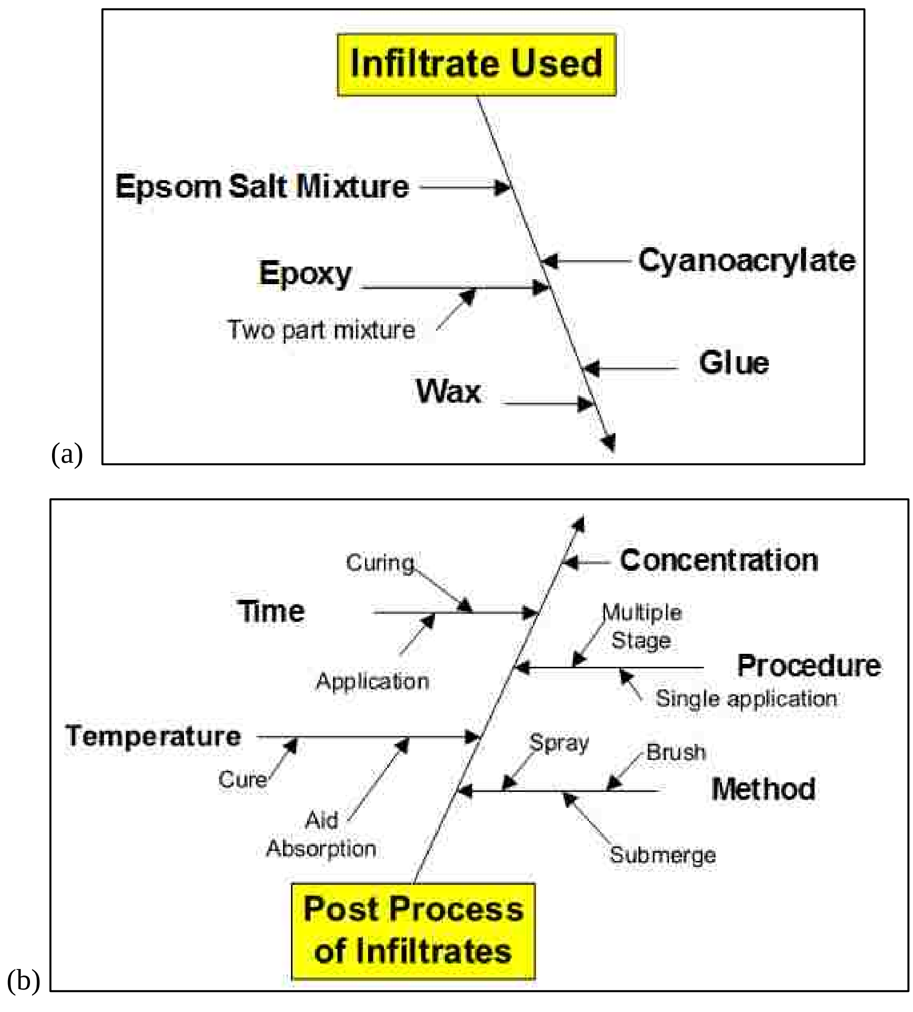

Figure 3 (a) Infiltrate Used – section of fishbone and (b) Post Process of Infiltrate – section of fishbone

The comprehensive study includes the three physical testing methods, with their specific geometry and test set-ups. The specimens were printed in three different build orientations and post processed with different types and levels of infiltrates. Force and distance results from the tests were obtained from the testing software. The absorption depth of the infiltrate was measured for all the specimens. The test specimens represent different build orientations to understand their impact on the different stresses present and predict the build directions for the optimal stresses desired. Curve fitting of the stress and strain observed are used to help to classify, compare and predict the impact or failure due to stress and/or deflection. These results further analyze their impact of the decisions affecting the management of resources to decide which factors are most important when making design decisions.

Presently, there is no complete experimental or theoretical foundation for designers to predict the mechanical characteristics of a 3D printed part, including employing a standardized testing methodology. Therefore, a complementary research outcome was establishing a robust approach for data collection, including standardizing specimen sizes, sample preparation and testing methods for components fabricated by the 3DP process.

CHAPTER 2

BACKGROUND

2.1 Background

Three dimensional printing (3DP) was developed by the Massachusetts Institute of Technology. The parts that were made in this process were typically for ‘proof of concept’, as the parts were generally very brittle (Upcraft & Fletcher, 2003). This is no longer the case as different materials and infiltrates can increase the characteristics greatly.

2.1.1 Building of the part

The building of a 3D printed part is achieved by the layering of powder material and bonding them together. The build bed will have a layer of power layered on the surface by the feed roller. The printer head/binder cartridge will then dispense the binding material on the powder at the desired location dictated by the slice produced from the CAD representation of the part being built. Once that slice is complete, the build surface will then lower into the build chamber and the feed roller will push another layer of power on top of the bed. The print head will only deposit binder based on the parts geometry. There is no need for extra support material as the base powder acts as the support structure each time a new layer is feed through. Once the building is complete, the build chamber will then be raised and the full printed part will then be revealed. The excess build powder will be brushed off and recycled for future use. Figure 4a is the schematic view of the 3D printing process and 4b is an illustrated summary of the 3DP process flow.

(a) 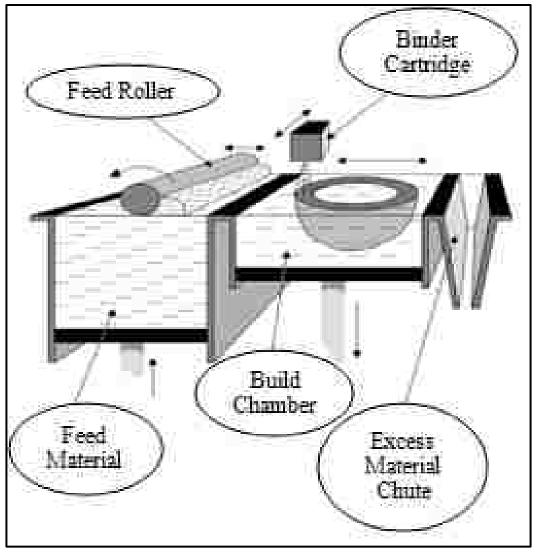

(**b**) 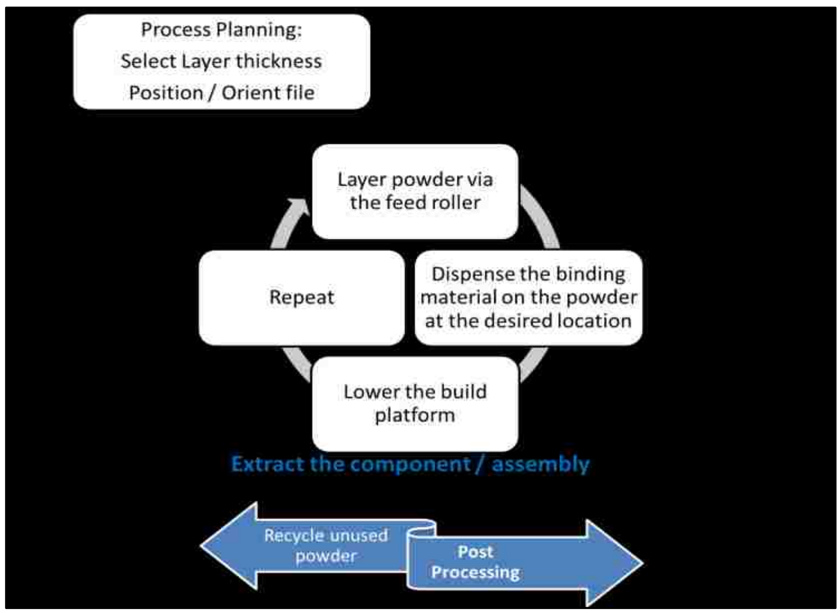

Figure 4 (a) Schematic view of the 3DP process (Upcraft & Fletcher, 2003)and (b) 3DP Process flow

When compared to other RP technologies, 3DP has shorter building times and consumes less expensive raw materials (Upcraft & Fletcher, 2003). These factors have made the printer more affordable. Once seen as a disadvantage, part being brittle and requiring infiltration, is now an advantage. This advantage is realized in the more diverse products that can be obtained from the variations in powder, binder, and infiltrates (Z Corporation, 2005). These factors and variables have led to many researchers looking to understand the different combinations and finding the correct one for their application.

2.2 Literature Review

The original equipment manufacturer (OEM), Z corp. (Z Corporation, 2005), provides basic information with respect to adjusting parameters and variables to reach the desired effect and characteristics of the final printed part, for various machines, base materials, and infiltrates. The information provides the general applications and characteristics that can be observed with their products, and the available information is limited. The goal is to be able to build a component with specified mechanical characteristics; consequently, a more in-depth understanding is needed when specific results and characteristics are preferred. As a result, researchers have tested and documented some of the variables that can be altered to understand their effects. These variables include: infiltrates, binder levels, layer thickness, and the curing method. The results were compiled through physical testing and measurements. Below in Table 2, various directions of researchers are summarized. (T-time , M-method, A-absorption)

Author	Tensile	Compression	Bending	Binder	Layer height	Infiltrate			Comments
						T	M	A	
Pilipovic, Raos & Sercer (2009)	X		X						Compared 3DP and Polyjet components
Frascati (2007)	X		X					X	Orientation has a significant effect
Gharaie, Morsi & Massood (2013)	X								
Galeta, Kladri & Karaka (2013)	X				X				Thinner layers are produce stronger components
Vaezi & Chua (2011).	X		X	X	X				
Zañartu & Ramos (2010)					X				
Suwanprateeb (2006)					X	X	X	X	2 phase experimental process, described well
Hsu & Lai (2010)	X		X	X	X				Dimensional stability and optimization
Yao & Tseng (2002)				X	X				Dimensional stability
Lu et al (2014)					X				Control algorithm

Table 2 Critical literature review summary

In most cases, researchers are most concerned with the tensile characteristics of the final part.

2.2.1 Build parameters

Researchers have been interested in the changing of the building parameter and the affect it will have on the mechanical characteristics of the printed part. These build parameters range from the part location on the build bed, direction of build, the thickness of build layers as well as the binder level.

2.2.2 Orientation

The orientation of the part can have two meanings, location and build direction. In terms of the location of the specimen on the build bed, researchers observed that it has no significantly effect on the mechanical characteristics of the printed part. With experimental results, authors Frascati (2007), Galeta (2013), and Yao & Tseng (2002), have all noted that the location of the part is not a major factor in the mechanical characteristics or dimensional analysis of the part. However, build direction was documented to have a significant effect on the test results. Build direction, as in orientation of the part, is a variable used to understand how the direction of build layers affect the parts reaction to directional forces. An example of the different orientation is illustrated below in Figure 5 and adapted from an article by Gharaie, Morsi, & Masood (2013).

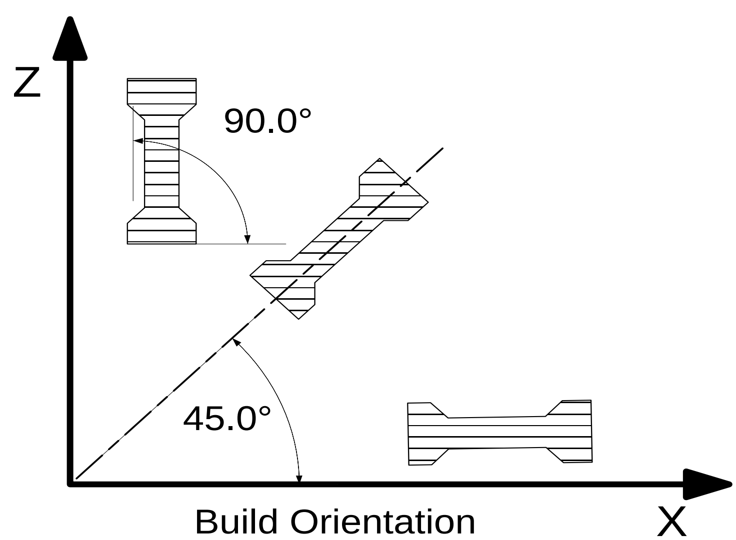

Figure 5 - Three different planes and Build Orientations adapted from, (Gharaie, Morsi, & Masood, 2013)

The above representation helps to visualize the different orientations and understand why the tensile specimens will react differently by directional forces applied on the layers. It was found in the study that the 45° build orientation exhibited the highest tensile strength while the 90° (transverse) orientation exhibited the worst. The results from the experiment can be seen in Figure 6 below.

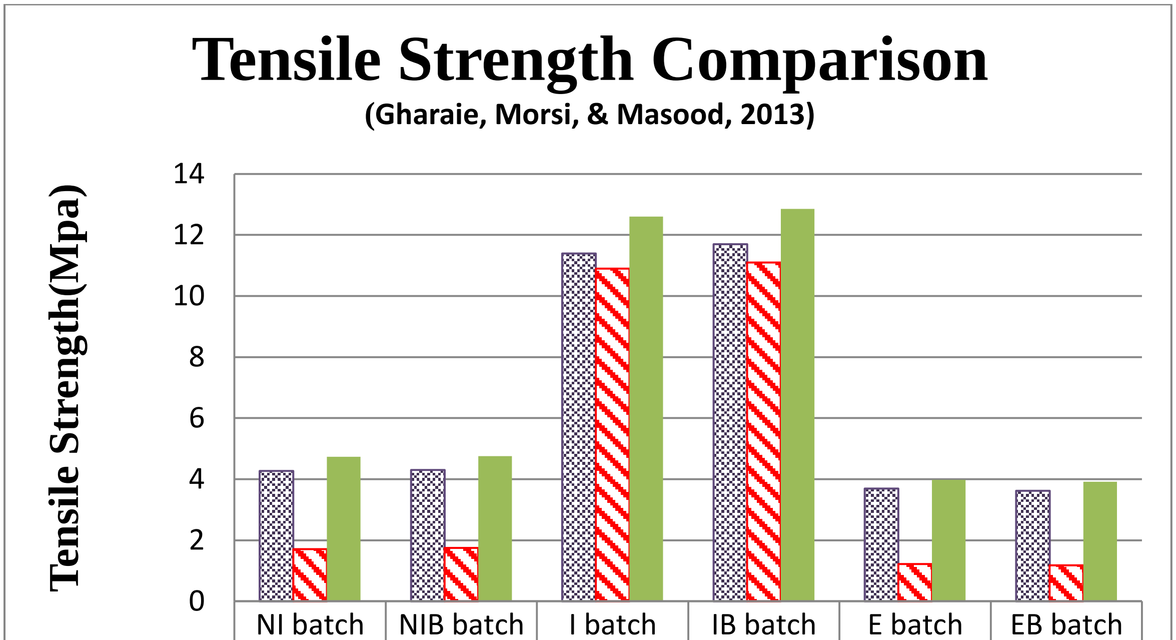

	NI batch	NIB batch	I batch	IB batch	E batch	EB batch
Axial	4.27	4.3	11.4	11.7	3.69	3.62
Transverse	1.71	1.75	10.9	11.1	1.222	1.18
45 degree	4.73	4.75	12.6	12.85	3.98	3.92

Figure 6 - Tensile Strength Comparison w/ Orientation (Gharaie et al., 2013)

It was also noted, by Frascati (2007), that the orientation had this effect because the bond between layers are not as strong as the layers themselves. The force need to separate the layers would be less than to stress crack through a number of layer. This is illustrated more clearly with a representation of the breaks formed in Figure 7.

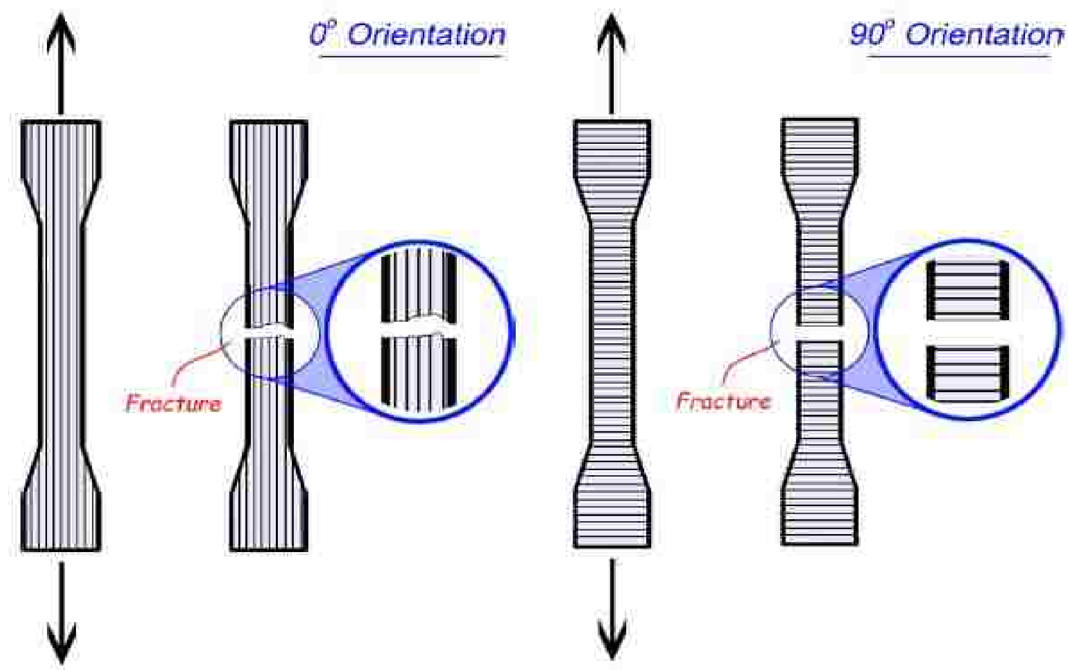

Figure 7 Fractures from tensile test based on orientation (adapted from Caulfield, McHugh & Lohfeld (2006)

Mixed results from the strength from orientation were observed by Galeta et al. (2013). They experimented with orientation of the build specimen but there was not a significant different in their test results. This could have been because the author omitted building the specimen in the Z direction, as it would have taken too much time (Galeta, Kladaric & Karakasic, 2013).

2.2.3 Layer Thickness and Binder level

Layer thickness and binder level are parameters that can be changed within the printer's software, therefore, it is easy to alter to compare results. It is observed in the article by Galeta et al. (2013) that test specimens that had the smaller layer thickness resulted in a higher tensile strength than that of the thicker layers. In the article by authors Vaezi & Chua (2011), their test experiment did not add infiltrates but only looked into the effects of binder saturation and layer thickness. They investigated two levels of binder saturation and layer thickness and they similarly observed that the thinner layers with higher binder saturation produced a stronger part. This is not surprising that the specimens with the highest binder content performed better because the build material itself is just powder and would not positively affect the parts strength. The results also show that when the binder saturation level remained constant, that the thin layer resulted in a stronger part. Similar to the other article, the observed increased strength in thin layers is due to the fact by having more layers, more binder was subsequently used building the specimen (Vaezi & Chua, 2011). Although experimenting with a different process of 3D printing, the author, Zañartu-Apara & Ramos-Grez (2010), also observes that the printed parts with thinner layers are stronger. It is their assumption, that when more binder is used it aids the material to be more compact resulting in a more dense part, and therefore stronger (Zañartu-Apara & Ramos-Grez, 2010).

Another research direction focuses on dimensional characteristics as opposed to the strength (Yao & Tseng, 2002). They used the Taguchi method to optimize the process parameters to create a better part based on dimensional tolerances. The process parameters were the layer thickness, binder levels in shell and core, and part location on the build plane. The optimal parameters, for the study conducted by Yao & Tseng (2002) to result in an improvement in performance, are presented in Table 3. The chart leads the reader to believe that the improved performance measures were a desired outcome. But if it were a desired outcome, there would be a comparison with more samples within the experiment. For example, some of the specimen measurements did not have a significant different in their measured height. It is observed that there is only 0.025% difference in height among some of the specimens with different process parameters.

Item	Time	Parameter Layer	Binder Used
(ZP11) Original	98 min	0.007inch (0.1778mm)	100 units
(ZP11) Optimal	91 min	0.007inch (0.1778mm)	90 units
Saved	7 min		10 units
(ZP 100) Original	207 min	0.0035inch (0.0889mm)	251 units
(ZP 100) Optimal	170 min	0.004inch (0.1016mm)	200 units
Saved	37 min		51 units

Table 3 Improved performance from new optimal parameters (Yao & Tseng, 2002)

Furthermore, the test piece used in the experiment was a cross resembling blocks. For a better representation of optimization with performance and dimensional tolerances, more complex geometry, which would include curvilinear surfaces, thick wall/thin wall conditions and fins, could have been incorporated.

2.2.4 Infiltrate

Infiltrates are normally used in post processing of the 3D printed part as the 'green' part is brittle. The common types of infiltrates used are wax, cyanoacrylate, epoxy and acrylic. These infiltrates, by their proprietary names from the Z-Corp (2006) supplier brochure, are listed with the summary of their qualities from in Table 4. The strength of the post processed part increases from left to right.

Unfinished	Wax Infiltrated	Z-Bond Infiltration	Z-Max Infiltration	Cosmetic finishing
•Fast •Inexpensive	•Fast •Inexpensive •Increased durability •Great color	•Fast •Durable •Excellent color	•Inexpensive •Very Durable	•Very Realistic
•Quick design check •Concept model	•Design check •Display model	•Display model •Shippable •Ergonomic model	•Functional parts	•Final design •Feedback

Table 4 Infiltrate summary of qualities from Z-Corp (2005)

In the article by Gharaie et al. (2013), using cyanoacrylate is an infiltrate produced a significantly stronger part then using an Epsom salt mixture or nothing at all. It is interesting to note that the specimens infiltrated with the Epsom salt mixture actually performed worse than having no infiltrate at all, when tensile testing (Gharaie et al., 2013). Many other authors not only documented the affects from cyanoacrylate but also compared the results to specimens infiltrated with resin. With the set up illustrated in Table 5, authors Galeta et al. (2013), examined and compared the result from wax, resin, and cyanoacrylate.

Layer thickness	0.1 mm						0.875 mm					
Infiltration	Wax		Epoxy resin		Cyanoacrylate		Wax		Epoxy resin		Cyanoacrylate	
Orientation	X	Y	X	Y	X	Y	X	Y	X	Y	X	Y
Experiment label	1XW	1YW	1XE	1YE	1XC	1YC	2XW	2YW	2XE	2YE	2XC	2YC

Table 5 - Combinations of the processing factors and experiment labels (Galeta, Kladaric & Karakasic, 2013).

The experimental result showed that the resin infiltrate produced a stronger specimen by nearly double the tensile strength of the cyanoacrylate but it performed 50% better than the wax specimens.

A more in-depth study and analysis by (Frascati, 2007) was executed with three phases, build location, build orientation and infiltrate. The third phase, infiltrate, included the use of 2 cyanoacrylate and 5 epoxies. Tensile strength and flexural strength were highest with the resin infiltrates. Among the resins, it is noted that the less viscous the resin, the higher the resultant strength was. The less viscous an infiltrate is, the more of it will be absorbed. It was noted and assumed by the author that cyanoacrylate has a shorter cure time therefore could not penetrate too deep, approximately 0.254mm. This could be the reason why the tests showed that the parts were not as strong as the resin parts as it was observed to penetrate approximately 0.765mm (Frascati, 2007). To help explain further about absorption, the author in the illustration seen below in Figure 8, shows the tensile strength compared to the amount of infiltrate absorbed.

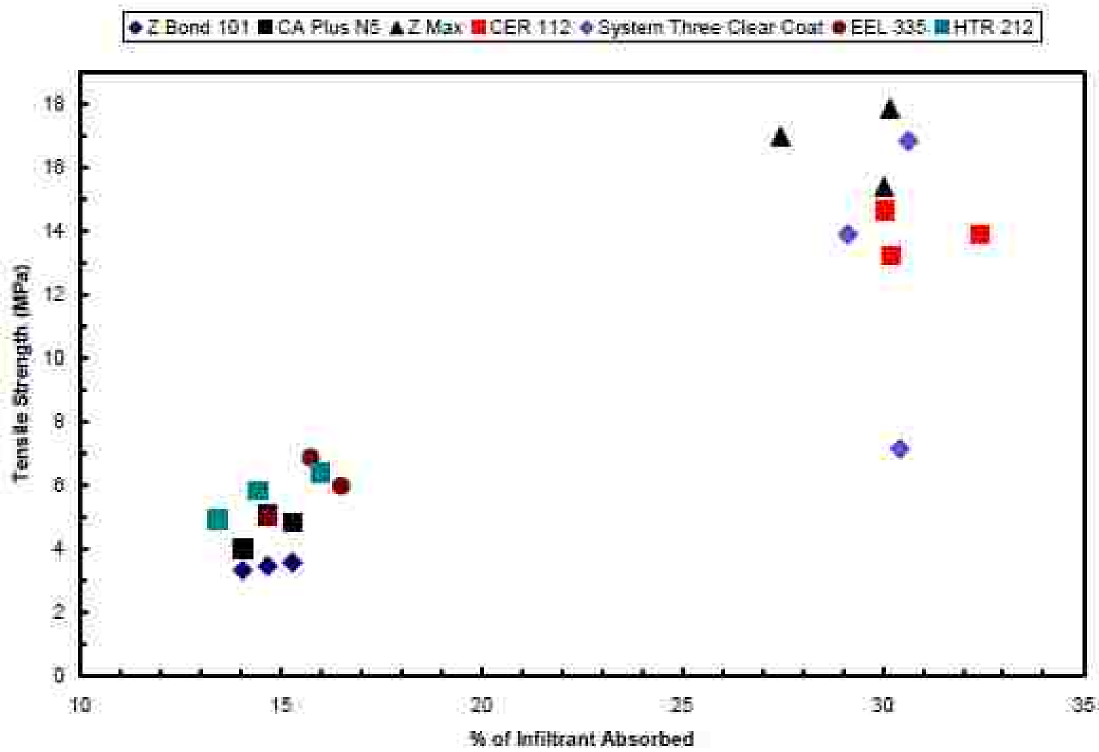

Figure 8 - tensile strength compared to the amount of infiltrate absorbed (Frascati, 2007)

The illustration does depict that the more infiltrate absorbed would result in a higher tensile strength. Under further analysis the measure used for the data is not the percentage of infiltrate absorbed but the percentage of weight the infiltrate added to the part. This could be misleading as the different infiltrates could vary in weight. Therefore, the results should be cross referenced with the actual weight of the infiltrate to understand the volume of infiltrate that was actually absorbed.

An article by Pilipović, Raos, & Šercer (2009), not only tested the 3D printer and its base material but also compared the resultant mechanical characteristics with 3 different types of build material using a Polyjet method. The infiltrates used were a cyanoacrylate and a resin. Along with a tensile test, the author tested the specimens' flexural strength in a three point bending test. The author states that the Polyjet processed specimens have responded better in the flexural test. As observed with other research papers, the orientation of the part is significant and in this study it is not known how the 3D printed parts were build. Disregarding the above mentioned variable, the author determines that the specific material that is used in the Polyjet process performed better but it is noted that out of the two 3D printer tests, the cyanoacrylate slightly outperformed the resin (Pilipović, Raos, & Šercer, 2009).

It is interesting to note that although each of the above articles included the application of infiltrates, none of them describe the application method or the application time. Therefore, it is impossible to compare the results from the different articles based specimen test results. Each of the authors could have used different methods or different amounts of infiltrates. The article that described a clear methodology in depth is published by Suwanprateeb (2006). In this article the author investigated a double infiltration technique. The same infiltrate was used in all the phases, a heat cured dental acrylic. The specific application of the infiltrate was submerging the part for ten minutes, and then cured in oven 105°C for 30 mins. The specimens compared were a single application and a double application and subjected to flexural testing. The samples were weighed to measure the weight gain resulting from infiltrating the part. It is observed that most of the gain was during the first infiltrate application (Suwanprateeb, 2006). The author notes that the pores of the material were mostly filled during the first phase resulting in a lower absorption in the second infiltrate application. The small amount of infiltrate absorbed in the second phase did not result in a significant change in the flexural strength of the specimens.

2.3 Analysis of Resources

For a comprehensive optimization model, understanding the resources usages is essential. Resources are the additional costs that are consumed or are affected by the different process strategies. While some of the resource differences would not alter some designers' decisions, others might find them the main focus for moving forward. Consequently, understanding the time and material characteristics is important.

2.3.1 Time

Time is an important resource when trying to finish a project that has a short window of opportunity. Therefore, building a part with specific strength might not be the main concern but building a relatively strong part the quickest way possible might be. Within the scope of time include both machine time and infiltration time.

Machine There is a time element for preparing the build file prior to the actual fabrication, but this element is external to this research. Keeping within the focus of this study, three different build directions are used for build time evaluation. The three build orientations investigated are horizontal (0°), angled (45°), and vertical (90°). To compare the different build directions, a common part and geometric shape was used. A 5.1 cm cylinder with a varying diameter was virtually simulated and he results are summarized below in Table 6 and illustrated in Figure 9.

Diameter and Biuld Direction		Amount of parts	Time	Layers	Total volume (cm^3)
0.3	0	1	9min	31	0.39
	45	1	1hr 30min	375	0.39
	90	1	2hr 3min	499	0.39
0.6	0	1	19min	62	1.57
	45	1	1hr 34min	397	1.57
	90	1	2hr 3min	499	1.57
1.3	0	1	33min	124	6.27
	45	1	1hr 49min	441	6.27
	90	1	2hours 3min	499	6.27
2.5	0	1	1hr 4min	249	25.58
	45	1	2hr 11min	530	25.58
	90	1	2hr 7min	500	25.58
5.1	0	1	2hr 10min	498	102.49
	45	1	3hrs 4min	705	102.49
	90	1	2hr 14min	500	102.49

Table 6 Summary of build times for cylinder with different dia. and build directions

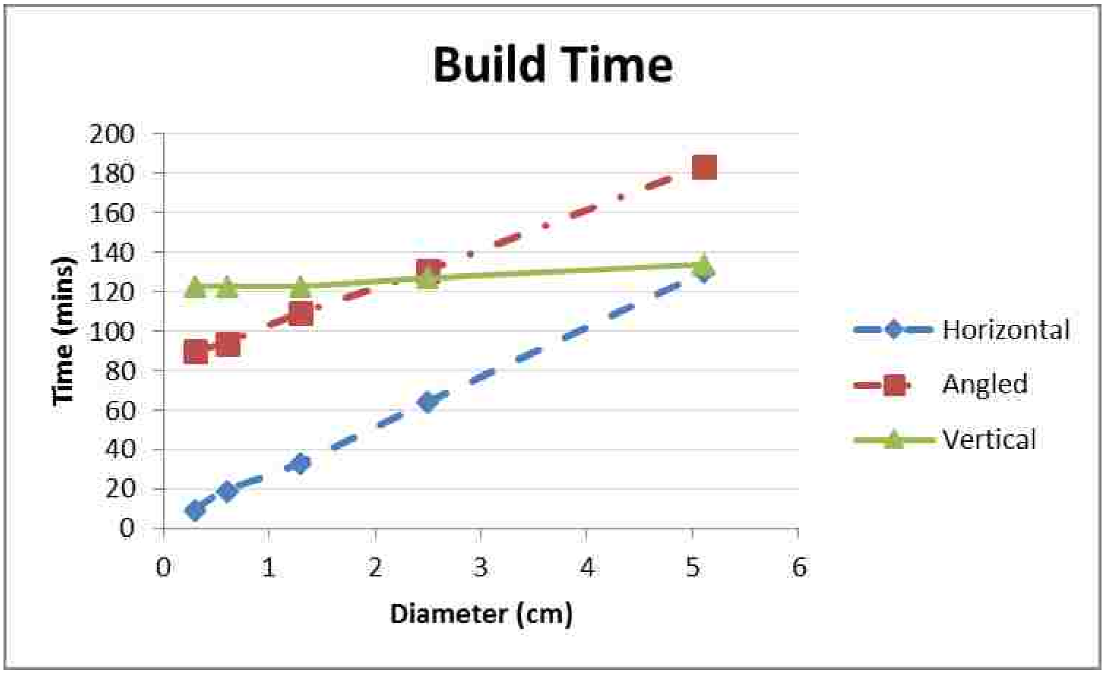

Figure 9 Graph of build times for cylinder with different dia. and build directions

From the results, it is clear that the smaller diameter parts take much less time when printed in the horizontal direction. While the smallest parts took the most time printed in the vertical direction, it remained constant until finally intersecting with the horizontal direction. The angled direction gradually took more time and after intercepting the vertical direction curve, it became the direction with the highest build time. Upon further study, the direction itself might not be the main source of the extra build time. The printing of the part includes depositing binder resembling the CAD geometer over many layers of powder. The number of layers used for the printing of the geometry in the different directions, as illustrated in Figure 10, has a similar trend to the build time.

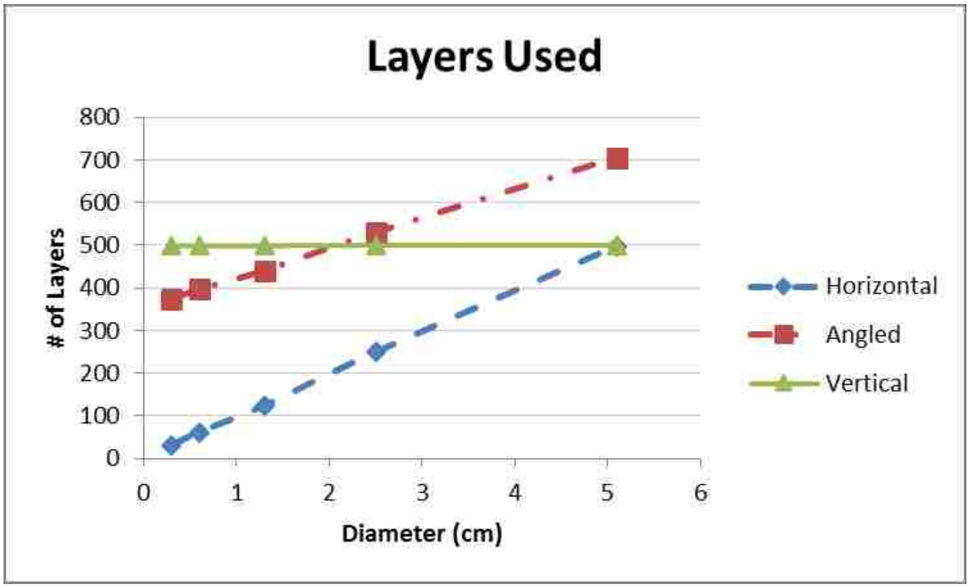

Figure 10 Graph of layers used for cylinder with different dia. and build directions

Infiltrate Application The infiltrate application time includes the specific application time used for each of the different infiltrates and the additional time needed for the mixing of the infiltrate and subsequent drying/curing of the part. A summary of the results from this study can be seen in Table 7.

Type of Infiltrate	Coding of Infiltrate	Special	Application (sec)	Curing	Mixing
Control	C	No infiltrate	n/a	n/a	
Cyanoacrylate	B		30	10 (mins)	
Polyurethane Glue	P1		60	6 (hours)	
Polyurethane Glue	P2	2hr Oven After Infiltration	60	2 (hours) oven + 6 (hours)	
Epoxy	R1	*	30	1 (hours)	10 Mins
Epoxy	R2	*	60	1 (hours)	10 Mins
Epoxy	Rg	* Not dried in Oven	120	1 (hours)	10 Mins
Salt Water	S1	Salt Solution 1**	5	3 (days)	5 Mins
Salt Water / Cyanoacrylate	Sb	Salt Solution 1**	5/30	3 (days)	5 Mins
Salt Water	S2	Salt Solution 2***	5	3 (days)	5 Mins
Salt Water / Cyanoacrylate	S2b	Salt Solution 2***	5/30	3 (days)	5 Mins

*Resin mixture 100:37 hardener by weight
**Salt Solution 1 (210:334) salt per water by weight
***Salt Solution 2 (105:334) salt per water by weight

Table 7 Summary of the time spent on infiltration from this study

It can be seen in the chart that while there is a time allotted for application and preparing the mixtures, the largest times include the drying and the curing. Other than the control, the shortest times include the cyanoacrylate and the epoxy. The actual shortest time would the epoxy (Rg) as it was not dried in the oven and was kept in its green state. The drawback from the top two sets of specimens is that they are chemicals that can be hazardous if not handled correctly. The descriptions from the accompanied packages along with special instruction are summarized in Table 8.

Infiltrate Type	Product Name	Description on Package	Special Instructions
Cyanoacrylate	HyperBond	5 cps thin triple distilled Adhesive Rapid Molds	Use with adequate ventilation Vapors irritate mucus membrane Avoid skin and eye contact
Epoxy	Z-Bond	High strength Epoxy infiltration system (resin and hardener) Zcorp	Eye skin and respiratory irritant Avoid breathing vapors Use with ventilation Wear suitable PPE
Polyurethane Glue	Elmer's	Ultimate Polyurethane glue (interior/exterior)	Use rubber gloves to avoid sticking/irritation May irritate eyes, skin Dangerous fumes when mixed with other products
Epsom Salt	100% Natural Mineral	Saltmasters	

Table 8 Summary of descriptions of special instructions from the accompanied packages

2.3.2 Materials

Materials used in the study and for 3D printing include the powder and binder during printing and the infiltrates while post processing.

Machine The machine consumables consist of binder, powder and printer heads. Three different build directions of the cylinders were virtual simulated for binder usage. The results are summarized below in Table 9 and illustrated in Figure 11.

Diameter and Biuld Direction		Amount of parts	Layers	Binder used (ml)	Total volume (cm^3)
0.3	0	1	31	5.1	0.39
	45	1	375	23.5	0.39
	90	1	499	30.1	0.39
0.6	0	1	62	7	1.57
	45	1	397	25	1.57
	90	1	499	30.4	1.57
1.3	0	1	124	11.1	6.27
	45	1	441	28.01	6.27
	90	1	499	31.2	6.27
2.5	0	1	249	20.7	25.58
	45	1	530	35.8	25.58
	90	1	500	34.1	25.58
5.1	0	1	498	44.8	102.49
	45	1	705	55.9	102.49
	90	1	500	44.9	102.49

Table 9 Summary of binder used for cylinder with different dia. and build directions

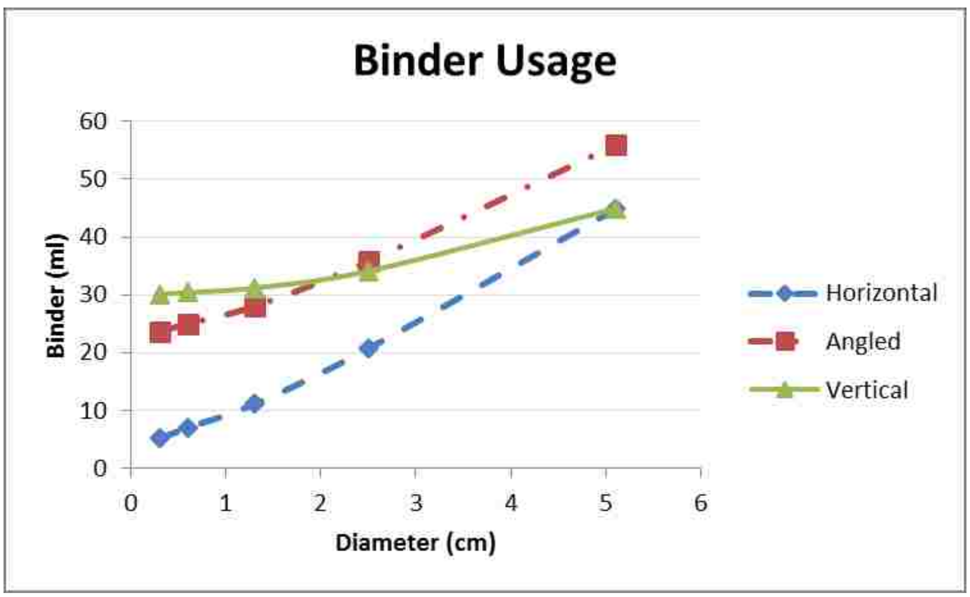

Figure 11 Graph of binder used for cylinder with different dia. and build directions

From the results, it is clear that the smaller diameter parts use much less time when printed in the horizontal direction. While the smallest parts used the most binder when printed in the vertical direction, it remained constant before an upturn and finally intersecting with the horizontal direction. The angled direction gradually used more binder and after intercepting the vertical direction curve, it became the direction with the highest binder usage. Upon further study, the direction itself might not be the main source of the extra binder usage. The printing of the part includes depositing binder resembling the CAD geometry over many layers of powder. The number of layers used for the printing of the geometry for the different directions, as illustrated earlier in figure 10, has a similar trend to the binder usage.

The binder is discharged through an HP printer head. This study did not use colour, therefore, the colour usage was not observed. Observations were only made on the black printer head cartridge. The black ink cartridge is used for dispensing the binder onto the power, even when no colour is being used. The cartridge has a use life that is recorded within the machine. As more binder is dispensed through the cartridge, the life of the cartridge is reduced. Once the machine determines that the useful life is complete, there will be no more printing until the cartridge is changed. Therefore, by using fewer layers per part, more parts could be printed before having to change the print head.

Each of the build directions produced identical parts and each consisted of the same volume, therefore, there was not a significant difference in the powder consumed. However, while there was no extra powder consumed, more powder is needed when building a part with the angled and vertical directions. This is due to the nature of 3D printing and using the powder layers as support material for subsequent layers. Thus, the more layers that the machine uses to print the part, the more powder is actually needed to produce the part.

Infiltrate The materials used for the infiltrates include not only the infiltrates themselves but also the materials that were used in the application of the infiltrates. The infiltrates varied not only in price but also in accessibility. The Epsom salt is the easiest to find and is the lowest price. This is followed by the polyurethane glue which can be found in many hardware stores in large container sizes. The cyanoacrylate is harder to find in larger sizes and will need to be special ordered but can be found for under $30 a bottle. The most expensive infiltrate used in this study was the epoxy. While there are many types of epoxy, this one is specifically made and marketed for the infiltration of 3D printed parts. Along with the Epsom salt mixture, the cyanoacrylate could be reused if it is quickly poured back into a sealed bottle after use. The other two infiltrated does not have this luxury As the polyurethane glue would already become thicker when exposed to air during application and the epoxy, being a mixture of resin and hardener, starts a chemical reaction when mixed which continues until it solidifies, thus rendering all non-used material useless.

Lastly, during the application process, there needs to be safety precautions for using some of infiltrates. Therefore, it must be mentioned that the epoxy and cyanoacrylate must be used in a well-ventilated environment with proper personal protective equipment including goggles and a respirator. While the two mentioned personal protection equipment can be reused and amortized over the amount of parts produced, the absence of either of them should eliminate those infiltrates as an option.

2.4 Exploratory testing

Preliminary exploratory testing was conducted to better understand the reaction of the different infiltrates with the 3D printed material. The test results was observing the absorption limitations of the infiltrates in the material which helped with the specimen selection for the design of experiment (DOE) The process flow of the infiltrate depth testing is illustrated in Figure 12.

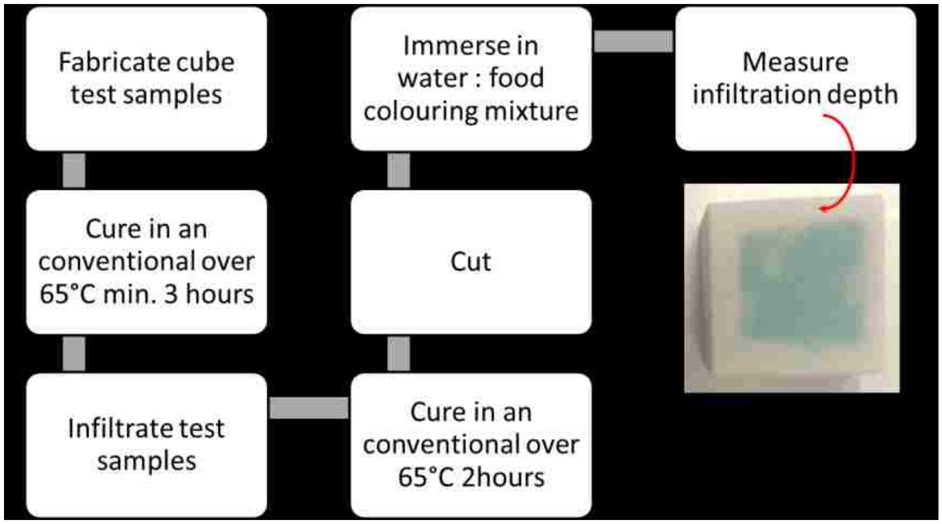

Figure 12 Process flow for infiltrate depth testing

2.4.1 Preparing the samples

The preliminary tests were conducted on prepared samples of the material cut from larger parts, printed from the machine. The larger parts were printed at an earlier date but did not have any post processing done to then except being cured by the lab room atmosphere. The test samples were cut into smaller pieces so that the material could be effectively viewed with the different levels of saturation that was eventually be used in the testing. The pieces were prepared to be no less than a half inch cube. The half inch minimum was chosen because of its resemblance to the eventual specimen diameter for further studying. A test piece that was too thin would not result in a true representation for the saturation time as the infiltrate could be absorbed for all directions and it would be difficult to determine the direction of absorption. A larger piece was not used as it could have been an inefficient use of material as it was still unknown that the part could be fully saturated.

As the parts were cured and stored within the lab and its environment, the prepared test samples were then placed in a convection oven at a temperature of 65°C (135°F) for a minimum of three hours. This was to ensure that any moisture absorbed back into the part from the regular humidity of the storage area in the lab was removed.

After drying the pieces, the different types of infiltrates were applied with the specific timed exposure. The infiltrates were allowed to saturate the part for a specific amount of time before the excess of the infiltrate was wiped away from the material surface. This would insure that no more infiltrate could be absorbed into the material part the time allowed. However, this did not restrict the continued travel or dilution of the absorbed amount of infiltrate. As illustrated in Table 10, the initial tests were conducted with polyurethane glue, cyanoacrylate, Epsom salt and epoxy as infiltrates.

Type of Infiltrate	Brand	Concentration	Abbreviation Used
Polyurethane glue	Armor Coat	full	P
Cyanoacrylate	Z-Bond 101	full	C
Epsom salt	Natural Mineral	7:9 (w/water)	S
Epoxy (resin: hardener)	Z-Max	100:41 (by volume)	R

Table 10 Infiltrates and Abbreviations Used for Exploratory tests

The times that the infiltrates were exposed to the test pieces, as seen in Table 11, ranged from 10 seconds to 5 minutes. The range of exposure time were chose to record a large range of distinct times and a method of tracking the speed at which it was absorbed.

	Application time and Abbreviation used					
	a	b	c	d	e	f
Seconds	10	30	60	120	190	300
Minutes	0.167	0.5	1	2	3	5

Table 11 Application times and Abbreviations Used

The parts were then set into the oven to cure at 65° for two hours and then set aside to finish curing in the natural environment of the lab for a minimum of two days. Shown in Figure 13 are the test samples being prepared and arranged for curing. It was assumed that the use of the convection oven would speed up the curing process without affecting the absorption depth. Once the cure time is completed, the parts are then cut in half with a hack saw, and the face smoothed by a file to facilitate the infiltrate measurement. It was assumed that the depth of the infiltrate would be uniform from all four of the walls and that the depth of the infiltrate would be easily observed by a distinct line representing the end of progression within the material.

Figure 13 In-Process Exploratory Testing Samples

2.4.2 Measuring the depth

Measuring the depth of the infiltrate absorption was not as straight forward as anticipated. Distinguishing between the material with or without the infiltrate was made difficult as there was only a slight shade change in the colour of the material. To make a more distinct line and to aid in the measurement another step in the preparation of the part is introduced, which consists of adding an additional material to highlight the infiltrate boundaries. The method and reasoning for adding the extra material was observed while viewing videos of different infiltrate application processes. At the end of the video, the researcher used copper dust to distinguish between a part that was post processed with an infiltrate and one that was not. The end result from this experiment is that the region with no infiltrate looked dark grey while the other was still white (Duann, 2012). As stated previously, the basic material used in the 3D printed part is porous in nature. As a result of adding an infiltrate, the pores of the material are filled within the infiltrate zone. Duann utilized copper dust because its small particles could be deposited in the pores of the material. The region with filled pores did not allow the copper dust to be deposited within the material. This same technique was implemented to view the depth line of where the infiltrate reached. Due to availability and cost, alternatives to copper particles were explored. Common ashes from a fireplace were used with good results, as did employing a colored liquid. The liquid is only absorbed by the material that is porous. Thus, a very distinct line can be viewed and used for depth measurements, as seen by the specimen preparation in Figure 14.

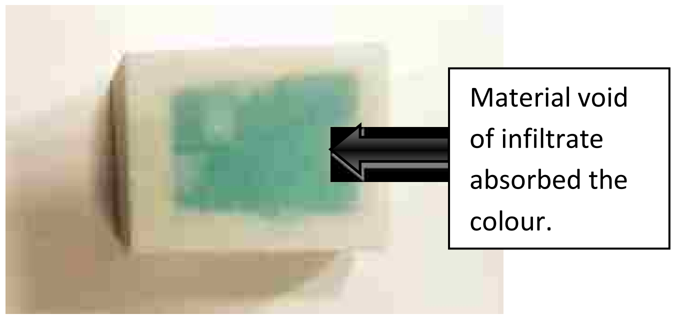

Figure 14 Illustration of Using Color to Observe Infiltrate Absorption

The depths are measured in inches using a Mastercraft ® digital Vernier caliper. The recorded depth was the measurement taken from the edge of the part to the distinct line representing the absence of infiltrate. The results for the initial round of test are seen in Table 12 and summarized in Figure 15.

		Application Time					
		a	b	c	d	e	f
Infiltrate Material	P	0.051 (1.3)	0.06 (1.52)	0.062 (1.57)	0.065 (1.65)	0.064 (1.63)	0.073 (1.85)
	C	0.073 (1.85)	0.074 (1.88)	0.069 (1.75)	0.065 (1.65)	0.068 (1.73)	0.072 (1.83)
	S	n/a	n/a	n/a	n/a	n/a	n/a
	R	0.089 (2.26)	0.18 (4.57)	0.218 (5.54)	0.223 (5.66)	.250 (6.35)	.250 (6.35)

Fully saturated part. (grey)
Part does not show any wall or barrier formation. (yellow)

Table 12 First Exploratory Test Results

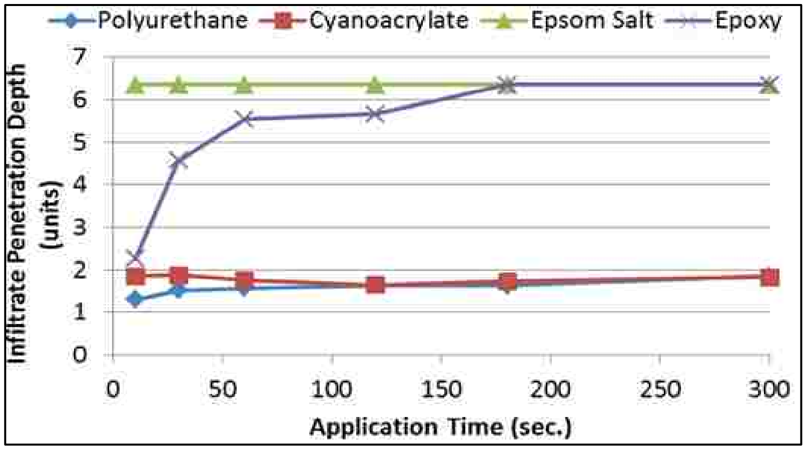

Figure 15 Exploratory test absorption depths

2.4.3 First test observations

It was observed from the first test that a distinct barrier could not be seen while using the Epsom salt mixture. To remedy this, an opposite post processing approach would be used in the second round of preliminary testing. Instead of using food colouring in a water mixture, the food colouring was added to the Epsom salt mixture so that a distinct line would be created where the absorption progress was halted.

It was also observed that both the polyurethane glue and the cyanoacrylate could have an infiltrate depth if allowed a longer application time. Therefore, another set of test specimens were prepared to explore this hypothesis.

Along with test specimens prepared for the new Epsom salt process and for the extended application time for the polyurethane and cyanoacrylate, test specimens were prepared to test the effects of: using a diluted ciliate and by using a two phase combination of Epsom salt mixture then cyanoacrylate. The diluted cyanoacrylate was a mixture of equal parts: Z-bond and acetone (recochem). The two phase trial started with fully saturating the piece with Epsom salt mixture with food colouring (to show full saturation), fully drying the piece, and then applying the cyanoacrylate similar to the first experiment. The results from the second test can be seen in Table 13.

		Application Time								
		a	b	c	d	e	f	30min	1hr	20hrs
Infiltrate material	P							0.037	0.036	0.041
	C							0.066	0.067	0.069
	C.5	0.095	0.083	0.058			0.066			
	Sf	0.046	0.046	0.046						
	Sf-C	very minimal detection								

Abbreviation Legend	
P	Polyurethane Glue
C	Cyanoacrylate
C.5	Cyanoacrylate/ Acetone (50%)
Sf	Epsom Salt w/food coloring
Sf-C	Epsom Salt w/food coloring, then Cyanoacrylate

Table 13 Second Expository Test Results

2.4.4 Second test observations

The results of the second test uncovered more variables that require to be investigated. Of the five new set of test, the cyanoacrylate absorption behaved as anticipated and can now be understood. It is observed that the depth of infiltration did not significantly change when cyanoacrylate was applied for a longer period of time. Therefore, when using this as an infiltrate, without dilution, the maximum depth of absorption observed is .065-.074 inches (1.65 – 1.88 mm).

The same results could not be said of the polyurethane glue. After cutting and preparing the samples, it was observed that the absorption depth was only half the depth as observed in the previous test, even though it had a longer application time. After reviewing the results and examining the procedures, it was discovered that there was a deviation in the processing of the test samples. The first test process included letting the test samples dry off in the convection oven of a minimum of two hours as it was thought at the time that this would have no effect of any of the sample or the infiltrates. Alternatively, this could be the very thing that altered the measurements for the absorption depth of this infiltrate. It is now assumed that the test part absorbed roughly the same amount of infiltrate but the heating of the sample actually lowered the viscosity of the glue. This enabled the glue, which was already absorbed, to penetrate deeper into the part. If this hypothesis is validated, it would lead to a new set of parameters for some of the infiltrates. Questions that could be examined further are: by adding heat to the infiltrate before absorption, could more of the infiltrate be absorbed; and does heating the part after infiltrate application, and the resulting change on depth, affect the strength of the part.

Also in the second set, tests were conducted using a diluted CA. The dilution was a 50% per volume mixture with acetone as the diluting agent. It was assumed that when this infiltrate was diluted, it would be more easily absorbed by the material. The samples pieces were processed and the results observed were not as expected. The first sample did indicate a deeper abortion of the material but this absorption depth actually decreased as the time was increased. The effects can be seen in Figure 16. The specimens that had the first applications and the shorter times are shown from left to right and clockwise (CW) respectively. A review of the finding and the sample preparation process was carefully examined.

Figure 16 Diluted Cyanoacrylate w/ Non-Uniform Absorption Compared w/ Time (Low to High, L-R and CLW)

There were two possible explanations that were identified: the mixture was starting to cure in the container as the tests were being taken; and the first test samples absorbed the part of the mixture with the lowest viscosity.

<u>Cure inside of container</u> The infiltrate mixture was mixed within a container and left in the open air until all the test pieces were subject to the appropriate application times. The test samples were arranged in ascending order of application time and processed in the same fashion. A random order of test pieces when applying this infiltrate should be used in the future to eliminate or understand this as a variable factor.

Absorbing lowest viscosity first The infiltrate mixture was mixed within a container. The application process was to submerge the piece in the container for the prescribed amount of time and then wiped of the excess before set aside to cure. Repeating the process explained earlier, the test samples were arranged in ascending order of application time and then processed in the same fashion. This order would allow the parts that were processes first and with the shortest time to theoretically absorb the least viscous part of the mixture. A random order of test pieces when applying the infiltrate along with using a different process of applying the infiltrate that does not include submerging the sample in the same container should be used.

Use of food coloring It was assumed that with the aid of food colouring, the depth of abortion for the Epsom salt mixture could be observed and measured. After preparing cutting a preparing the samples for measurement, there were two observations. First, all of the samples were still moist in the centre and the material was very soft. Second, the food colouring did not significantly penetrate into the material. These two observations can be seen in Figure 17 as a picture was taken to document preserve the findings.

Figure 17 Epsom Salt Mixture Prepared Samples (soggy center)

These observations would leave us to believe that the mixture did in fact become fully absorbed by the material, in as little as ten seconds, as the samples were still damp in the middle even though the food colouring did not indicate this. Further understanding is needed as it would seem as though the sample's material (white) just absorbed all the colour out of the mixture as it traveled to the center of the part. In this case, the material acted as a filter for the colour. This theory has given rise to the refuting of a uniform absorption of the infiltrate mixture in the material. The material could also be acting as a filter by separating the salt from the mixture and allowing just the water to be absorbed the rest of the depth. To eliminate and/or understand this as a factor, samples were made with two levels of salt concentration. The higher concentration of salt might should leave a more distinct border that can be measured indicating the depth of absorption.

The last of the test specimens was the trials for a two phased infiltrate approach. The first phase had the piece fully saturated with the Epsom salt mixture with food colouring that was used in the accompanying set of tests. Like in the accompanying test, it was thought that the food colouring would give a validation that the material had been full saturated by the mixture. When preparing the single phase test pieces for measuring, it was noticed that the material in the middle of the part was still damp but did not have colour with it. The absence of colour did not disqualify this test because by the part showing signs of dampness, it is confidently reported that the material was fully saturated by the mixture. As a result of the other parts being damp, these pieces were left to cure for another three days in the hopes that the part would be fully dry before adding the next infiltrate in stage two. Without incident, the stage two infiltrate was applied and set aside to cure before being processed. When the parts were cut and processed, it was observed that all the pieces, regardless of application time, appeared to have very minimal detection of a barrier. The part looked very similar to the samples that used the salt mixture and food colouring as an infiltrate. To achieve a better understanding of this case, a few more test samples were added to the specimen list. Similar to the reasoning proposed above, it is assumed that the salt was filtered by the material and clogged the pores near the surface, thus not allowing the absorption of the cyanoacrylate. This can be determined in the future by a testing two phase samples that would include the application of water then cyanoacrylate. This test would show that it could be added to the material after water and that the salt mixture somehow blocked the absorption.

Research performed to date has presented minimal information from the design community to determine a best practice approach for using infiltrates and standardizing the test methods to understand their effects and to the ability to compare and replicate results.

2.5 Data Collection

The data collected for this research consisted of: machine build times and binder usage for the different build orientations; the build orientations of the specimens; the post processing time for the infiltrates, measured infiltration depths; response curves for force vs. time/crosshead displacement; and the resultant ultimate strength for the different tests.

The build orientations were organized and manipulated within the Z-printer software before physical printing was conducted. After the printing of the specimens and in machine curing, the specimens were retrieved from the machine bed and marked with a black marker. The flat end of each of the specimens were marked with the batch number, build orientation and location of specific specimen, in black marker. This data was collected and subsequently used as its identifier throughout the experiment. The orientations were marked X for horizontal, Y for vertical and A for angle. The location was recorded by a numbering system that ascending from the first sample in the SW corner of the build chamber to the east and then returning to the west for the next row north.

The physical testing of the specimens produced a specific Excel ® data file for each specimen, which contains the measured force with the corresponding crosshead displacement and elapsed time.

After the destructive tests were conducted on the specimens, the broken portions were collected and sorted. The broken specimens were viewed in groups for visual trends in breaking area locations and geometry. After the observations were recorded, each of the specimens had a piece of their test area cut with a saw. That area was then measured for the infiltration depth by the method mention earlier in the paper.

CHAPTER 3

DESIGN OF EXPERIMENTS

3.1 Design of Experiments

This project incorporates a very thorough analysing of the many different variables that could alter the mechanical characteristics of the 3D printed material. The porous type material, which is used in this RP technology, can be manipulated to vary its properties quite substantially. Other authors have observed this variance and even the company suggest different post processing methods for the level of strength desired in the printed part

3.1.1 Experiment Process Flow

There are many steps within the process and at different times the variables are added. The process flow map below in Figure 18, illustrates the items that take place during the experiment and at which point key decisions were made.

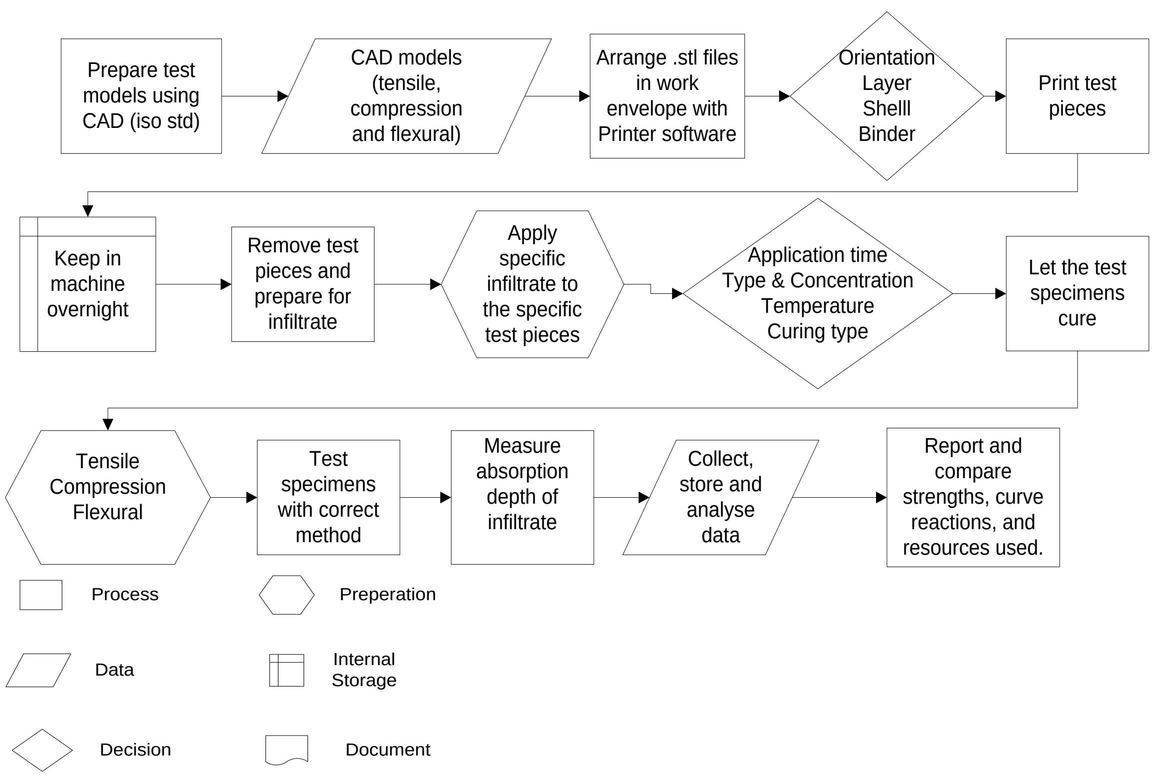

Figure 18 - Process flow chat of experiments overview

The first two decision items, dealing with build and post processing parameters, that are on this process flow chart represent change variables that can affect the mechanical characteristics of the specimens.

3.2 The Output Measurables

The measured outputs for the experiments are the results for the three types of testing: tensile, compression, and flexural. The raw data consists of the applied forces and associated cross head travel. This data is transformed into classic stress- strain curves to extract the key mechanical characteristics, and includes: the ultimate tensile, compressive, and flexural strengths, along with the associated moduli of elasticity and the linear regions. These three tests provide a comprehensive representation between the post processing variables and standard design performance parameters.

3.3 Factor levels

3.3.1 Infiltrate

There are many types of infiltrates that are commonly used and recommended by the manufacturing company. For this experiment, the base types of infiltrates used are CA, Epsom salt mixture, epoxy, polyurethane glue and a control sample with no infiltrates.

3.3.2 No infiltrates

These samples incorporated all the build parameters, and provide a baseline for the subsequent analyses.

3.3.3 Cyanoacrylate

Cyanoacrylate is also referred to as super glue. With mixed results from altering the concentration for a predictable absorption depth, it was determined that just one level was used for this infiltrate.

3.3.4 Epsom Salt mixture

The Epsom salt mixture to be used in the experiment is set at two factor levels. These levels include two different Epsom salt concentrations. The concentration of the solutions were the recommended 7:9 and a reduced concentration of 3.5:9 (Epsom salt: water, by volume).

3.3.5 Epoxy

The epoxy used for the experiment is a two part epoxy sold by z-corp. under the brand name of Z-max. The mixture includes the two parts, resin and hardener, measured by volume to a concentration of 100:41. This is the recommended mixture concentration on the supplier's package for the use as an infiltrate. The two levels of this product are the differences in the application time. As a result from the change of application time, the infiltrate is absorbed to different depths. Therefore, it can be observed how the amount of infiltrate absorbed could alter the mechanical characteristics of the material.

3.3.6 Polyurethane glue

This infiltrate was added to explore different type of infiltrates that are not commonly used. This type of glue is readily available and therefore could make a great alternative to any of the proprietary infiltrates. Therefore, this experiment analyzes the changes in the mechanical characteristic of the 3D material compared to the other more popular infiltrates. Two factor levels are examined with this infiltrate. These levels were determined from observations on the absorption depths paired with the processing parameters, during the exploratory phase. It was observed that heat affected the absorption depth of the product. The two levels, summarized in Table 14, include the absorption and cure at room temperature and absorption at room temperature while curing will be in the oven at 65°C.

	Temperature	
	Absorption	**Cure**
1	room	room
2	room	65°C (135°F)*

* Curing in oven for 2 hours

Table **14** Variable **set-up for Polyurethane Glue Trials**

The infiltrate, when heated, become less viscous and is absorbed to a greater depth. This was observed when exploratory tests showed that parts cured with heat was observed to have a higher absorption depth than the pieces that were cured at room temperature, even though no more material was applied. Therefore, these test specimens help to compare the effects on the characteristics of the material with respect to absorption depth and concentration of this infiltrate on the material.

3.3.7 Two Phase

A two phase infiltrate application was conducted by applying the Epsom salt mixture (7:9) and followed by the application of cyanoacrylate. The salt mixture was given time to cure before the cyanoacrylate is applied. This test aided in determining if two infiltrates could be combined to produce a mixed effect on the material. It was observed from exploratory testing that the cyanoacrylate did not penetrate deep into the material and could have been caused by the amount of salt within the material after the water was evaporated. Therefore, a second level of the two phase was used. This included a lower concentration of salt in the mixture.

3.3.8 Orientation

The orientation of the specimen can also have an effect on the mechanical characteristics of the material. The process of building the part in a 3D printer involves stacking layers of material. Subsequently the direction of these layers have an effect on its reaction to specific directional forces. The three most common build orientations, as illustrated in Figure 19 with test specimens, are vertical, horizontal, and 45°. The three orientations have been documented to have an effect on the mechanical characteristics of part. Therefore, the addition of this factor aided in a more comprehensive understanding of the effects of infiltrates and selection process of builders.

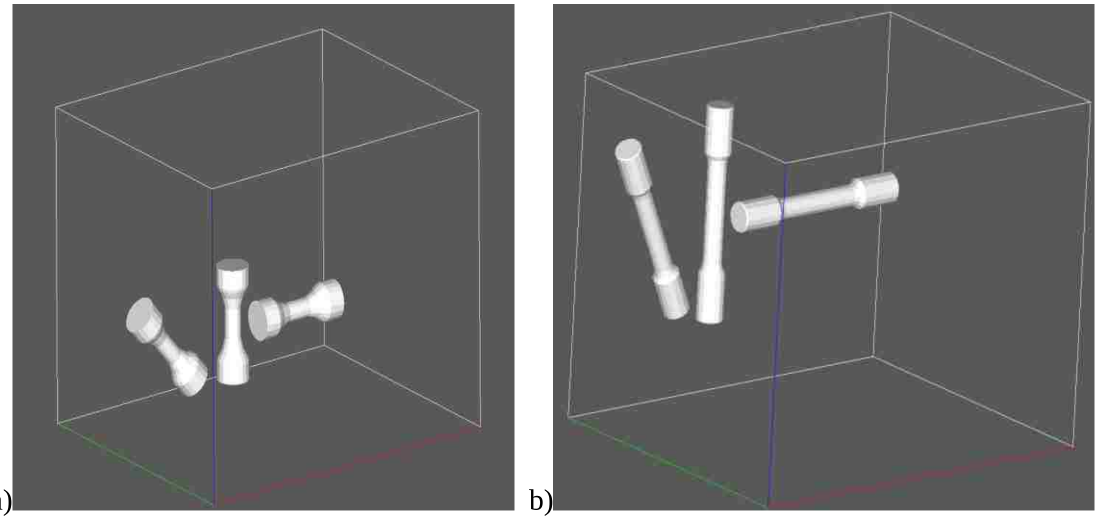
a) b)

Figure 19 Orientation of a) Compression and b)Tensile specimens

3.4 Analysis of Variance

The experiment and resultants are set up to perform an analysis of variance (ANOVA). This type of testing is used to further examine the results observed from changing the variables. An ANOVA is a way to compare experiments and determine if the variance in the resultant is significant in relation to the variance of the sample group. The knowledge from this testing provides statistical proof representing changes in the measured effects from that of the changes within the sample groups (Montgomery, 2009). For each of the different types of testing, tensile, compression and flexural, there are many specimens printed and tested. This included the combined 10 levels of infiltrate and the 3 build orientations. For each of the specific specimen type, there are replicates of at least three samples. Therefore, for each build direction of a specific test with a particular infiltrate type, had three specimens printed. The breakdown of the levels and samples can be seen in Table 15. For each of the samples, data was collected and analyzed for absorption depth. The measured results are used to compare and correlate the results from the applied test conducted.

Infiltrate	
Base	Levels
Control	1
Cyanoacrylate	1
Epsom Salt Mixture	1
	2
Epoxy	1
	2
Polyurethane Glue	1
	2
2 Phase	1
	2
	10 Total

Specimen Building	
Orientation	Levels
Vertical	1
Horizontal	1
45 Deg.	1
	3 Total

Test / Specimen	
Type	Levels
Tensile	1
Compression	1
Flexural	1
	3 Total

Table 15 Specimen Variable Breakdown

3.5 Curve fitting response characteristics

The second part of this project is to evaluate if the mechanical characteristics of the material can be confidently predicted. To accomplish this, each of the infiltrated specimens has their stress-strain curve analysed and fitted with the similar curves. By adding the infiltrate, the mechanical strength changed, and so did its reaction to the forces. This curve fitting aids in the understanding and predicting of the materials reaction within the bonded curve boundaries. The reaction trends of the infiltrates are compared to other known samples as well as other infiltrates within this study. The process of curve fitting for the deflection and reaction of the material can be seen below in Figure 20.

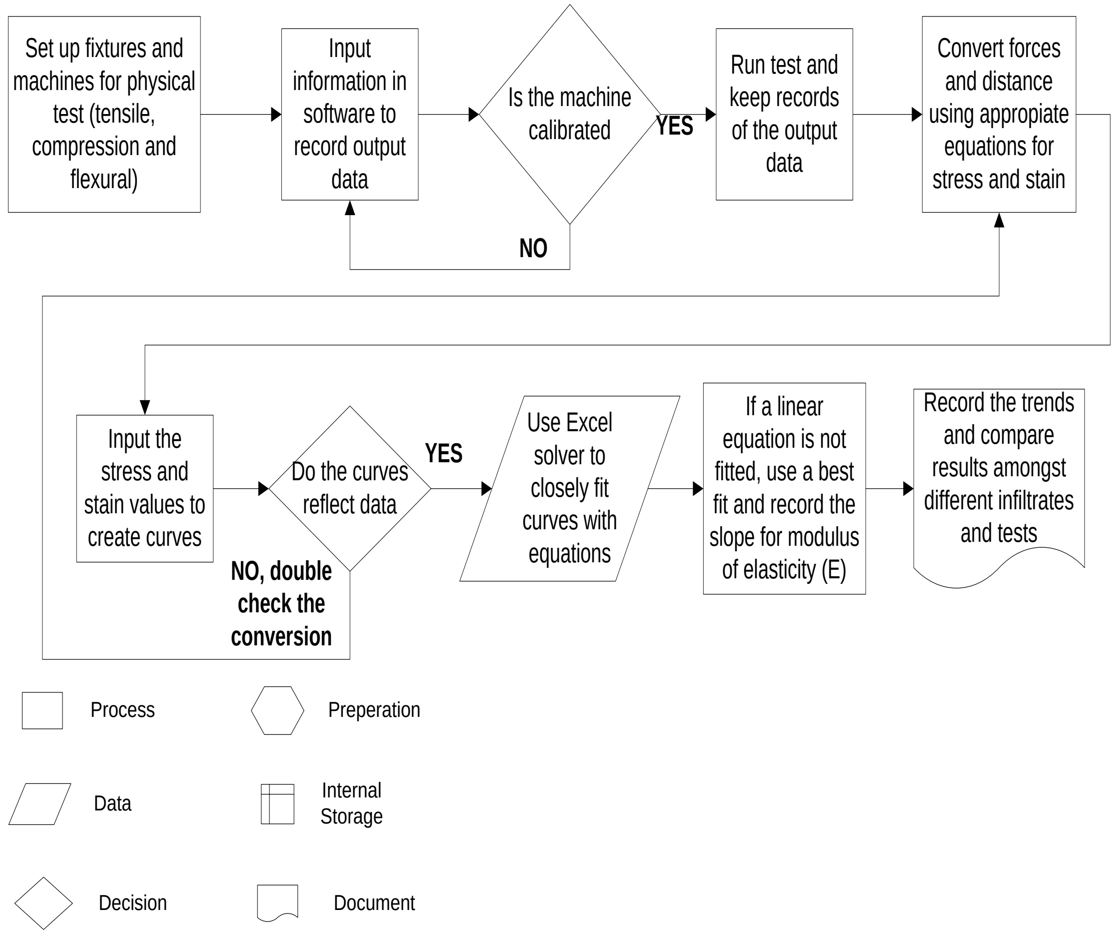

Figure 20 Process flow chart of Validation overview.

CHAPTER 4

PHYSICAL TESTING - TENSILE

4.1 Test method

The tensile test was conducted at the University of Windsor on a MTS Criterion Model 43. The results from the testing were prepared from the accompanied software, MTS Test Suite Elite. To observe the tensile strength of the material, prepared specimens were set up in the machine between two grips, the machine set-up for tensile testing. The top grip of the fixture, the crosshead, extends the specimen at the steady rate until the equipment and software observed a drop in load resistance. The drop in load resistance signifies that the specimen fractured. An illustration of the set-up with labels can be referred to in Figure 21.

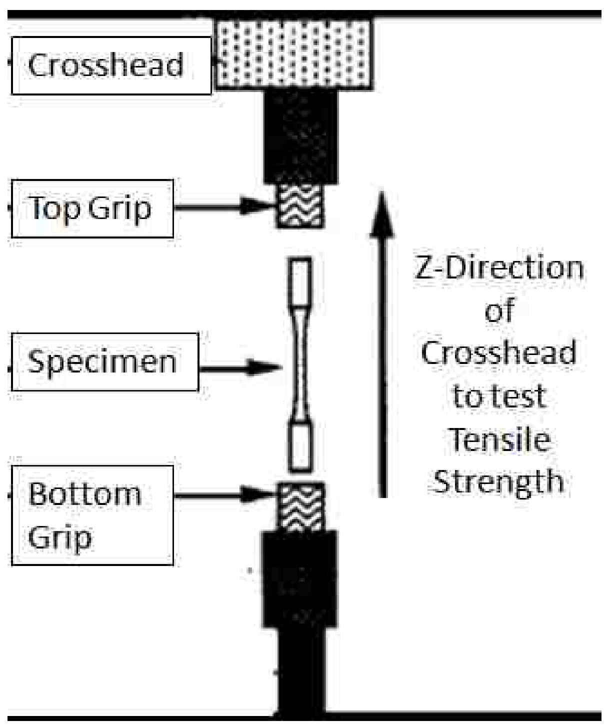

Figure 21 Illustration of the set-up for tensile testing in the MTS machine

The grips are standard equipment which are controlled (open and close) hydraulically. They would normally lock on the thick end pieces of the specimen and held in place by the compressive gripping force of the chucks.

4.2 Tensile Samples

To date, there is no ASTM standard specimen geometry for a 3D printed part for tensile testing. The printed material is very brittle and could be represented as a ceramic. Therefore, the geometry used for testing was adapted from the standard C1273 − 05 (Reapproved 2010) which is "Tensile Strength of Monolithic Advanced Ceramics at Ambient Temperatures1". The original geometry for the standard is illustrated in Figure 22.

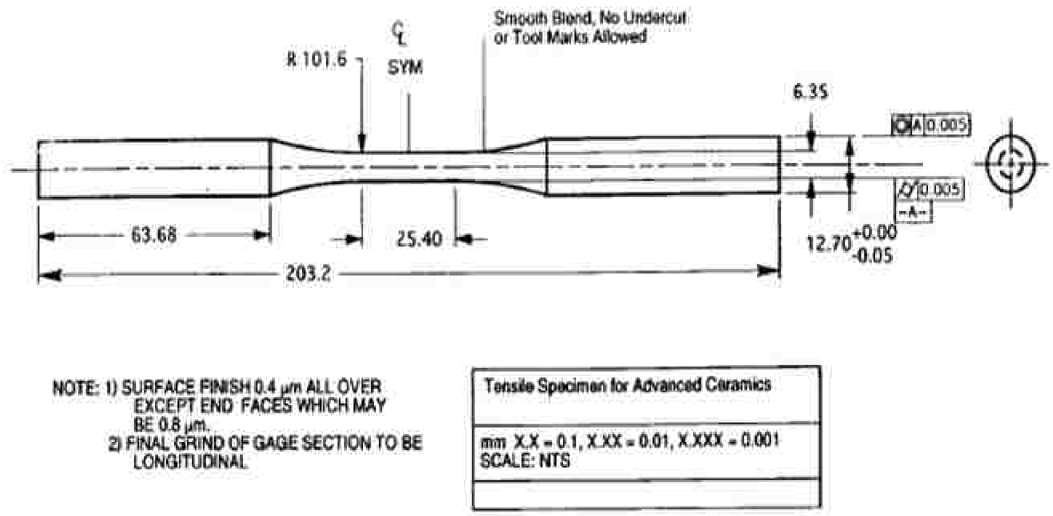

Figure 22 Example of a cylinderical, tensile specimen (adapted from ASTM std. C1273)

While the above is straight from the specific standard, and first iterations were produced with alterations, another standard geometry was observed to closely resemble the proposed new geometry. Therefore, to keep more commonality with a given standard, the specimen in this study uses the exact dimensions of specimen number 3 of the standard methods for "Tension Testing Wrought and Cast Aluminum – and Magnesium – Alloy Products". Specimen 3 and all the other specimen sizes and dimensions are illustrated in Appendix A.

The new geometry for the specimens was rendered using NX-ideas and saved in an .stl format that was later imported into the Z-printer software, which is illustrated in Figure 23.

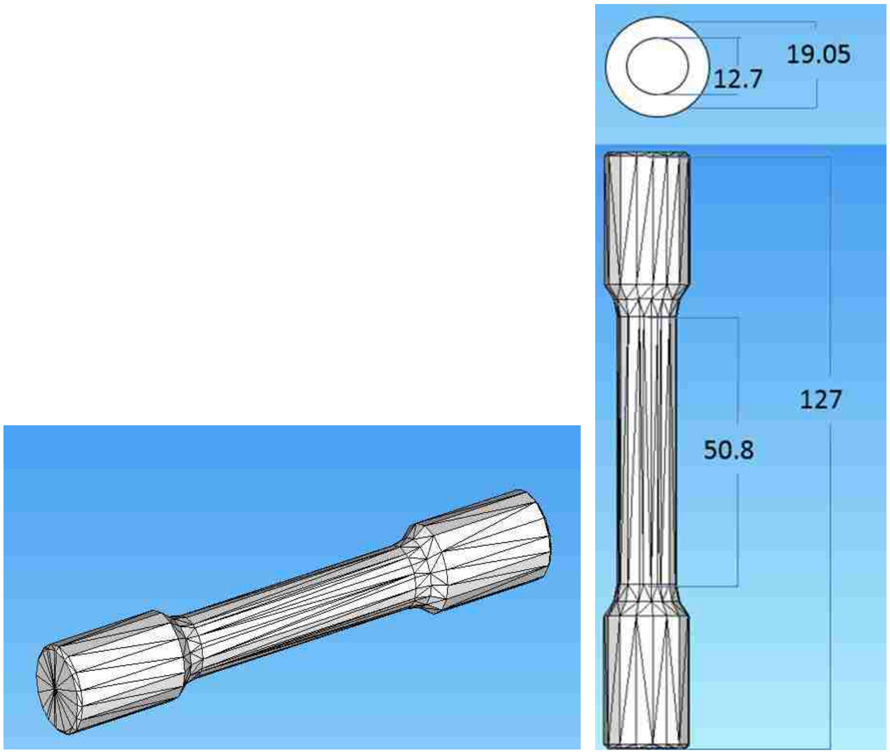

Figure 23 Illustration of the tensile specimens rendered in NX-Ideas

The specimens were post processed with not only their build direction but with their planned infiltrate type and duration. Illustrated in Table 16 below are the specimen types that were built with regards to infiltrate, corresponding type code and the build direction.

Infiltrate					
Infiltrate	Type Code	Build Direction			
		Horizontal (0°)		Angle (45°)	Vertical (90°)
		X	Y		
Control	C	2	2	3	3
Cyanoacrylate	B	2	2	3	3
Epsom Salt Mixture	S1	2	2	3	3
	S2	2	2	3	3
Epoxy	R1	2	2	3	3
	R2	2	2	3	3
Polyurethane Glue	P1	2	2	3	3
	P2	2	2	3	3
2 Phase	S1b	2	2	3	3
	S2b	2	2	3	3

Table 16 Infiltration and build breakdown for tensile specimens

4.3 Special Fixture

A specific setup was required for tensile testing as the material was observed to be too fragile. When using a few test pieces to finalize the set-up, it was noted that the force used to grip the part for the experiment was crushing the material and with less force applied, the specimen would slip within the jaws of the gripper. Therefore, a fixture was made so that the part would not break during the clamping but still allow the specimen to have the force applied to pull the part to fracture within the test area. A novel fixture was made for both ends of the specimen using copper pipe fittings (male and female adapters). Copper fittings were used for the variety of sizes available and for the ease of cutting compared to other material. The exploded view of the fixture is illustrated in Figure 24.

Figure 24 Parts and full assembly of tensile specimen holding fixtures

The male end adapter has two different inner diameters (¾" and ½"). Once cut in half, its shape could accommodate the small diameter of the test area while the larger diameter accommodated the end sections. The transition between the two diameters was at a radius similar to the one used in the specimen creation. This transition radius would be the part of the fixture that would be “pulling” the specimen when the force is applied. The female end was used to secure the male fitting together with the specimen. To finish of the fixture, an aluminum cap was turned. The small diameter section was feed through the female end while the large diameter was seated within the fitting. The protruding aluminum end stock was used as the stock to the machine’s grippers. Aluminum was used for the gripping stock because previous methods using wood and copper would not withstand perform well under continuous cycles of the clamping forces. A picture of tensile test being conducted using the specimen holding fixtures can be seen in Figure 25.

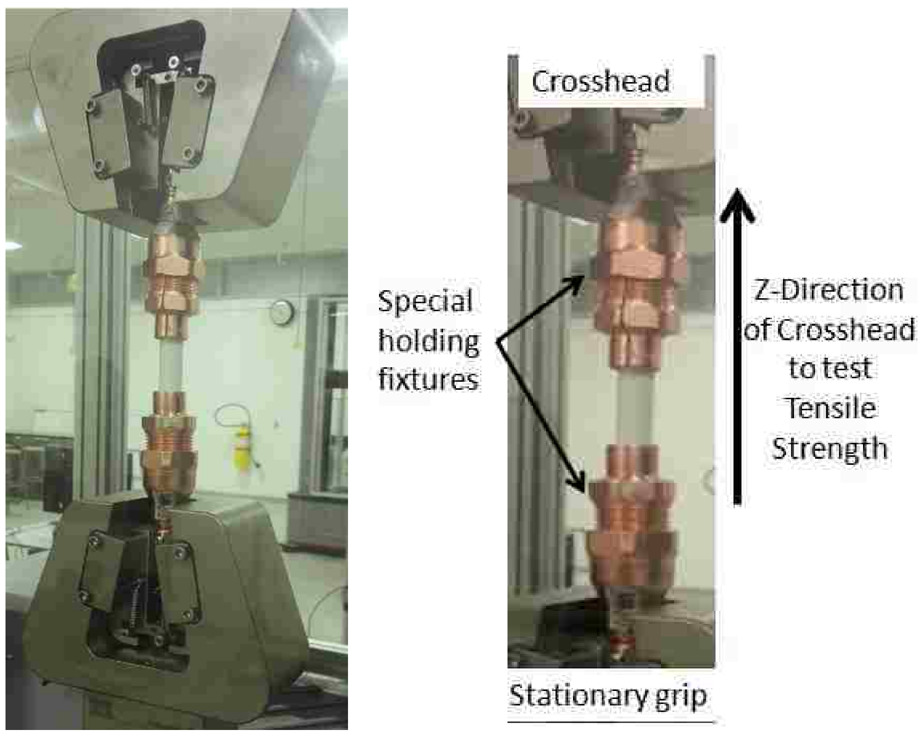

Figure 25 Special holding fixture is machine and details called out

4.4 Results

The results associated with the strength and stresses of the specimens were retrieved from the test run data of the specific specimen. The testing software produced a table with three columns: measured force (kN), crosshead distance traveled (mm), and elapsed time (seconds). An example of the readout can be seen in Appendix B. This test run data was then used for stress calculations and graphs.

4.4.1 Tensile Stress

The tensile tests were run until the specimen was observed to be at critical failure. The crosshead with top grip would ascend gradually until the software would observe a sudden drop in the recorded force by the transducer. Illustrated in Figure 26, are examples of each of the different infiltrate types and how they are graphically represented, including recorded force and crosshead travel distance and Figure 27 is a picture of a test specimen after critical failure.

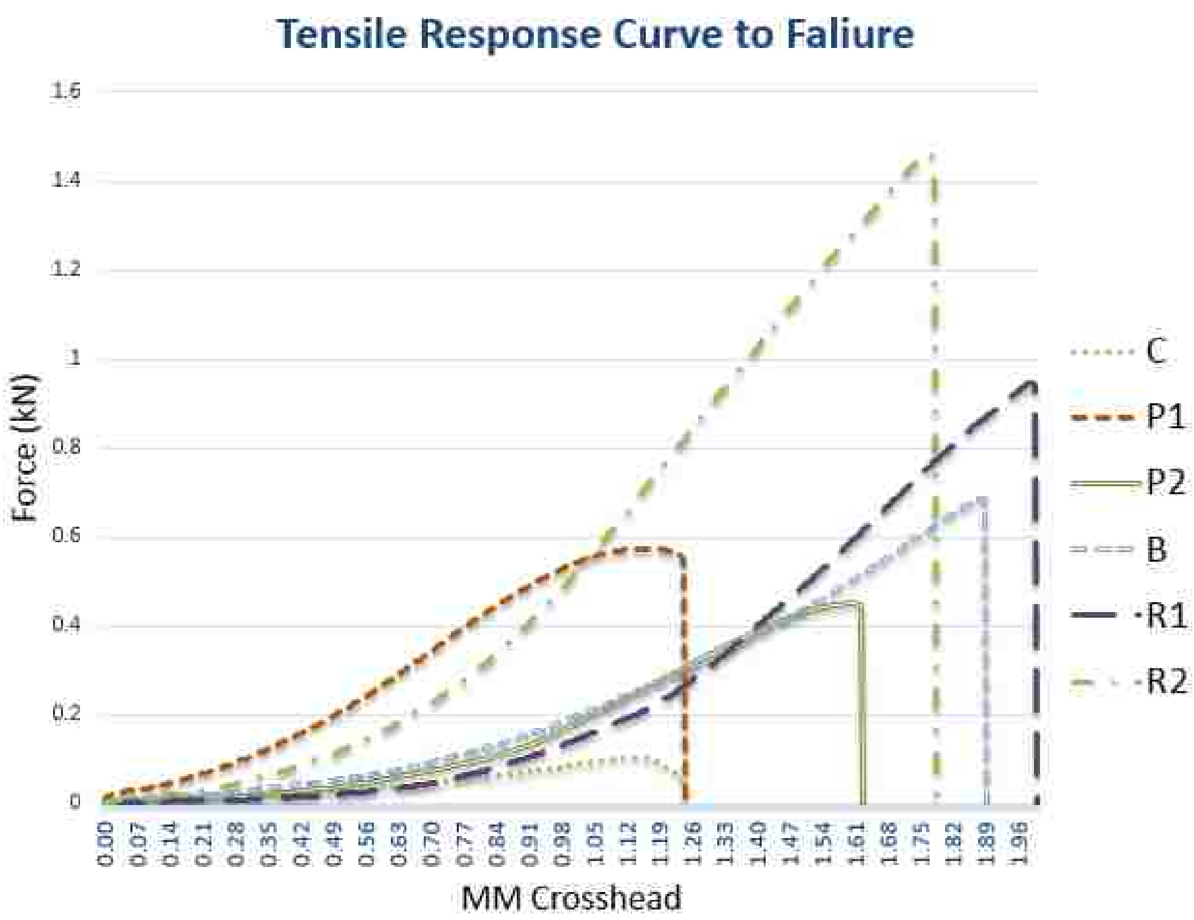

Tensile				
Infiltrate	Code	Run	Max Force (kN)	ΔX (mm)
Control	C	37	0.105	1.15
Epoxy	R1	72	0.947	1.99
	R2	48	1.461	1.77
Cyanoacrylate	B	19	0.687	1.89
Polyurethane	P1	22	0.575	1.16
	P2	89	0.451	1.60

Figure 26 Example of different infiltrate types and their response curves.

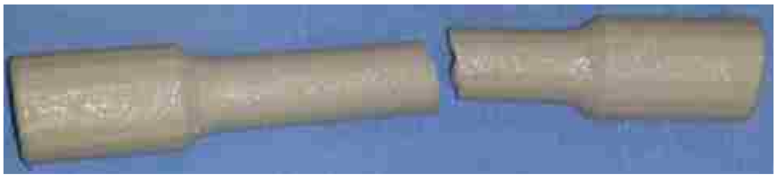

Figure 27 Tensile test specimen after critical failure

While there were many specimens tested for the different infiltrate types, the graph above has just one sample from each of the infiltrate types represented. This was needed to allow the graph to be readable and help to distinguish between the different line types. A graph produced with all the tensile test runs can be seen in Appendix C. The responses that were chosen were the tests runs of the different infiltrate types that recorded the highest applied force among its group. The legend of the graph included the line type, type code and the corresponding test run of the specimen.

The tensile strength for a uniaxially loaded rod specimen is calculated using the following equation;

$$S_u = \frac{P_{max}}{A}$$

S_u - Tensile Strength, MPa
P_{max} – Maximum force, N
A- Original Cross-sectional area, mm^2

$$A = \frac{\pi d^2}{4}$$

d – Average diameter of gauge section

Equation 1 Tensile Strength for round cross-section

The maximum strength of the specimens was determined from the highest point on the response curve. These results from the test runs were then grouped within their respective infiltrate type. Results from the tensile tests, summarized in a boxplot in Figure 28, show an increase in strength with the application of infiltrates, as compared to the control. It is observed that the specimens with epoxy application, (R1 and R2), recorded the highest strengths.

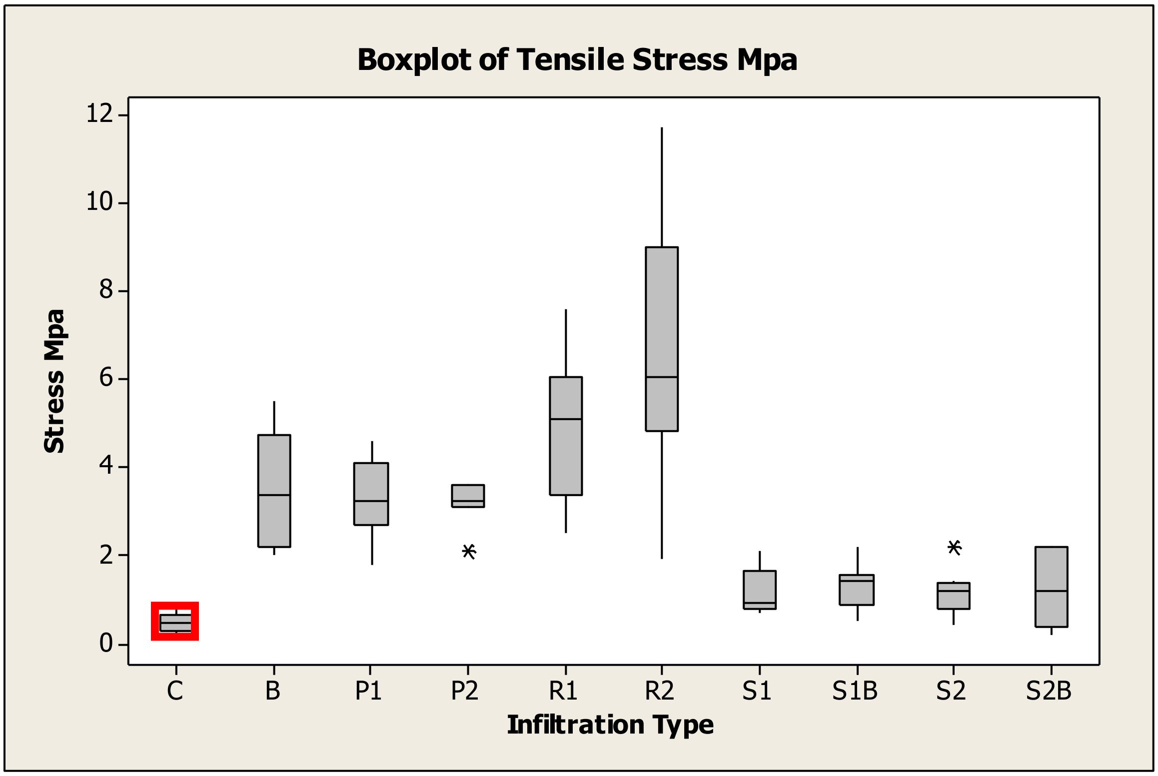

Figure 28 Boxplot results for tensile strength

It is clear that in the box plot, there is a large variation and spread within the categories of infiltration types. While there are some fluctuation between specimens of the same material, or in this case infiltration type, this variation could be due to the different build directions that the part was printed. The average strengths observed for the infiltration types and build directions are represented below in Figure 29 with a bar graph.

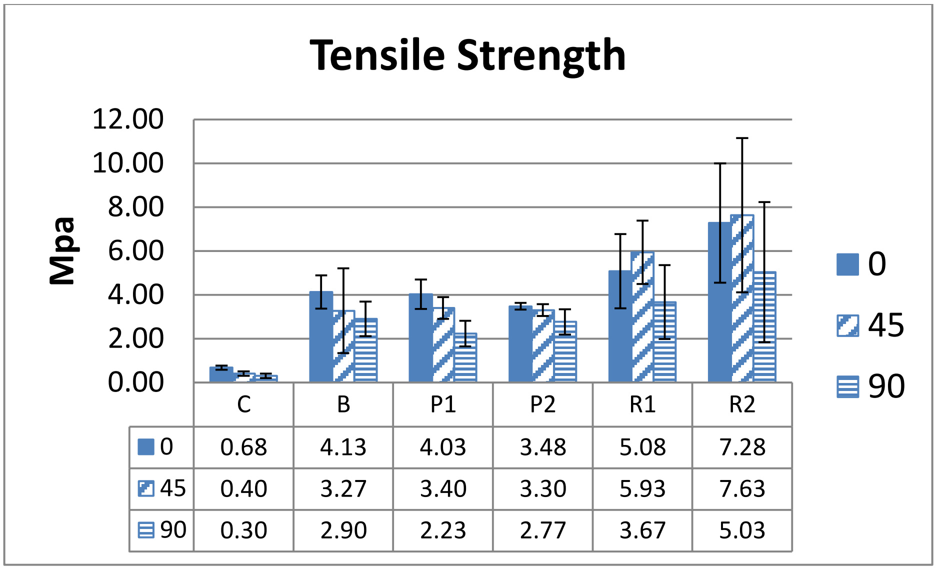

Figure 29 Average tensile strength observed for build direction

From the graph and the accompanied table it can be seen that while the epoxy specimens performed the best on average, they did not outperform the other infiltrates by a large margin. Besides the results from the 45° direction from the R1, the cyanoacrylate and both the polyurethanes had very similar results. It is interesting to note that each of the infiltrate types had the performance ranked as 0 °, 45° and then 90°, expect for the epoxy sets. They had the first and second inverted, 45° then 0° but still had the 90° build direction producing the weakest specimens within their set.

4.4.2 Underperforming Infiltrate types

The poor performing infiltrate types that were the salt mixtures and 2 phase types. As it is represented in the previous box plot, these 4 infiltration types did not perform well during the tensile testing. As illustrated in Figure 30, the underperforming specimens had similar tensile strength as the control.

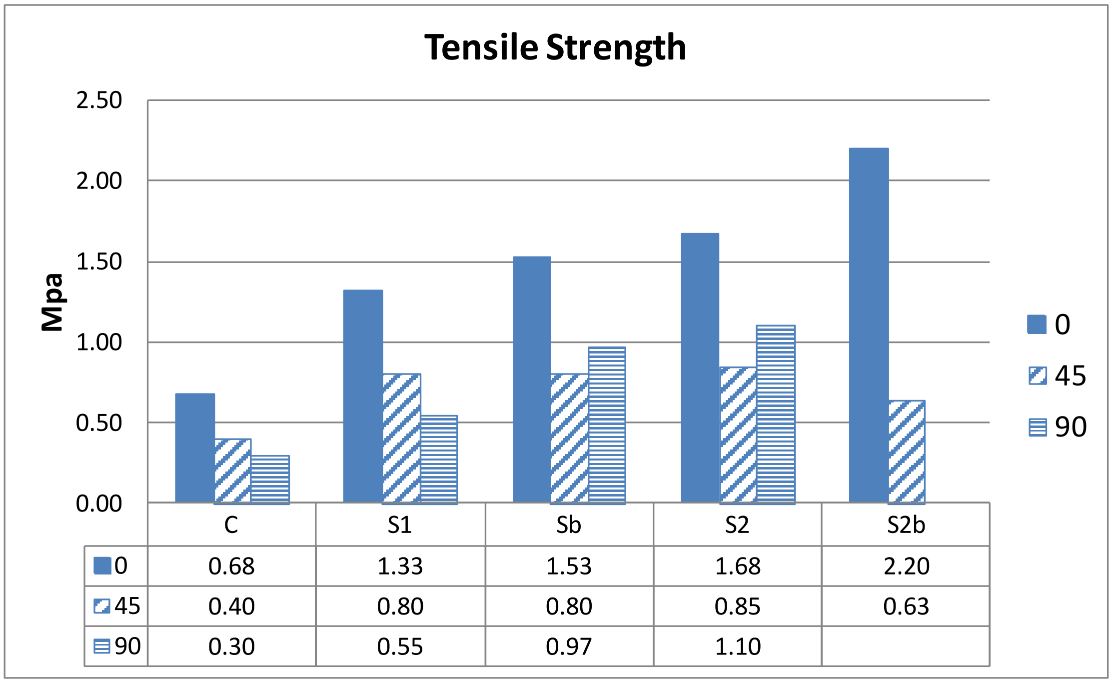

Figure 30 Average tensile strength observed for underperforming specimens

These parts were still very brittle and weak and either did not even outperform or barely outperformed the controlled material specimens that did not have any infiltrate. Some of these parts were also found to be warped. The part was fully saturated by the salt water and deformed while drying and is illustrated in Figure 31.

Figure 31 Deformed tensile specimen from salt mixture

The possible distortion of the parts after infiltration was not an outcome considered as it was not previously mentioned within literature. The studies by Yao & Tseng (2002) and Hsu & Lai (2010) analysed the dimensional stability and of the printed parts with respect to binder levels and layer thickness. Each study recommended optimal settings for printing parts based on a dimensional analysis of a green part. Neither of the studies took into consideration the impact and effects that the application of infiltrates have on the dimensional output. As seen in this study, and the above picture, infiltrates have an effect and should have been included into the studies.

4.4.3 Depth of Infiltration

The absorption depth of the infiltrate was measured for all the specimens. After the specimens were broke in the physical testing, they were cut with a small hacksaw and the observed depth was measured manually with a vernier caliper. The summary for the observed depths for the tensile tests are illustrated below in Figure 32.

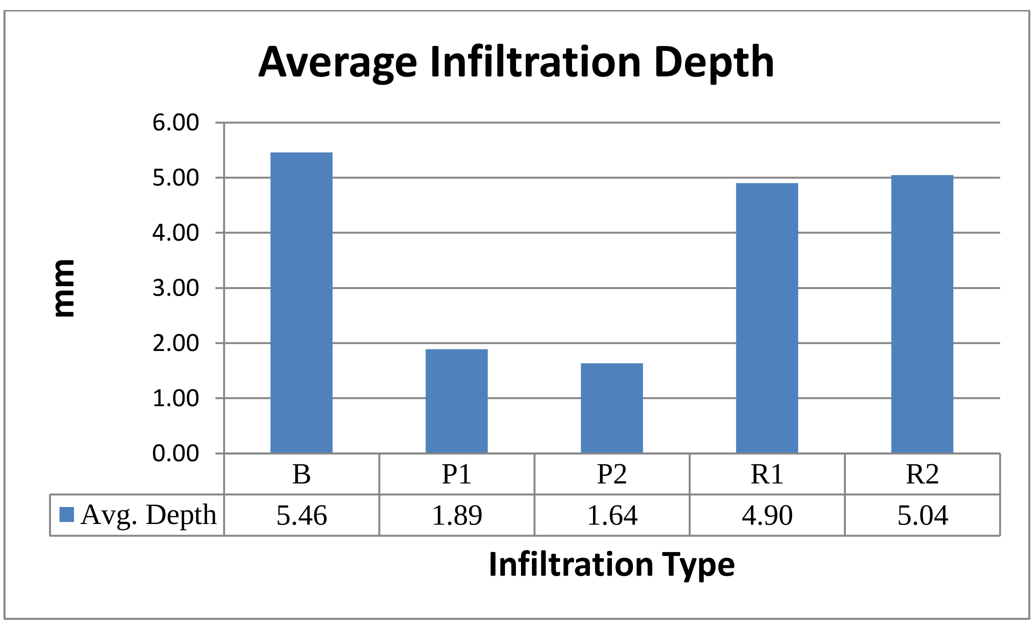

Figure 32 Average depth of infiltrate for tensile specimens

The cyanoacrylate and the epoxy sets recorded the deepest average absorption. The polyurethanes sets were much shallower. The absorption depths for the different application times are consistent with the hypothesis for the epoxy set. The R2, which had a longer application time, was observed to absorb more of the infiltrate. Alternatively in the polyurethane set, the average absorption was measured with a greater depth with the specimens that did not have the extra oven time. It was assumed that by putting the specimen in the oven after application, the heat would make the material more viscous and able to penetrate deeper.

While examining the absorption depths more closely, the infiltrate types were broken down into their respective build directions. The results are summarized in Figure 33.

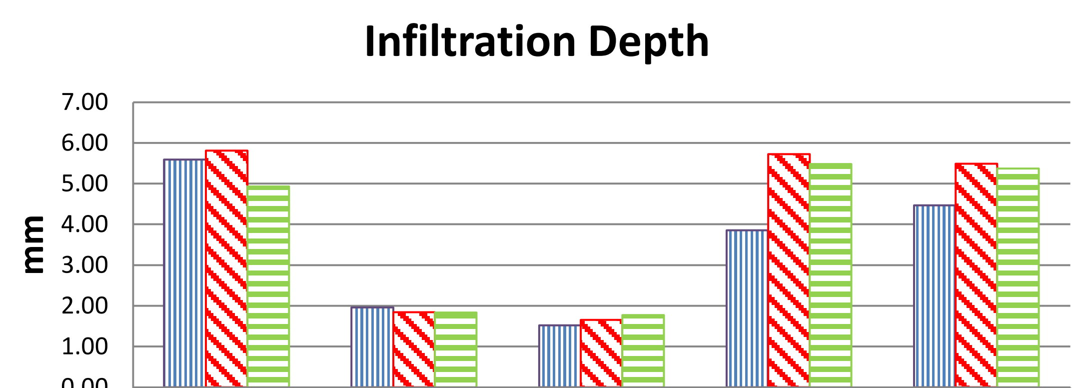

	B	P1	P2	R1	R2
0	5.59	1.96	1.52	3.85	4.47
45	5.81	1.85	1.65	5.72	5.49
90	4.93	1.84	1.77	5.48	5.37

Figure 33 Average depth of infiltrate with build direction, for tensile specimens

There are minor differences in absorption depths within the infiltrate sets. The largest differences were observed within the epoxy set, specifically the 0° horizontal direction. This direction produced the shallowest absorption depth of the three build directions for both of the types. The two polyurethane sets produced similar absorption depths. Having the depths similar disproves the hypothesis that when P2 was heated in the oven after application, a deeper absorption would be the result. It was also observed that the deeper the infiltrate was absorbed, the stronger the specimen was. As that could be the case, it is clear to suggest that there are more factors involved than just the infiltrate depth. An example of this could be seen with the lower absorption of the epoxy set in the 0° horizontal build direction. While a significant shallower depth was observed, the strength of those specimens was observed to be much higher than the 90° vertical build direction.

4.5 Observations and Summary

It was observed that there were differences among the specimens and their tensile test run recordings and measurements. Aside from reporting the raw data, the unbalanced data sets were analyzed within the Minitab software using a general linear model, one way ANOVA and the Tukey grouping method to see if the variables had a significant effect on the measured outcome. The first factors analysed were all the infiltrate types and their respective orientations and comparing their effect on the measured stress of the specimen. The P-value of these variables, as see in Table 17, are .000 and .004 respectively. With reference to values within ANOVAs, variable with a P-value less than or equal to .05 would indicate that it would have a significant effect of the outcome. Therefore, it shows that both variables have a significant effect of on the tensile strength of the specimen.

General Linear Model: Stress Mpa versus Type, Orientation

Factor	Type	Levels	Values
Type	fixed	10	1, 2, 3, 4, 5, 6, 8, 9, 10, 11
Orientation	fixed	3	1, 2, 3

Analysis of Variance for Stress Mpa, using Adjusted SS for Tests

Source	DF	Seq SS	Adj SS	Adj MS	F	P
Type	9	331.819	338.552	37.617	24.12	0.000
Orientation	2	18.817	18.817	9.408	6.03	0.004
Error	77	120.089	120.089	1.560		
Total	88	470.725				

S = 1.24884   R-Sq = 74.49%   R-Sq(adj) = 70.84%

Table 17 ANOVA table: Tensile stress vs. all infiltrate types and build orientations

These results were for all the specimens and test runs conducted during the experiment. It was noted earlier that there were some of the infiltrate types that were tests underperformed. These underperforming infiltrate types were omitted from some of the graphs and results because they added noise and confusion. They were deemed underperforming as they were grouped together with the control during the Tukey method. Illustrated in Table 18, they are grouped together which identifies that there is not a significant difference between the results for the types which includes the control.

```
Grouping Information Using Tukey Method

Type   N   Mean  Grouping
  6   10  6.710  A
  5   10  4.910  A B
  2   10  3.500    B C
  3   10  3.300    B C D
  4   10  3.210    B C D E
  9    9  1.300          E F
 11    5  1.260      C D E F
 10    9  1.178            F
  8    6  1.150        D E F
  1   10  0.480            F

Means that do not share a letter are significantly different.


Tukey 95% Simultaneous Confidence Intervals
All Pairwise Comparisons among Levels of Type

Individual confidence level = 99.83%
```

Legend	
1	Control
2	Cyancrylate
3	Polyurethane (1)
4	Polyurethane (2)
5	Epoxy (1)
6	Epoxy (2)
7	Epoxy (Rg)
8	Salt (1)
9	Salt (1)B
10	Salt (2)
11	Salt (2)B

Table 18 Underperforming tensile types - Tukey method

Therefore, the same could be examined for observing the significance. The comparisons were analysed again without the underperforming specimens and control. The new results still show that the type and orientation had a significant effect on the outcome, as illustrated in Table 19.

```
General Linear Model: Stress Mpa versus Orientation, Type

Factor       Type   Levels  Values
Orientation  fixed       3  1, 2, 3
Type         fixed       5  2, 3, 4, 5, 6


Analysis of Variance for Stress Mpa, using Adjusted SS for Tests

Source       DF   Seq SS   Adj SS  Adj MS     F      P
Orientation   2   21.753   21.753  10.877  4.35  0.019
Type          4   90.049   90.049  22.512  9.00  0.000
Error        43  107.594  107.594   2.502
Total        49  219.396


S = 1.58183   R-Sq = 50.96%   R-Sq(adj) = 44.12%
```

Table 19 ANOVA table: Tensile stress vs. selected types at all orientations

The orientation now indicates less significance than with all the sets. As mentioned earlier in the results, most of the directions had a similar trend, except the epoxy sets. With a smaller number of specimens in the analysis, the epoxy sets were able to shift the results for significance.

To compare the absorptions depths, the measured results were grouped into 9 different levels. The first level represented the minimum that could be measured, as it is the observed depth of the binder shell on the part. The subsequent levels were groups within .025" intervals as summarized in Table 20.

Level	Depth (inch)
1	0 - 0.050
2	.051 - 0.075
3	.076 - 0.100
4	.101 - 0.125
5	.126 - 0.150
6	.151 - 0.175
7	.176 - 0.200
8	.201 - 0.225
9	.226 - 0.250

Table 20 Group intervals used for infiltration depth levels

The results from analysing the absorption depth as a factor were similar to those of the orientation. While using all the results from the specimen test runs and infiltrate types, it was observed, and illustrated in Table 21A that the absorption depth of the infiltrate was significant.

After removing the underperforming infiltrate types, the resultant still show that the absorption depth is a significant factor. The new results summary can be observed below in Table 21B.

A)

General Linear Model: Stress Mpa versus Depth c

Factor	Type	Levels	Values
Depth c	fixed	9	1, 2, 3, 4, 5, 6, 7, 8, 9

Analysis of Variance for Stress Mpa, using Adjusted SS for Tests

Source	DF	Seq SS	Adj SS	Adj MS	F	P
Depth c	8	307.484	307.484	38.435	18.8	0.000
Error	80	163.241	163.241	2.041		
Total	88	470.725				

B)

General Linear Model: Stress Mpa versus Depth c

Factor	Type	Levels	Values
Depth c	fixed	8	2, 3, 4, 5, 6, 7, 8, 9

Analysis of Variance for Stress Mpa, using Adjusted SS for Tests

Source	DF	Seq SS	Adj SS	Adj MS	F	P
Depth c	7	69.942	69.942	9.992	2.81	0.017
Error	42	149.454	149.454	3.558		
Total	49	219.396				

S = 1.88638   R-Sq = 31.88%   R-Sq(adj) = 20.53%

Table **21** ANOVA table: Tensile stress vs. absorption depth A) All specimens B) Selected specimens

The new observations would more closely reflect the results of the absorption depths. The underperforming type all had the minimum recorded absorption depths and could have altered the test to show significance. While the depth as a factor showed less significant impact, it was the difference between the high strength and absorption depth of the epoxy verses the lower strength and absorption of the polyurethane types that impacted the significance. The absorption depth, while a significant factor cannot be used to confidently predict the strength of an infiltrated part. The type and build orientation have to be included when choosing a design. This is illustrated in Figure 36 with a scatter plot showing the average strength of the infiltrate type with the measured absorption depth of the specimen. Within the epoxy (R2), there is a strength and depth correlation with the angled and horizontal build directions. This is only disrupted by the significant lower strength of the vertical build direction with a deep absorption depth.

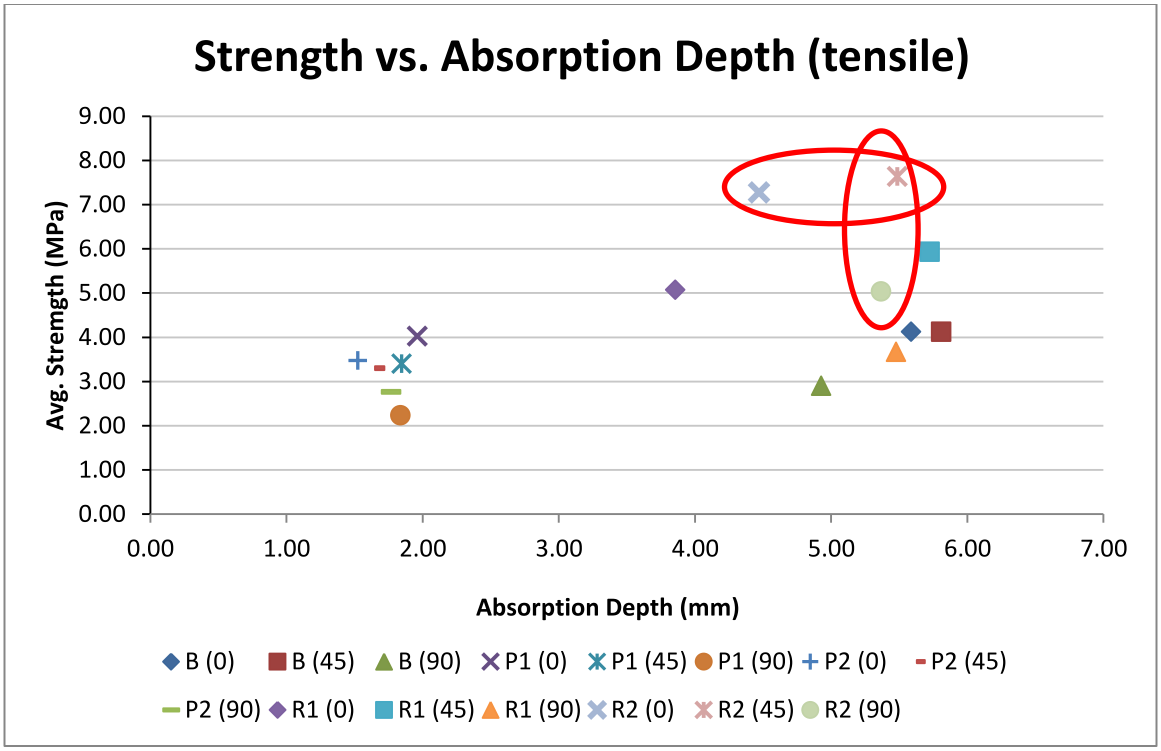

Figure 36 Strength vs. Absorption depth (tensile)

Orientation is a significant factor within the same infiltrate type. With the results of all the infiltrate types, it is safe to say that while the ranks might have differed, it is clear that the 90° vertical build direction produces the lowest tensile strength regardless of the infiltrate type.

CHAPTER 5

PHYSICAL TESTING – COMPRESSION

5.1 Test method

To observe the compressive strength of the material, prepared specimens were set up into the machine between two plates, the machine set-up for compressive testing. The top plate of the fixture, the crosshead, would descend onto the specimen at the steady rate until the equipment and software observed a drop in load resistance. The drop in load resistance would signify that the specimen fractured. An illustration of the set-up with labels can be referred to in Figure 35.

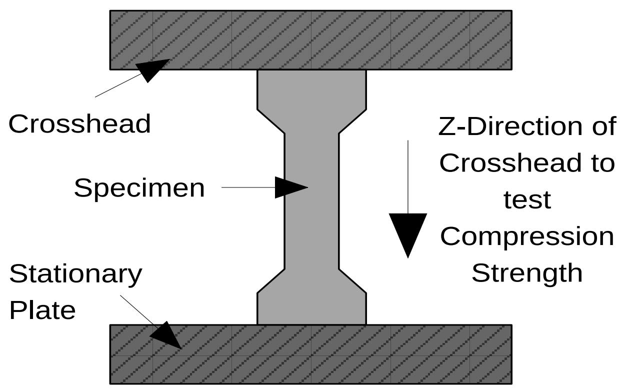

Figure 35 Illustration of the set-up for Compressive testing in the MTS machine

The plates are standard equipment which are ground flat and securely locked into the fixture. To run the test, the crosshead is manually lowered to the top of the specimen before the automated test could start.

5.2 Compression Samples

The specimens printed for the compressive test were specific to the testing. To date, there is no standard specimen geometry for printed part for compressive testing. The geometry used was an adaptation of a current ASTM standard. The printed material is very brittle and could be represented as a ceramic. Therefore, the geometry was adapted from the standard C1424 – 10 which is "Standard Test Method for Monotonic Compressive Strength of Advanced Ceramics at Ambient Temperature1". The original geometry for the standard is illustrated in Figure 36.

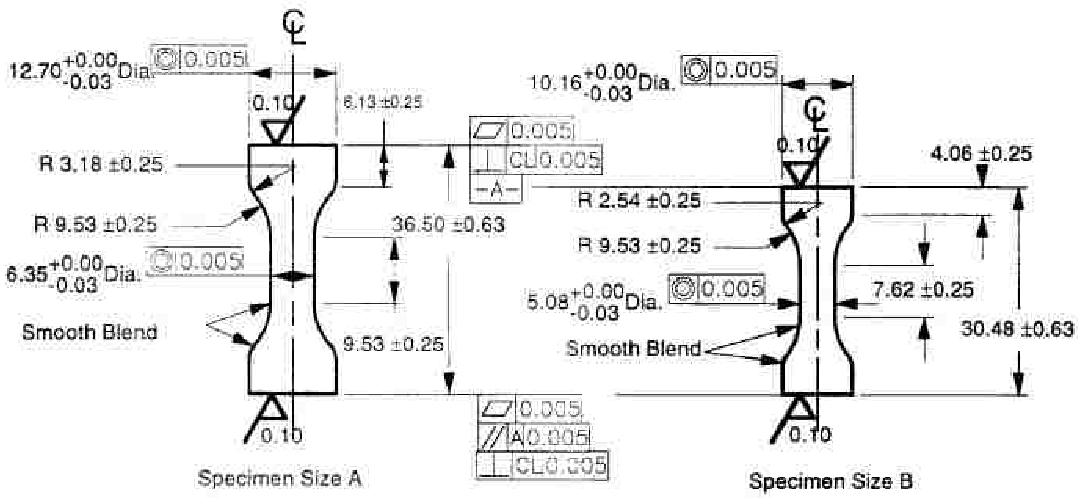

Figure 36 Original geometry for compressive test specimen from ASTM C1424 – 10

The specimen size A was modified to include a 12.7 mm diameter within the gauge length. All other measurements, from specimen size A, were then enlarged double their original size to match the enlarging of the main diameter. The new geometry for the specimens was rendered using NX-ideas and saved in .stl format that was later imported into the Z-printer software, which is illustrated in Figure 37.

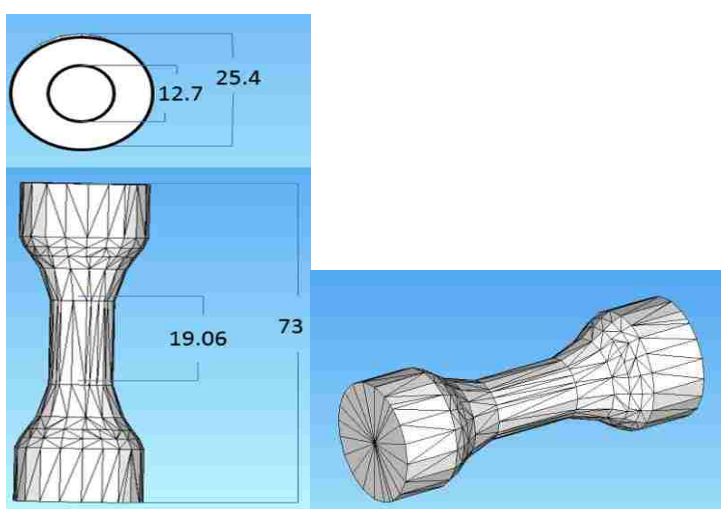

Figure 37 Illustrations of CAD representation of compression specimens within the Z-printer software

The specimens were post processed with not only their build direction but with their planned infiltrate type and duration. Illustrated in the Table 22 below are the specimen types that were built with regards to infiltrate, corresponding type code and the build direction.

Infiltrate					
Infiltrate	Type Code	Build Direction			
		Horizontal (0°)		Angle (45°)	Vertical (90°)
		X	Y		
Control	C	2	2	3	3
Cyanoacrylate	B	2	2	3	3
Epsom Salt Mixture	S1	2	2	3	3
	S2	2	2	3	3
Epoxy	R1	2	2	3	3
	R2	2	2	3	3
Polyurethane Glue	P1	2	2	3	3
	P2	2	2	3	3
2 Phase	S1b	2	2	3	3
	S2b	2	2	3	3

Table 22 Infiltration and build breakdown for tensile specimens

5.3 Results

Data collection for the compressive specimens were performed within the MTS software and manually measured by the author. The results associated with the strength and stress of the specimens were retrieved from the test run data of the specific specimen. The testing software produced a table with three columns: measured force (kN), crosshead distance traveled (mm), and elapsed time (seconds). An example of the readout can be seen in Appendix D. This test run data was then used for stress calculations and graphs.

5.3.1 Compression Stress

The compressive tests were run until the specimen was observed to be at critical failure. The crosshead plate would descend gradually until the software would observe a sudden drop in the recorded force by the transducer. Illustrated in Figure 38 and summarized in Table 23, are examples of each of the different infiltrate types and how they are graphically represented, including recorded force and crosshead travel distance and Figure 39 is a picture of a test specimen after critical failure.

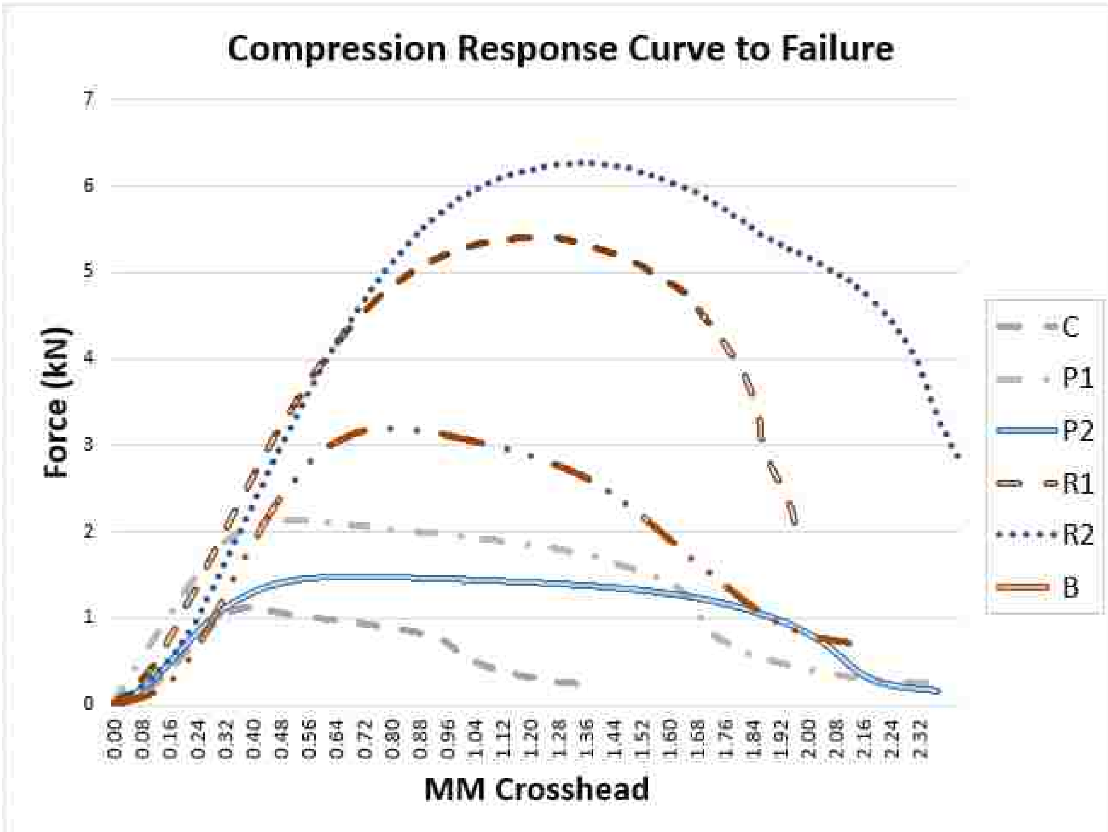

Figure 38 Example of different infiltrate types and their response curves.

Compression				
Infiltrate	Code	Run	Max Force (kN)	ΔX (mm)
Control	C	49	1.121	0.40
Epoxy	R1	37	5.405	1.22
	R2	27	6.264	1.35
Cyanoacrylate	B	90	3.205	0.79
Polyurethane	P1	30	2.131	0.53
	P2	19	1.485	0.72

Table 23 Example of different infiltrate types and their response curves.

Figure 39 Compression test specimen after critical failure

While there were many specimens tested for the different infiltrate types, the figure above includes just one sample from each of the infiltrate types. This was needed to allow the graph to be readable and help to distinguish between the different line types. A graph produced with all the compression test runs can be seen in Appendix E. The responses that were chosen were the tests runs of the different infiltrate types that recorded the highest applied force among its group. The legend of the graph included the line type, type code and the corresponding test run of the specimen.

The compression strength of the specimen is calculated using the following equation;

$$S_u = \frac{P_{max}}{A}$$

S_u - Compression Strength, MPa
P_{max} – Maximum force, N
A- Original Cross-sectional area, mm^2

$$A = \frac{\pi d^2}{4}$$

d – Average diameter of gauge section

Equation 2 Tensile Strength for round cross-section

The maximum strength of the specimens was determined from the highest point on the response curve. These results from the test runs were then grouped within their respective infiltrate type. Results from the compressive tests, summarized in a boxplot in Figure 40, show an increase in strength with the application of infiltrates, as compared to the control. It is observed that the specimens with epoxy application, (R1 and R2), recorded the highest strengths.

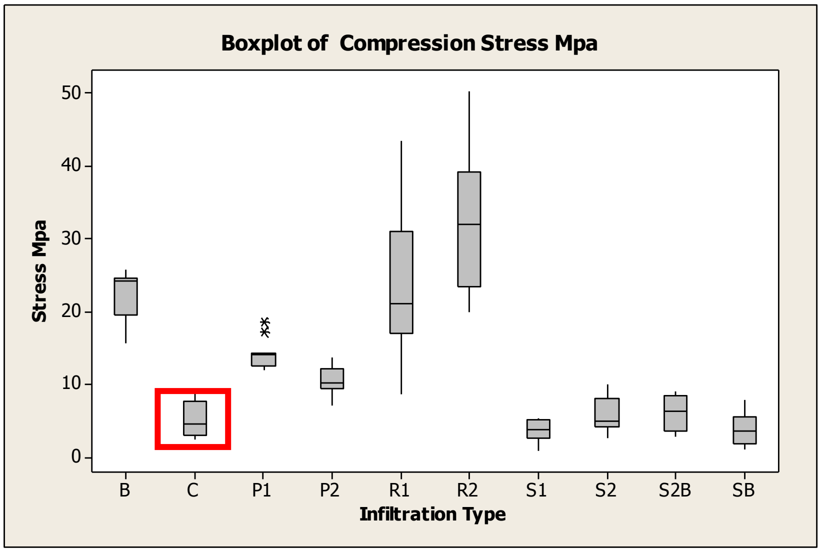

Figure 40 Boxplot of average compression strength

It is clear that in the box plot, there is a large variation and spread within the categories of infiltration types. While there are some fluctuation between specimens of the same material, or in this case infiltration type, this variation could be due to the different build directions that the part was printed. As mentioned before, there were three build directions for the compression specimens, the 0° (horizontal), the 45° (angular), and the 90° (vertical) direction. The average strengths observed for the infiltration types and build directions are represented below in Figure 41 with a bar graph.

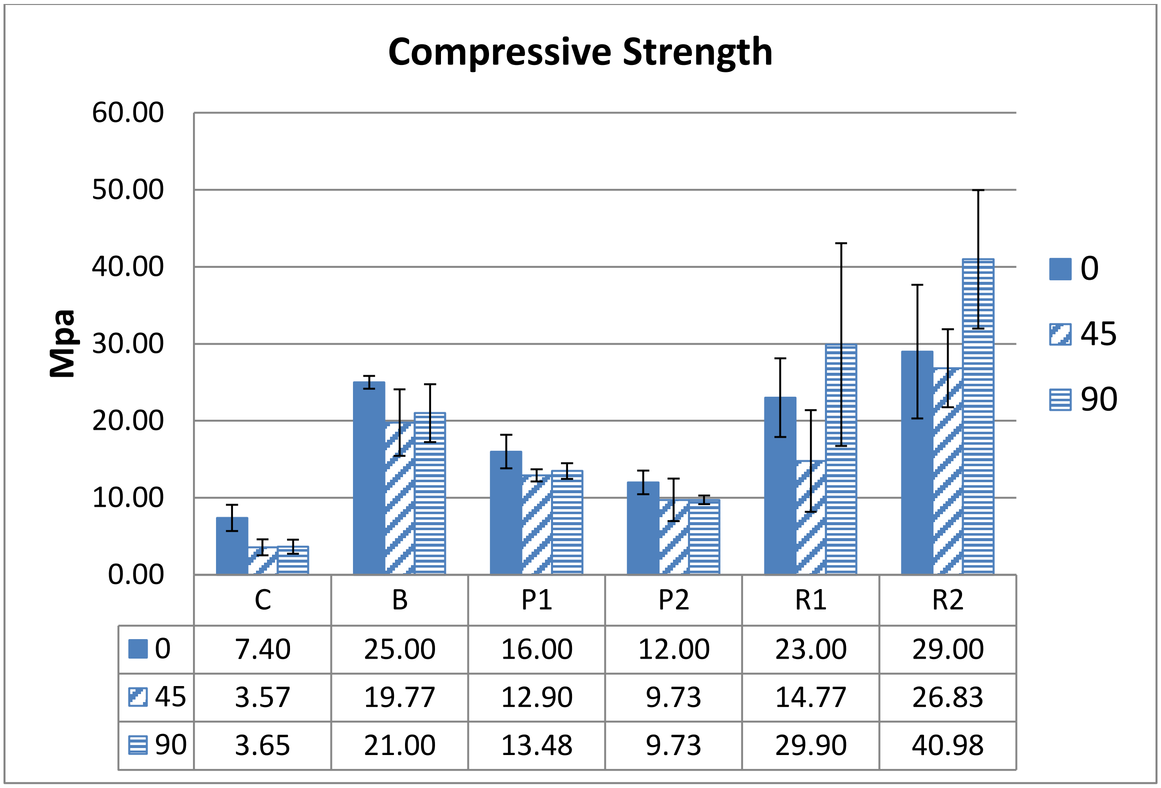

Figure 41 Bar graph of the observed compressive strength of different build directions

From the graph and the accompanied table it can be seen that while the epoxy specimens performed the best on average, the cyanoacrylate outperformed the low application time epoxy in 2 out of the 3 build directions. It is interesting to note that each of the infiltrate types had the performance ranked as 0 °, 90° and then 45°, expect for the epoxy sets. They had the first and second inverted, 90° then 0° but still had the 45° build direction producing the weakest specimens within their set.

5.3.2 Underperforming Infiltrate types

There are less infiltrate types represented in the above graph. The infiltrate types that were removed from the charts were the salt mixtures and 2 phase types. The grouping Tukey method, illustrated in Table 24, was used to show that these groups of infiltrates were not significantly different than the control infiltrate type.

```
Grouping Information Using Tukey Method

Type   N    Mean  Grouping
 6    11  32.664  A
 5    11  23.409    B
 2    11  22.127    B
 3    11  14.227      C
 4    10  10.500      C D
11     7   6.066        D
 9    11   5.909        D
 1    11   4.991        D
 8     9   3.778        D
10    10   3.750        D

Means that do not share a letter are significantly different.


Tukey 95% Simultaneous Confidence Intervals
All Pairwise Comparisons among Levels of Type

Individual confidence level = 99.84%
```

Legend	
1	Control
2	Cyancrylate
3	Polyurethane (1)
4	Polyurethane (2)
5	Epoxy (1)
6	Epoxy (2)
7	Epoxy (Rg)
8	Salt (1)
9	Salt (1)B
10	Salt (2)
11	Salt (2)B

Table 24 Underperforming compression types – Tukey method

Also sharing a letter is the polyurethane level 2. This infiltrate type was not taken out as it also shares a letter with the other polyurethane set which is found to be significantly different than the underperforming types.

5.3.3 Depth of Infiltration

The absorption depth of the infiltrate was measured for all the specimens. After the specimens were broke in the physical testing, they were cut with a small hacksaw and the observed depth was measured manually with a vernier caliper. The summary for the observed depths for the compression tests are illustrated below in Figure 42.

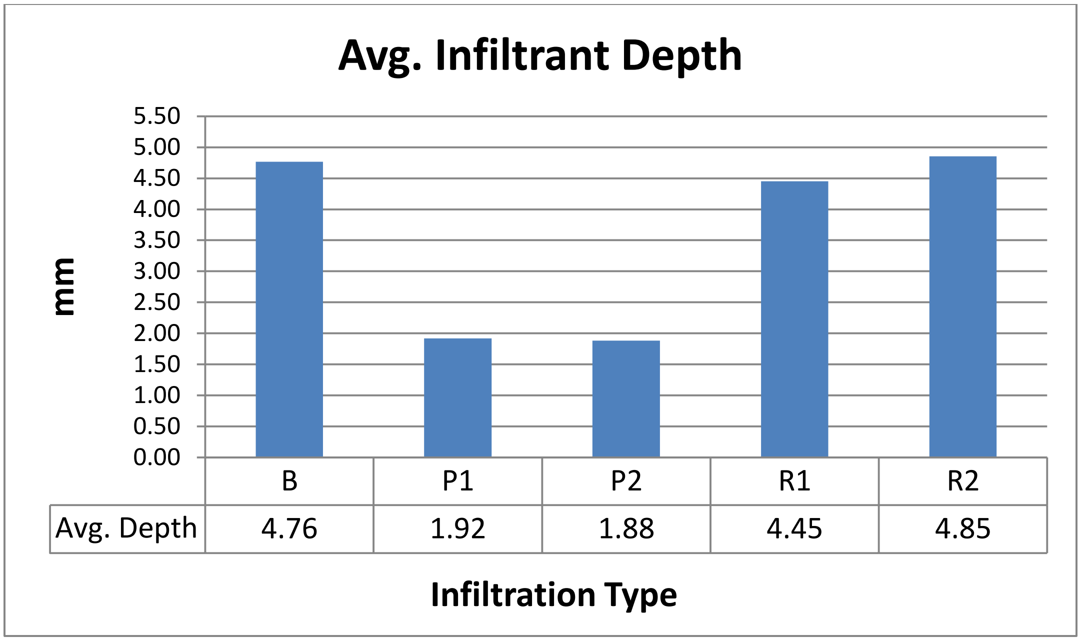

Figure 42 Observed absorption depths for the compression tests

The cyanoacrylate and the epoxy sets recorded the deepest average absorption. The polyurethanes sets were much shallower. The absorption depths for the different application times are consistent with the hypothesis for the epoxy set. The R2, which had a longer application time, was observed to absorb more of the infiltrate. Alternatively in the polyurethane set, the average absorption was measured with a greater depth with the specimens that did not have the extra oven time. It was assumed that by putting the specimen in the oven after application, the heat would make the material more viscous and able to penetrate deeper.

5.4 Observations and summary

It was observed that there were differences among the specimens and their tensile test run recordings and measurements. Aside from reporting the raw data, these unbalanced data sets were analyzed within the Minitab software using the general linear model and one way ANOVA to see if the variables had a significant effect on the measured outcomes. First item measured were all the build orientations and their respective infiltrate types and comparing their effect on the measured stress of the specimen. The P-value of these variables, as seen in Table 25, are .005 and .000 respectively. With reference to values within ANOVAs, a variable with a P-value less than or equal to .05 would indicate that it would have a significant effect of the outcome. Therefore, it shows that both variables have a significant effect on the compressive strength of the specimen.

General Linear Model: Stress Mpa versus Orientation, Type

Factor	Type	Levels	Values
Orientation	fixed	3	1, 2, 3
Type	fixed	10	1, 2, 3, 4, 5, 6, 8, 9, 10, 11

Analysis of Variance for Stress Mpa, using Adjusted SS for Tests

Source	DF	Seq SS	Adj SS	Adj MS	F	P
Orientation	2	272.03	274.09	137.05	5.70	0.005
Type	9	9650.38	9650.38	1072.26	44.61	0.000
Error	90	2163.11	2163.11	24.03		
Total	101	12085.52				

S = 4.90251 R-Sq = 82.10% R-Sq(adj) = 79.91%

Table 25 ANOVA table: Compressive stress vs. all types and orientations

These results were for all the specimens and test runs conducted during the experiment. It was noted earlier that there were some of the infiltrate types that were tests underperformed. These underperforming infiltrate types were omitted from some of the graphs and results because they added noise and confusion. Therefore, the same could be examined for observing the significance. The comparisons were analysed again without the underperforming specimens and control. The new results still show that the type and orientation had a significant effect on the outcome, as illustrated in Table 26.

General Linear Model: Stress Mpa versus Orientation, Type

Factor	Type	Levels	Values
Orientation	fixed	3	1, 2, 3
Type	fixed	5	2, 3, 4, 5, 6

Analysis of Variance for Stress Mpa, using Adjusted SS for Tests

Source	DF	Seq SS	Adj SS	Adj MS	F	P
Orientation	2	401.97	346.60	173.30	4.29	0.019
Type	4	3123.16	3123.16	780.79	19.35	0.000
Error	47	1896.66	1896.66	40.35		
Total	53	5421.79				

S = 6.35251 R-Sq = 65.02% R-Sq(adj) = 60.55%

Table 26 ANOVA table: Compressive stress vs. selected types at all orientations

The orientation now shows less significance than earlier. Even with a smaller number of specimens in the analysis, differences between the strength observed at the different orientation, especially the epoxy sets, were able to shift the results for significance.

To compare the absorptions depths, the measured results were grouped into 9 different levels. The first level represented the minimum that could be measured, as it is the observed depth of the binder shell on the part. The subsequent levels were groups within .025" intervals as summarized in Table 27A. The infiltrate types that were underperforming were not among the specimen sets compared. The resultant shows that depth is a significant factor. The results summary can be observed below in Table 27B.

A)

Level	Depth (inch)
1	0 - 0.050
2	.051 - 0.075
3	.076 - 0.100
4	.101 - 0.125
5	.126 - 0.150
6	.151 - 0.175
7	.176 - 0.200
8	.201 - 0.225
9	.226 - 0.250

B)

ANOVA: Stress Mpa versus Depth c

```
Factor   Type   Levels  Values
Depth c  fixed       8  2, 3, 4, 5, 6, 7, 8, 9


Analysis of Variance for Stress Mpa

Source   DF       SS      MS      F      P
Depth c   7  3717.34  531.05  14.33  0.000
Error    46  1704.45   37.05
Total    53  5421.79


S = 6.08714   R-Sq = 68.56%   R-Sq(adj) = 63.78%
```

Table 27 A) Infiltration and build breakdown for tensile specimens B) ANOVA table: Compressive stress vs. absorption depth

Unlike the tensile test, the specimens that were found to have the highest compressive strength also had the deepest infiltrate absorption. The epoxy sets and the cyanoacrylate were observed to have much higher results in both categories compared to the polyurethane. This is illustrated in the scatter plot of the specimen's strength with absorption depth in Figure 44.

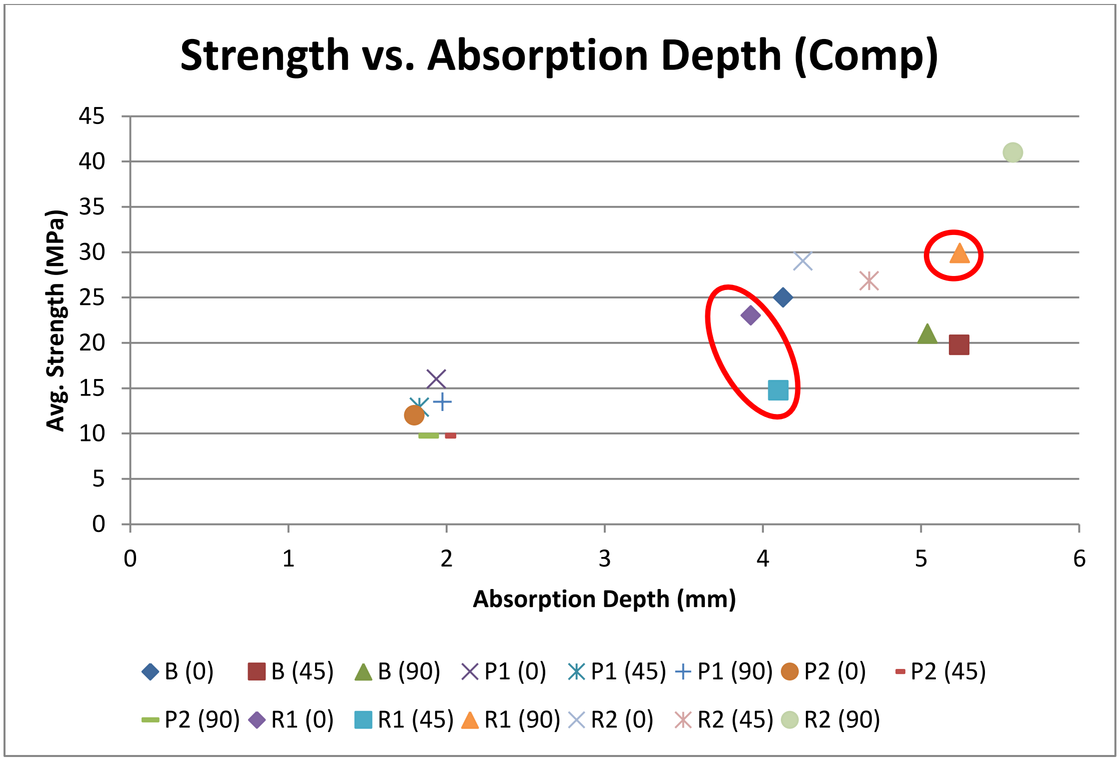

Figure 44 Strength vs. Absorption Depth (compression)

While the test shows that the deeper absorption was a significant effect, the results could also be reflective that the infiltrate type is a significant effect on the absorption as well as the strength. One observation is that while the ranks might have differed, it is clear that the 45° angle build direction produces the lowest compression strength regardless of the infiltrate type. This is made clear in the highlighted markers in the above plot. The epoxy (R1) has a linear correlation with depth and strength for the horizontal and vertical build but the angled build, while having similar absorption as the horizontal, is observed to be significantly weaker.

CHAPTER 6

PHYSICAL TESTING – FLEXURAL

6.1 Test method

The flexural test was conducted at the University of Windsor on a MTS Criterion Model 43. The results from the testing were prepared from the accompanied software, MTS Test Suite Elite. The flexural test method used was the three point bending method, and illustrated in Figure 45.

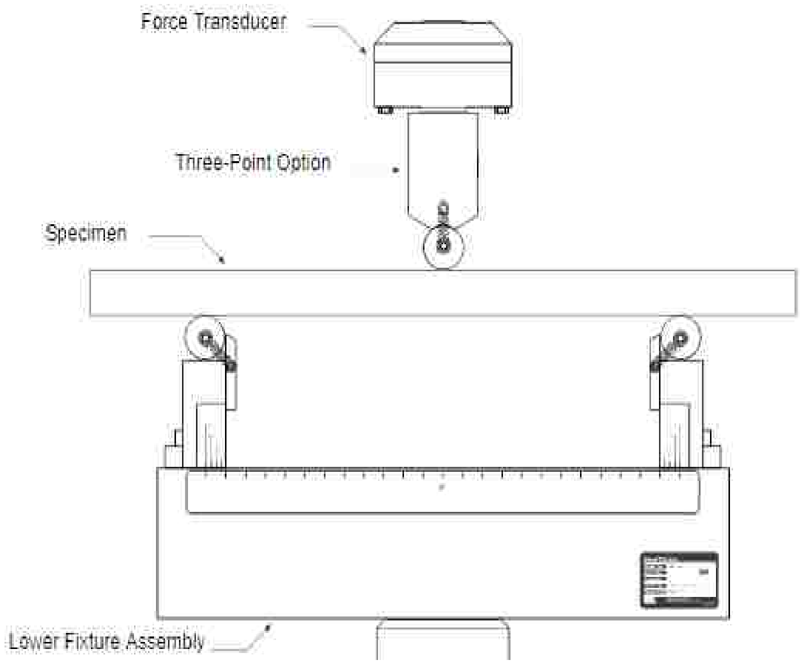

Figure 45 Illustration of fixture for three pint bending, adapted from (MTS, 2010)

The fixture for this method was the MTS Model 642.10B. The three points were comprised of 15mm rollers and the lower fixture rollers were spaced 7cm away from center, to the outside of the roller. This gave a span of 125mm between the centers of the rollers.

A rod shape specimen was used a test samples to keep consistent with other test conducted as the symmetry reduces the number of build orientations observable. The machine tested the samples by lowering the crosshead at a rate of 2mm/min onto the specimen that was places on top of the rollers. The specimens were 171mm which is long enough to have excess material over the rollers and no samples were pushed into the fixture because it was not long enough.

The machine's force transducer would descend, with the top roller, onto the specimen at the steady rate until the equipment and software observed a drop in load resistance. The drop in load resistance would signify that the specimen fractured.

6.2 Flexural Samples

There were two specimen sizes built for flexural testing. The geometry for the specimen was a rod shape, both 171.45mm long with diameters of 12.7mm and 19.05mm. The specimens were rendered using NX-ideas and saved in an .stl format and imported into the Z-printer software, which is illustrated in Figure 46.

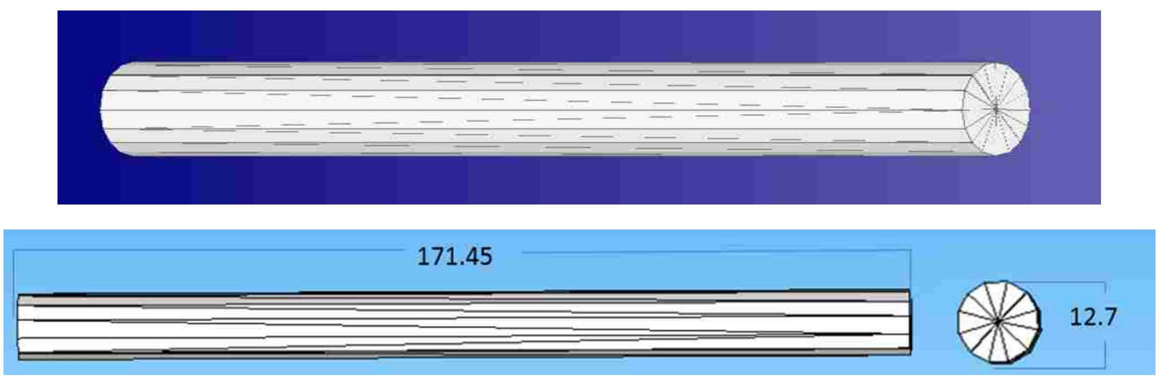

Figure 46 Illustration of CAD representation of Flexural specimen within Z-printer software.

Illustrated in the Table 28 below are specimen types that were built with regards to infiltrate, corresponding type code and the diameter.

Infiltrate			
Infiltrate	Type Code	Built Specimen	
		Small Dia.	Large Dia.
Control	C	Yes	Yes
Cyanoacrylate	B	Yes	Yes
Epsom Salt Mixture	S1	Yes	Yes
	S2	Yes	n/a
Epoxy	R1	Yes	Yes
	R2	Yes	n/a
	Rg	Yes	n/a
Polyurethane Glue	P1	Yes	Yes
	P2	Yes	n/a
2 Phase	S1b	Yes	n/a
	S2b	Yes	n/a

Table 28 Infiltration and build breakdown for tensile specimens

6.3 Results

Data collection for the flexural specimens were performed within the MTS software and manually measured by the author. The results associated with the strength and stresses of the specimens were retrieved from the test run data of the specific specimen. The testing software produced a table with three columns: measured force (kN), crosshead distance traveled (mm), and elapsed time (seconds). An example of the readout can be seen in Appendix F. This test run data was then used for stress calculations and graphs.

6.3.1 Flexural Stress

The flexural tests were run until the specimen was observed at critical failure. The top roller would descend gradually until the software would observe a sudden drop in the recorded force by the transducer. Illustrated in Figure 46 and summarized in Table 29, are examples of each of the different infiltrate types and how they are graphically represented, including recorded force and crosshead travel distance.

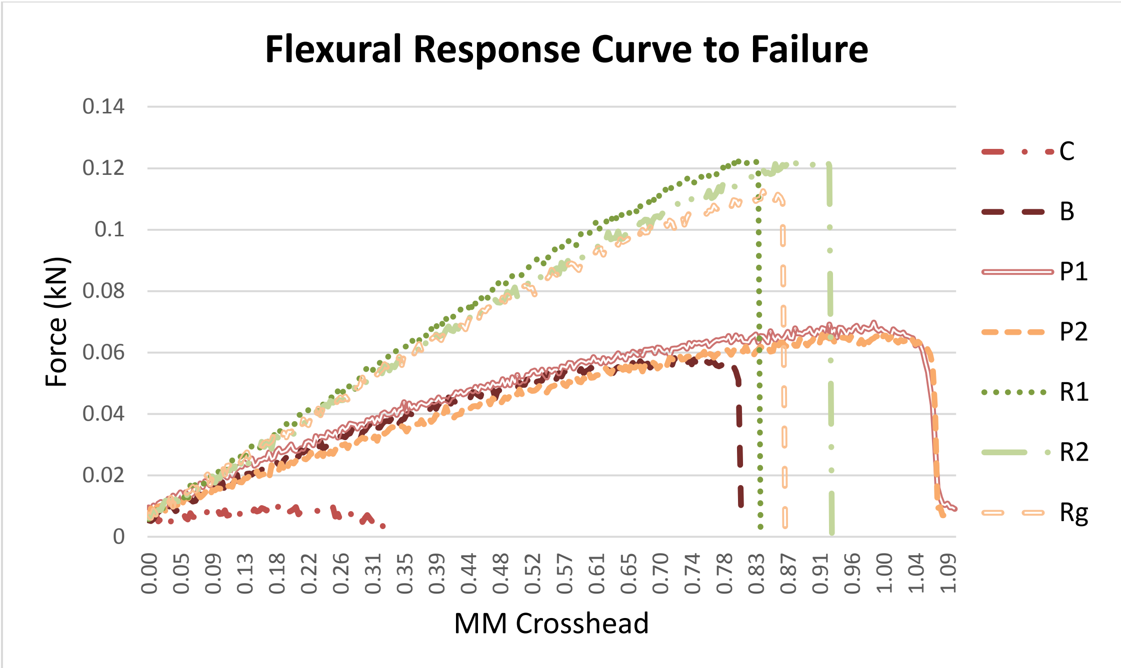

Figure 46 Example of different infiltrate types and their response curves - flexural.

Flexural				
Infiltrate	Code	Run	Max Force (kN)	ΔX (mm)
Control	C	3	0.010	0.19
Epoxy	R1	11	0.123	0.83
	R2	10	0.123	0.92
	Rg	27	0.113	0.84
Cyanoacrylate	B	28	0.059	0.75
Polyurethane	P1	6	0.070	0.99
	P2	20	0.066	1.01

Table 29 Summary of maximum results from response curve – flexural.

While there were many specimens tested for the different infiltrate types, the figure above includes just one sample from each of the infiltrate types. This was needed to allow the graph to be readable and help to distinguish between the different line types. A graph produced with all the flexural test runs can be seen in Appendix G. The responses that were chosen were the tests runs of the different infiltrate types that recorded the highest applied force among its group. The legend of the graph included the line type, type code and the corresponding test run of the specimen.

The flexural strength of the specimen is calculated using the following equation;

$$\sigma = \frac{8PL_o}{\pi D^3}$$

σ - Flexural Stress
P - Peak force observed
L_o - Length between rollers
D – Diameter of specimen

Equation 3 Flexural Strength for round cross-section

The maximum strength of the specimens was determined from the highest point on the response curve. The results from the test run were then grouped within their respective infiltrate type. The average strengths observed are represented below with bar graphs. Results from the flexural tests, summarized in a boxplot in Figure 47 and graph in Figure 48, show an increase in strength with the application of infiltrates, as compared to the control. It is observed that the specimens with epoxy application recorded the highest strengths.

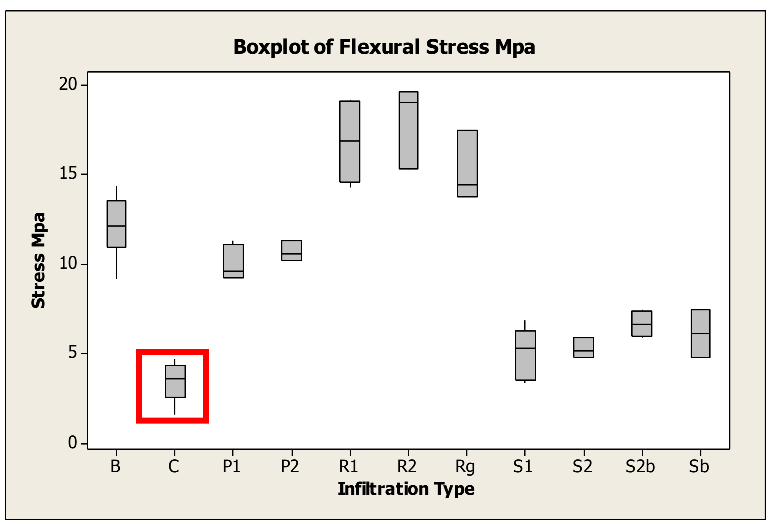

Figure 47 Bar graph illustrating the observed flexural strength of small diameter specimen

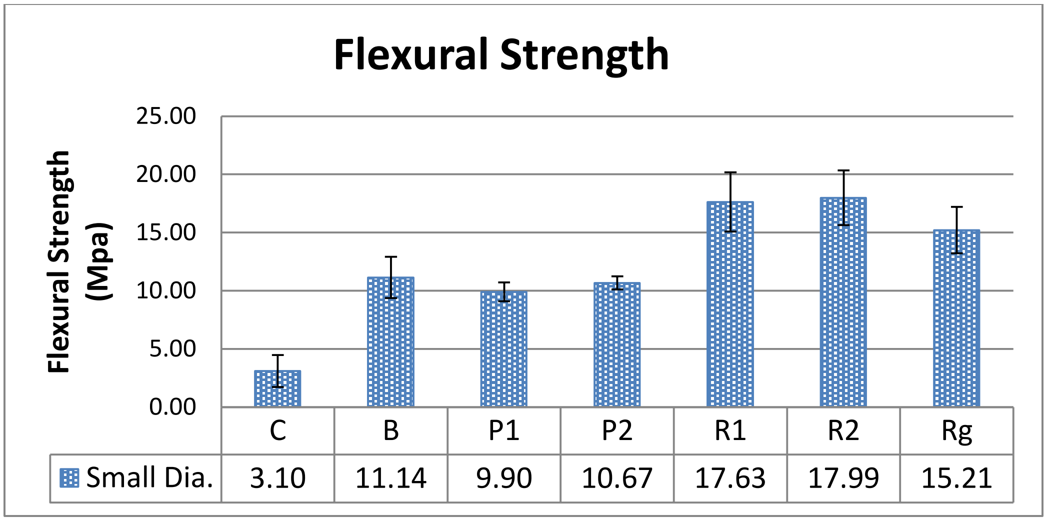

Figure 48 Flexural strength for selected infiltrate types

The flexural tests were conducted using only one build orientation, horizontal (0°). The build orientation was chosen because it is assumed to represent the build direction with the highest recorded strength for this test and because it has a significant lower building time than the other two orientations, therefore, would be more representative of the orientation that designers would choose for long parts. Because one orientation was used, a larger second diameter specimen was added for comparison of results (19.05mm). The larger diameter specimens did record a higher force at failure, but when the ultimate flexural strength was calculated, the sample groups performed very similar to their smaller diameter sample group, as illustrated in Figure 49.

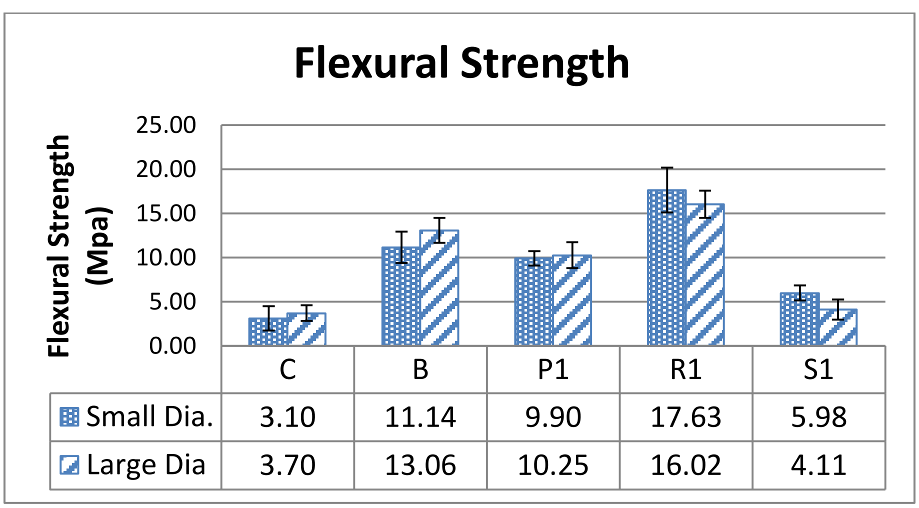

Figure 49 Bar graph illustrating the observed tensile strength of specimens with two diameters

6.3.2 Depth of Infiltration

The depth of infiltration was measured using the method described earlier. The measured depths of the infiltrates with the small diameter flexural specimen can be seen in Figure 50.

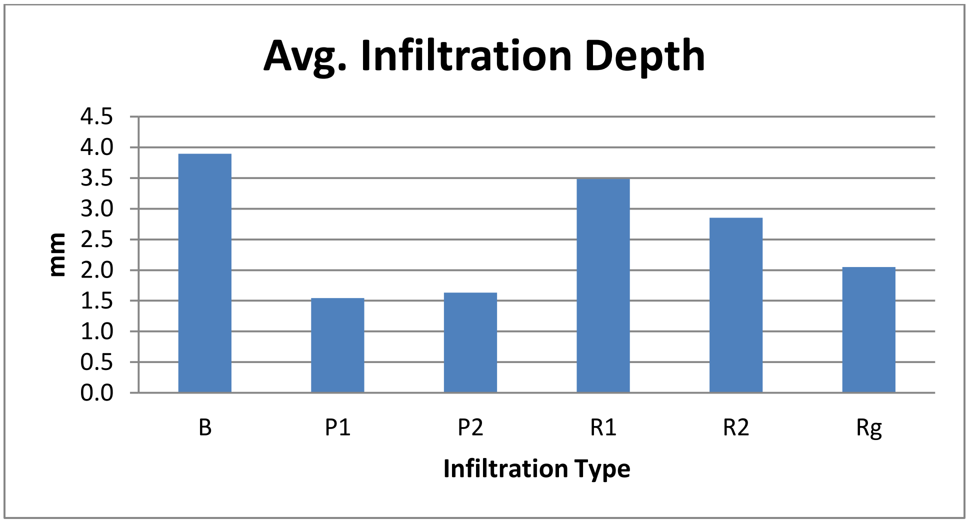

Figure 50 Average absorption depth for small dia. flexural specimens

The cyanoacrylate recorded the deepest average absorption followed closely by the epoxy specimens and then the polyurethane set. The absorption depths for the different application times are consistent with the hypothesis for the polyurethane set. The P2, which had a longer application time, was observed to absorb more of the infiltrate. Alternatively in the epoxy set, the average absorption was measured with a greater depth with the specimens that had a lower application time. This depth difference did not have a significant impact on the strength of the specimen as a higher average strength was observed. Also within the epoxy set was the green sample. The green sample had the shallowest absorption depth of the set and also had the lowest strength. The depth of infiltration seen in Figure 51 on the large diameter specimens was similar to their small diameter counterparts.

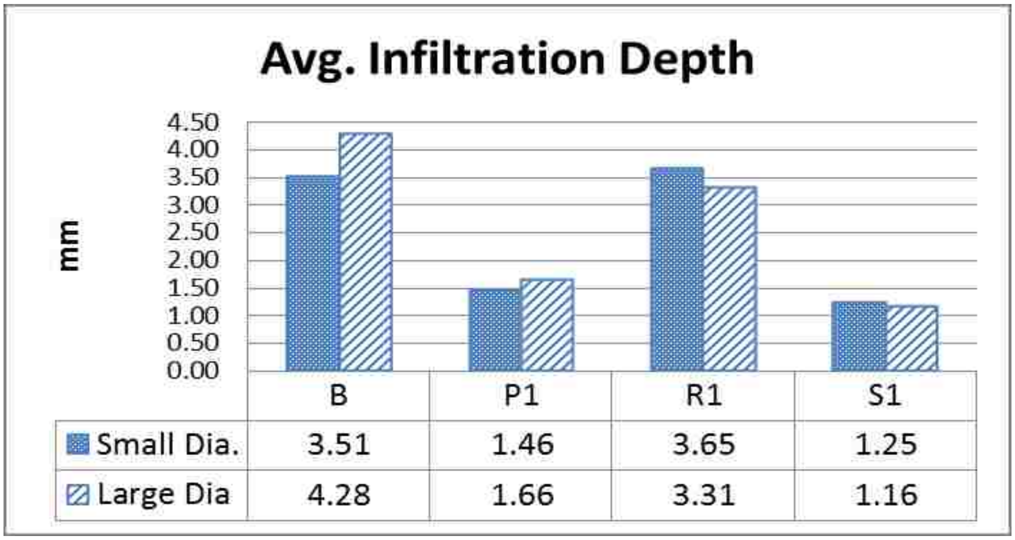

Figure 51 Average absorption depth for small and large dia. flexural specimens

The above chart looks similar to the strength chart of the two diameters. It can be seen upon further examination, that the minor differences between the strength of two sets of diameters can be correlated with the measured infiltrate absorption depth.

6.3.3 Observations and Summary

There were two diameters of specimens printed for select infiltration types. While the larger diameter specimens could withstand a higher peak load during the test, it was directly proportional to the increase in diameter. Thus, the actually flexural strength of the material was relatively consistent. It was also observed that the direction of the printed part, within the horizontal build direction, did not have a significant effect of the outcome. The P-value of this variable, as see in Table 30, is .602. With reference to values within ANOVAs, factors with a P-value less than or equal to .05 would indicate that it would have a significant effect of the outcome. The outcome for these tests is the material flexural strength.

General Linear Model: Stress Mpa versus X or Y, Type

Factor	Type	Levels	Values
X or Y	fixed	2	1, 2
Type	fixed	11	1, 2, 3, 4, 5, 6, 7, 8, 9, 10, 11

Analysis of Variance for Stress Mpa, using Adjusted SS for Tests

Source	DF	Seq SS	Adj SS	Adj MS	F	P
X or Y	1	0.01	0.64	0.64	0.28	0.602
Type	10	1130.59	1130.59	113.06	48.66	0.000
Error	35	81.32	81.32	2.32		
Total	46	1211.92				

Table 30 ANOVA table: Flexural stress vs. all types and horizontal orientations

The above table indicates that the type of infiltrate has a significant effect on the flexural strength of the material. This is further detailed in the grouping of types using the Tukey method, illustrated in Table 31.

Grouping Information Using Tukey Method

Type	N	Mean	Grouping
6	3	17.990	A
5	6	16.827	A
7	3	15.210	A B
2	6	12.100	B C
4	3	10.673	C D
3	5	10.038	C D E
11	4	6.650	E F
10	2	6.105	D E F
9	3	5.257	F
8	6	5.047	F
1	6	3.398	F

Means that do not share a letter are significantly different.

Tukey 95% Simultaneous Confidence Intervals
All Pairwise Comparisons among Levels of Type

Individual confidence level = 99.85%

Legend	
1	Control
2	Cyancrylate
3	Polyurethane (1)
4	Polyurethane (2)
5	Epoxy (1)
6	Epoxy (2)
7	Epoxy (Rg)
8	Salt (1)
9	Salt (1)B
10	Salt (2)
11	Salt (2)B

Table 31 Flexural specimen - Tukey method

It is observed in this method that there is not a significant difference in the test result between the control and all the salt mixtures. These sets are classified as underperforming because they did not show significant improvement with the extra post processing.

Another measured variable is the depth of absorption for the infiltrate for the different types. The results from the ANOVAs (Table 32A) show that the depth of absorption is a significant factor affecting the material flexural strength. The absorption depth was simplified within 9 different levels. The breakdown, (Table 32B), was produced with .025” intervals. The first interval was .50 as it reflects that a measurement could not be observed under this interval because the presence of the binder shells.

A)

One-way ANOVA: Stress Mpa versus Depth c

```
Source   DF       SS      MS      F      P
Depth c   7   899.21  128.46  16.02  0.000
Error    39   312.71    8.02
Total    46  1211.92

S = 2.832   R-Sq = 74.20%   R-Sq(adj) = 69.57%


                              Individual 95% CIs For Mean Based on
                              Pooled StDev
Level   N    Mean  StDev  ----+---------+---------+---------+-----
1      16   4.810  2.022  (-*-)
2      15   9.346  3.011         (--*-)
3       3  15.313  1.932                (-----*----)
4       5  15.604  4.123                  (---*---)
5       4  13.870  3.869              (----*----)
6       2  15.795  2.015                (-----*------)
7       1  13.260      *         (---------*---------)
9       1  19.180      *                  (---------*---------)
                          ----+---------+---------+---------+-----
                            6.0      12.0      18.0      24.0

Pooled StDev = 2.832
```

B)

Level	Depth (inch)
1	0 - 0.050
2	.051 - 0.075
3	.076 - 0.100
4	.101 - 0.125
5	.126 - 0.150
6	.151 - 0.175
7	.176 - 0.200
8	.201 - 0.225
9	.226 - 0.250

Table 32 A) ANOVA table: Flexural stress vs. absorption depth B) Absorption level breakdown

The depth is a significant factor as the results of the polyurethane sets were observed to have a low absorption and low strength compared to the higher strength and deeper absorption of the cyanoacrylate and the epoxy sets.

CHAPTER 7

PHYSICAL TESTING – OVERALL SUMMARY

Physical testing is necessary to understand how variable effect of the strength of the material. The strength of the material is dependent on the type of physical testing being conducted. The strength of the materials is different while in tensile, compression or during flexural testing. The differences observed are illustrated in Figure 52 A&B. The graph is a summary of the ultimate stress that was observed for the different testing methods.

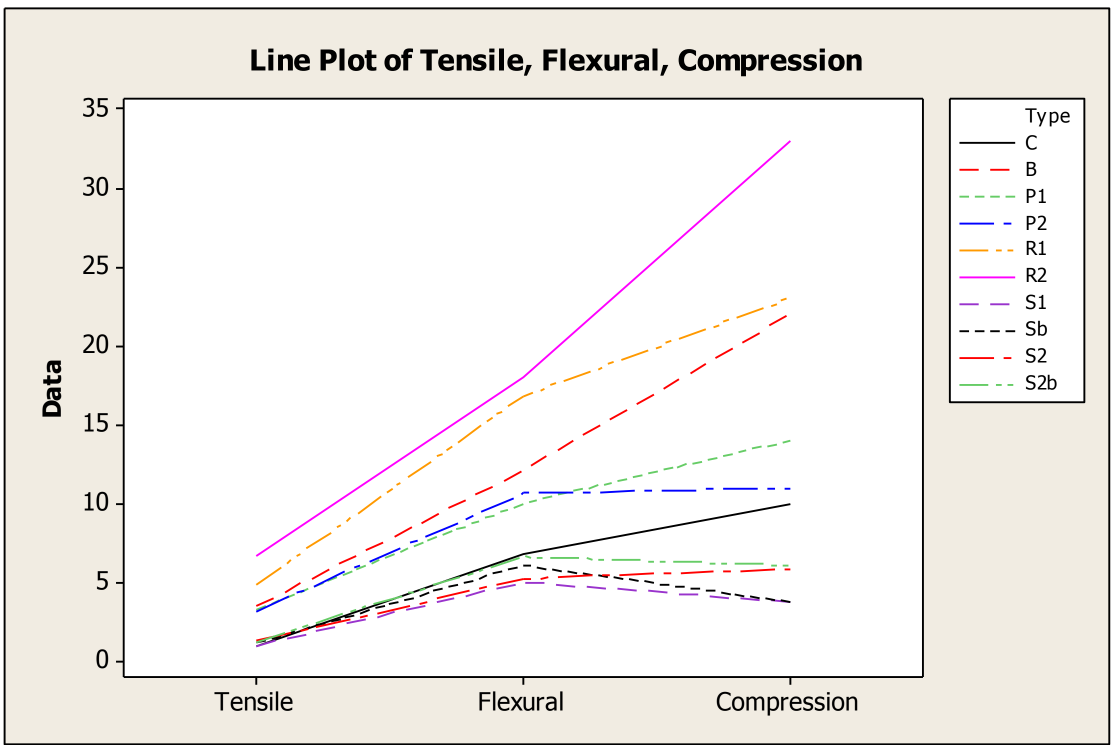

A)

B) 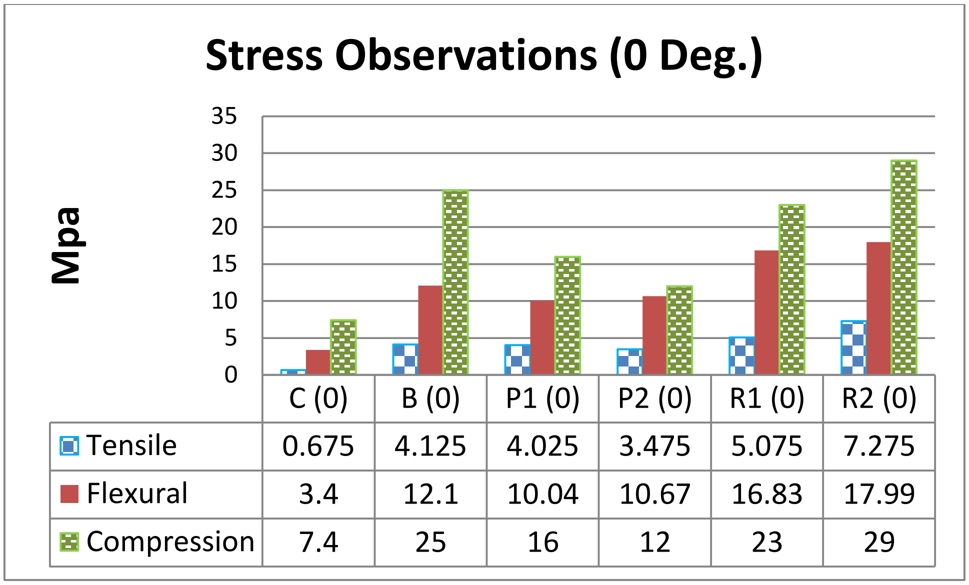

Figure 52 Summary graph of physical testing a) Line Graph b) Bar graph

The data used for the comparison and chart are the top performing infiltrate types and at the 0° horizontal build orientation. This orientation was used so that a proper comparison could be reached as that was the only build orientation available for the flexural testing.

To analysis this further, regressions to predict the outcomes were made. Tables 33 (A,B, and C) summarize the equations that could be formed from the information.

A) 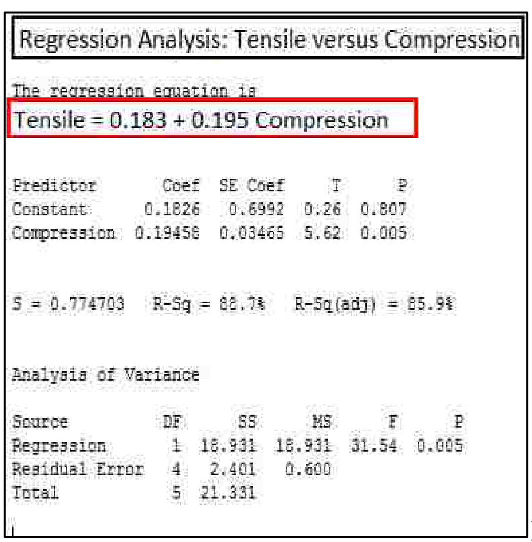

Regression Analysis: Tensile versus Compression

The regression equation is
Tensile = 0.183 + 0.195 Compression

Predictor	Coef	SE Coef	T	P
Constant	0.1826	0.6992	0.26	0.807
Compression	0.19458	0.03465	5.62	0.005

S = 0.774703 R-Sq = 88.7% R-Sq(adj) = 85.9%

Analysis of Variance

Source	DF	SS	MS	F	P
Regression	1	18.931	18.931	31.54	0.005
Residual Error	4	2.401	0.600		
Total	5	21.331			

B) 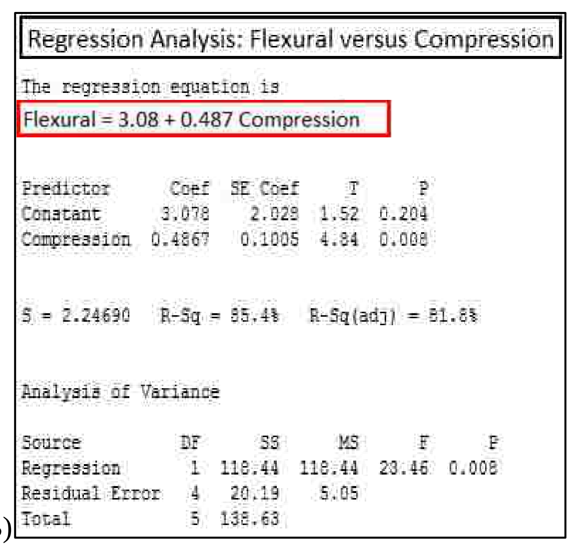

Regression Analysis: Flexural versus Compression

The regression equation is
Flexural = 3.08 + 0.487 Compression

Predictor	Coef	SE Coef	T	P
Constant	3.078	2.028	1.52	0.204
Compression	0.4867	0.1005	4.84	0.008

S = 2.24690 R-Sq = 85.4% R-Sq(adj) = 81.8%

Analysis of Variance

Source	DF	SS	MS	F	P
Regression	1	118.44	118.44	23.46	0.008
Residual Error	4	20.19	5.05		
Total	5	138.63			

C)

Regression Analysis: Tensile versus Flexural

The regression equation is

Tensile = -0.838 + 0.382 Flexural

Predictor	Coef	SE Coef	T	P
Constant	-0.8381	0.5675	-1.48	0.214
Flexural	0.38207	0.04442	8.60	0.001

S = 0.523003   R-Sq = 94.9%   R-Sq(adj) = 93.6%

Analysis of Variance

Source	DF	SS	MS	F	P
Regression	1	20.237	20.237	73.98	0.001
Residual Error	4	1.094	0.274		
Total	5	21.331			

Table 33 Regression Analysis A)Tensile vs. Compression B) Flexural vs. Compression C) Tensile vs. Flexural

The formula solved by the software can be used as a baseline and as a early predictive tool in determining the complementary strengths by calculating from a base test.. By looking at the graph, it can be understood that since they all increase in strength at difference rates from tensile to compression, the designer would not be able to rely on the outcome when choosing for specific strengths.

During this experiment, it was observed that each of the variables tested affected the results to different degrees and/or with opposite effects. One such variable is the orientation. There were three build orientations; 0° horizontal (1), 45° angled (2), and 90° vertical (3). The results for the different orientations were compared for tensile and compression. The averages were aggregated from leveling off the results among the infiltrate types. Therefore, the infiltrate types were not compared to each other but scaled within [1,2] from their respective set for to get the performance numbers. It was observed that the lowest performer for tensile was 90° and the second was 45°. As illustrated in Figure 53, these low multipliers were then inversed for compression. Interesting, for both tensile and compression, the 0° build orientation remained as the top performer, on average, for the infiltrate types.

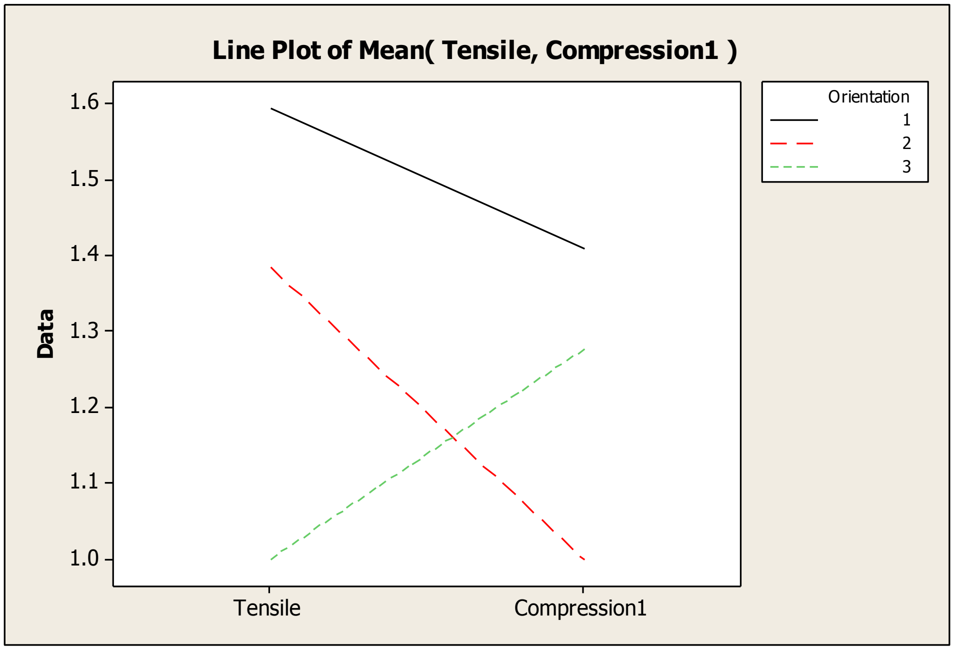

Figure 53 Scaled results from infiltrate types and the orientation

Methods to predict the strength for the different stresses from post processing the different infiltrates could not be too precise. Therefore, a summary table of results that could be expected or achieved, as shown in Table 34, should be referenced.

Infiltrate	Type Code	Ultimate Strength in MPa		
		Tensile	Flexural	Compression
Control	C	0.6 - 0.8	1.5 - 4.65	2.5 - 9
Cyanoacrylate	B	2 - 5.5	9.13 - 14.37	15.6 - 25.8
Epsom Salt Mixture	S1	0.7 - 2.1	3.36 - 6.81	.9 - 5.3
	S2	0.5 - 2.2	4.79 - 5.88	2.7 - 9.9
Epoxy	R1	2.5 - 7.6	14.27 - 19.18	13.8 - 43.4
	R2	4.5 - 11.7	15.31 - 19.64	19.9 - 50.2
	Rg	n/a	13.77 - 17.48	n/a
Polyurethane Glue	P1	1.8 - 4.4	9.21 - 11.28	12 - 18.5
	P2	2.1 - 3.6	10.21 - 11.29	7 - 13.7
2 Phase	S1b	.4 - 2.2	4.79 - 7.42	1 - 7.8
	S2b	0.2 - 2.2	6.03 - 7.42	3.6 - 9

Table 34 Summary table of expected ultimate strengths

These results are only a representation from the methods, material and machines used of this experiment.

CHAPTER 8

CURVE FITTING

8.1 Curve Shape and Reaction

The mechanical characteristics of material can also be described as not just how much force the material can withstand but how it reacts to that force. This characteristic can be helpful to designers when they are determining and trying to predict how the part will fail or designing a part that will not fail under specific loads. As mentioned earlier in the paper, the 3D printed material is very brittle and therefore, could be classified as a ceramic. Other brittle material include: glass, stone and cast iron. Brittle material, during tensile tests, normally fails without a change in elongation. This abrupt fracture lends that there is not much difference between the ultimate strength and breaking strength of the material. It is also noted that strain at the point of facture is much less than ductile materials. Ductile materials would stretch and possibly neck before fracture occurs.

For most brittle materials, the ultimate compression strength is much larger than the ultimate tensile strength. Microscopic cracks or cavities and other presence of flaws can weaken the material in tension but it does not affect its compressive resistance. (Beer, Johnston, DeWolf, & Mazurek, 2008) This is illustrated below in Figure 54 with the stress strain curve for concrete. Tension is in the positive hemisphere and compression is in the negative hemisphere. Like other brittle material the concrete observes a linear elastic region. It is linear because the stress is proportional to the increase in strain. After its yield point, the strain increases quicker than the stress. In compression, the higher stresses achieved produces a linear region that is much larger. Also, the failure does not occur at the highest recorded stress but actually on the gradual downward gradual curve as stress is reduced and strain is increasing. One noteworthy item is that just like most brittle material, concrete has the same modulus of elasticity (E) , slope of stress-strain, in both tensile and compression.

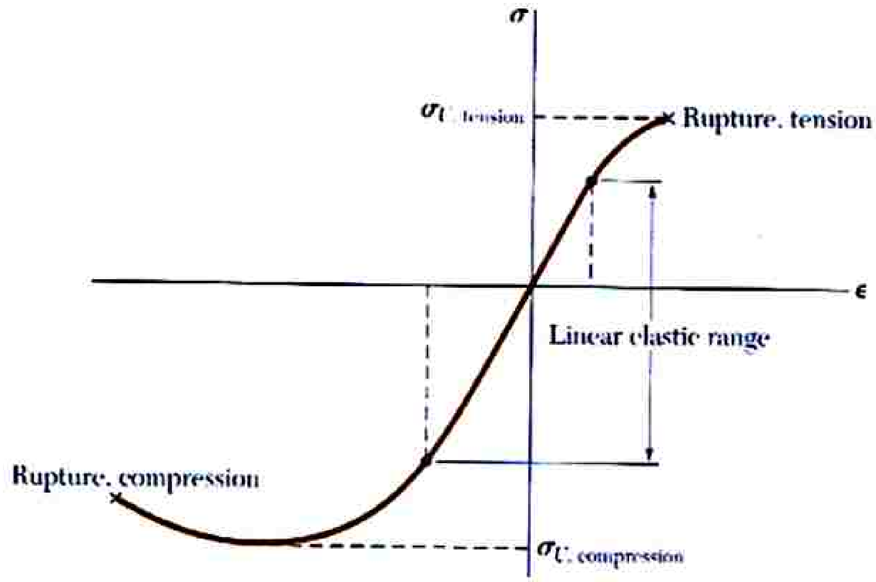

Figure 54 Stress strain curve for concrete adapted from (Beer, 2008)

8.2 Tensile

The curves that were selected to examine more closely are the curves illustrated earlier in the paper. Below illustrated in Figure 55 are the curves selected for the measuring curve shape. These samples are selected from the highest performing test runs of each of the infiltrate types.

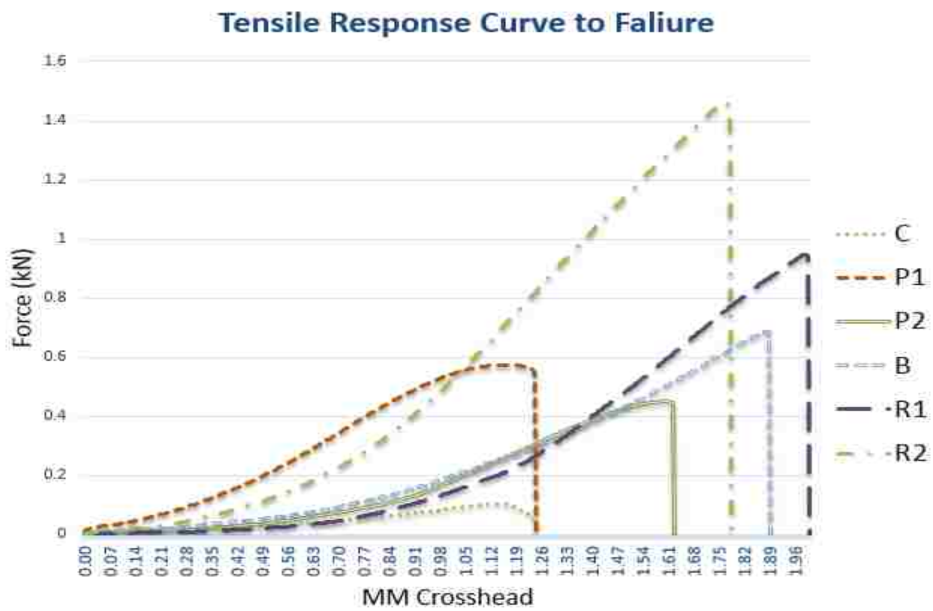

Figure 55 Select tensile response curves

Each of the curves were separated and graphed individually to examine the curves more closely. While each of the specimens was built using the same material, the infiltration type produced different stress-strain curves. The curves observed could be represented by one, two or three different curves.

The cyanoacrylate specimen could be represented by just one curve. While fitting the curve, one polynomial equation was used to closely match the stress-strain curve. Illustrated in Figure 56 is the stress-strain curve along with the fitted polynomial curve with equation. Also represented in the graph is a line that matches the final arc of the curve. This slope is used later for comparing modulus of elasticity among specimens.

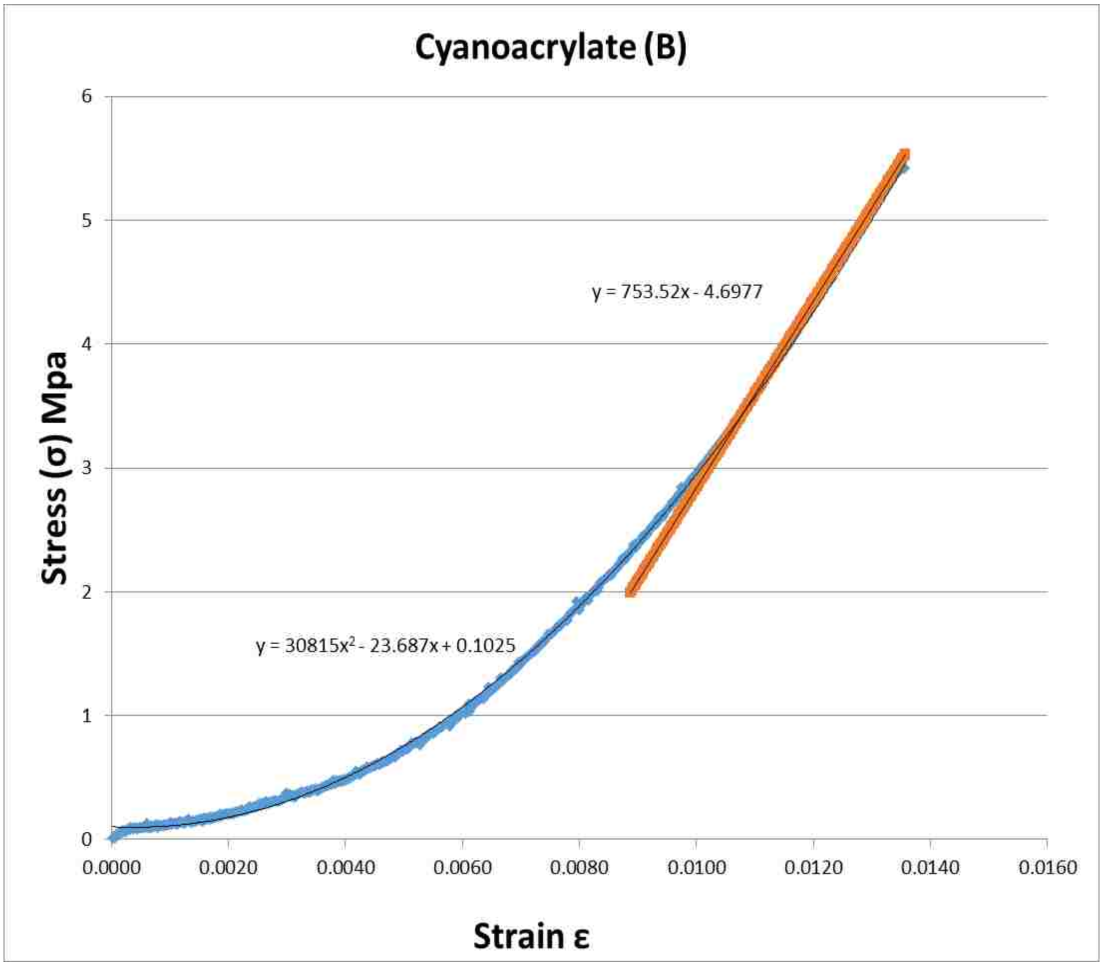

Figure 56 Tensile stress – strain curve for cyanoacrylate

While the above curve could be represented by just one polynomial equation, the epoxy (R2) specimen (illustrated in Figure 57), needed an additional linear equation to get the proper curve fitting. The first part it is noticeable that the stress is not increasing at a constant rate until the strain is at .007, and then a linear region is observed. This linear region's slope is used as the specimen's modulus of elasticity.

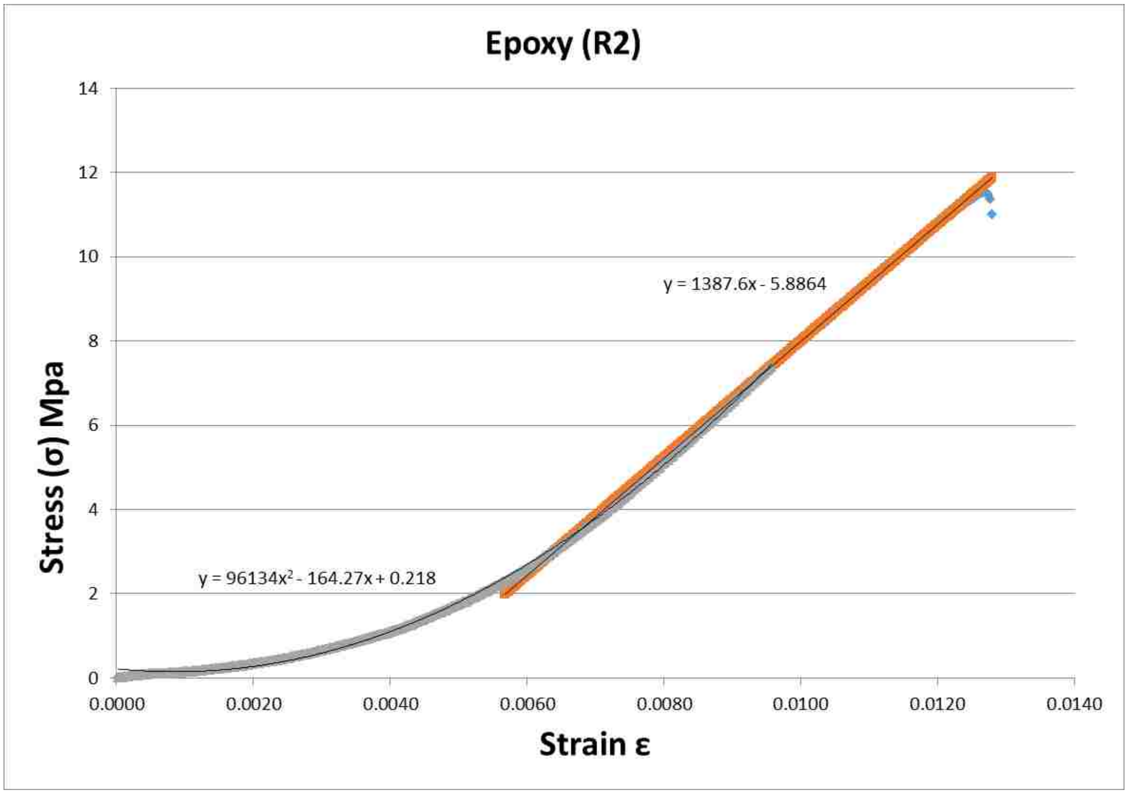

Figure 57 Tensile stress – strain curve for epoxy (R2)

Finally the third type of curve within the tensile test is fitted with three curves. The most extreme case is illustrated below in Figure 58, with the stress-strain curve of polyurethane (P1). It has a polynomial curve to start, followed by a linear region and then ending with another polynomial curve. This would give the curve a more S-type pattern. This same pattern can be seen with the other polyurethane sample in Appendix H.

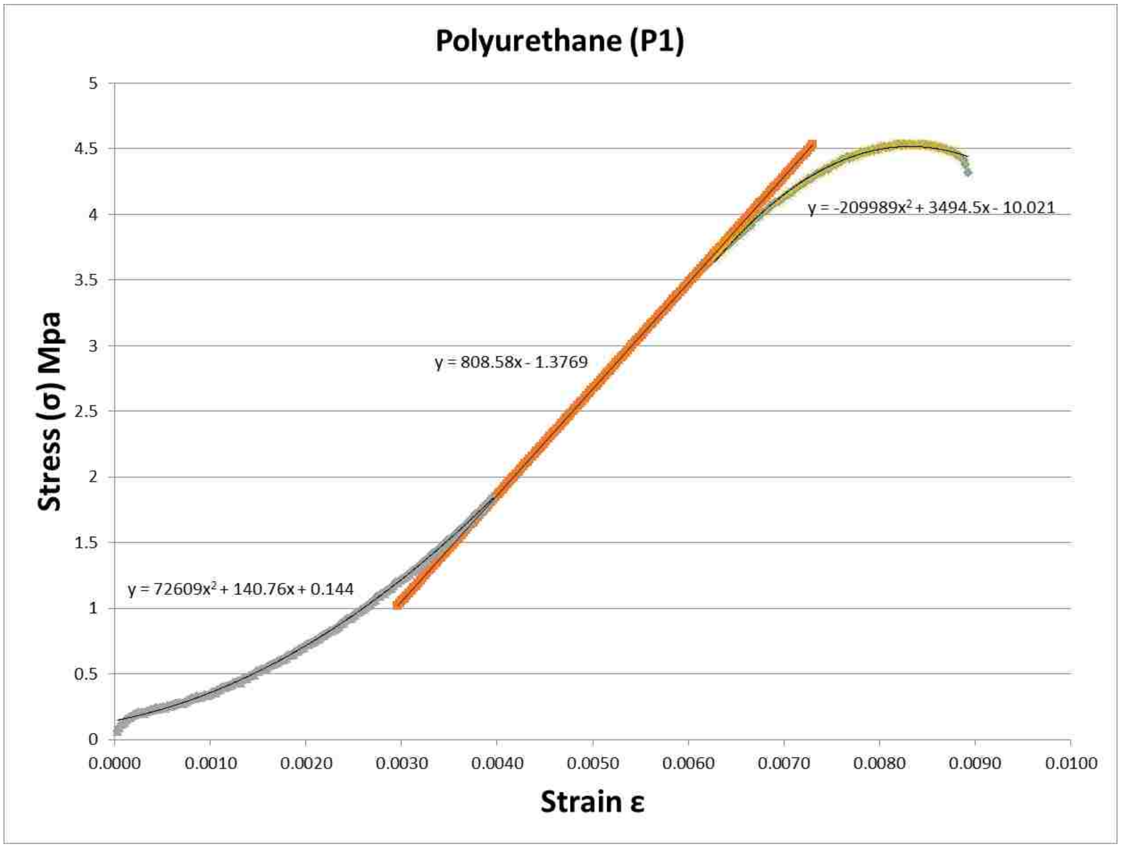

Figure 58 Tensile stress – strain curve for polyurethane (P1)

Other variations of three curves needed to fit the tensile curve, illustrated in Appendix I, are for the control (logarithmic, polynomial, linear) and the epoxy (R1) (linear, polynomial, linear).

Some of the infiltration type might have had the same type of curves to fit but each was at different magnitudes and was bounded in different areas. Table 35 is a summary of the different curve types, equations and bounded sections. The region number is given along with the linear equation that is used as the specimen's modulus of elasticity (E).

Tensile						
Infiltrate	Code	Run	Equation	Region #	Curve Shape	Bound
Control	C	37	y = 0.0449ln(x) + 0.4441	1	Logarithmic	[0,.002]
			y = 15104x2 - 41.936x + 0.1927	2	Polynomial	[.002,.0063]
			y = 160.223x - 0.46883	3 (E)	Linear	[.0063,.08]
Epoxy	R1	72	y = 45.495x + .007012	1	Linear	[0,.0038]
			y = 70514x2 - 526.06x + 1.2187	2	Polynomial	[.0038,.0101]
			y = 1080.228x - 7.759	3 (E)	Linear	[.0101,.0143]
	R2	48	y = 96134x2 - 164.27x + 0.218	1	Polynomial	[0,.00866]
			y = 1387.62x - 5.88637	2 (E)	Linear	[.00866, .0128]
Cyanoacrylate	B	19	y = 30815x2 - 23.687x + 0.1025	1	Polynomial	[0,.0135]
			y = 753.522x - 4.697	(E)	Linear	[.0104,.0135]
Polyurethane	P1	22	y = 72609x2 + 140.76x + 0.144	1	Polynomial	[0,.004]
			y = 808.578x - 1.3769	2 (E)	Linear	[.004,.0062]
			y = -209989x2 + 3494.5x - 10.021	3	Polynomial	[.0062,.0089]
	P2	89	y = 25150x2 - 19.879x + 0.058	1	Polynomial	[0,.0073]
			y = 591.669x - 2.8827	2 (E)	Linear	[.0073,.0103]
			y = -217622x2 + 5060.7x - 25.871	3	Polynomial	[.0103,.0116]

Table 35 Summary of the different curve types, equations and bounded sections for tensile

8.3 Compression

The curves that were selected to examine more closely are the curves illustrated earlier in the paper. Below illustrated in Figure 59 are the curves selected for the measuring curve shape. These samples are selected from the highest performing test runs of each of the infiltrate types.

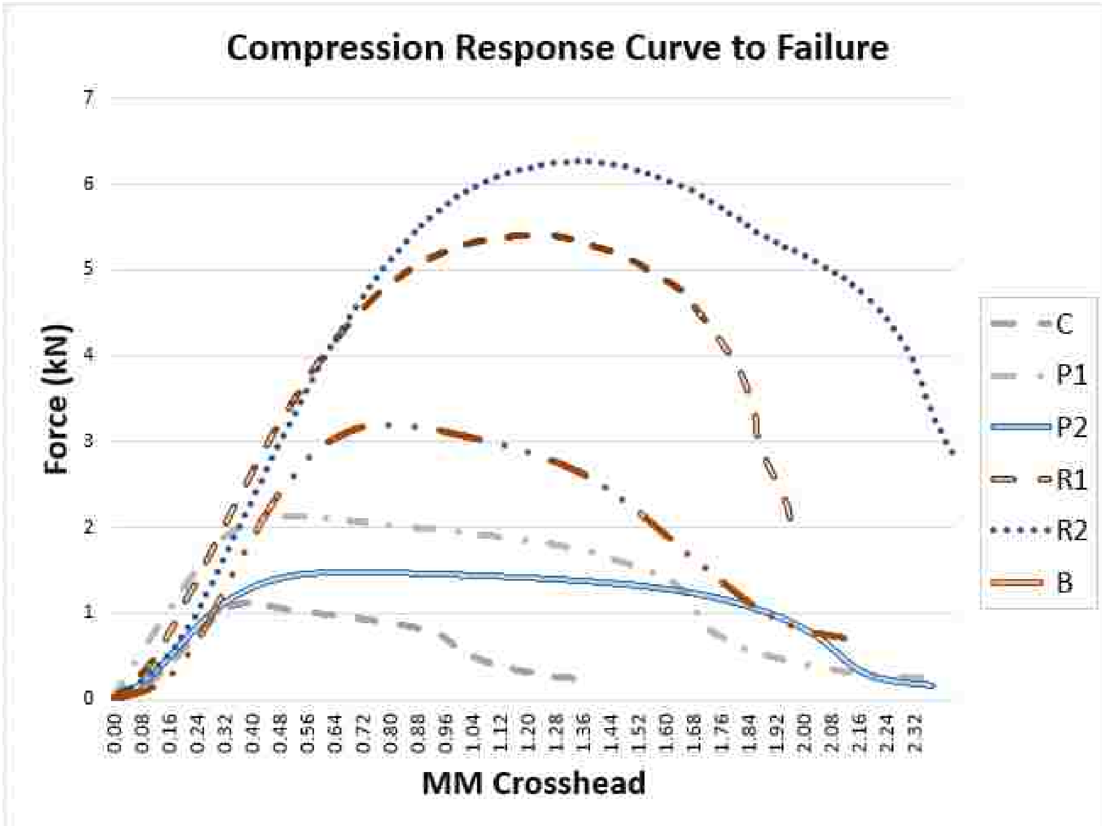

Figure 59 Select compressive response curves

Each of the curves were separated and graphed individually to examine the curves more closely. While each of the specimens was built using the same material, the infiltration type produced different stress-strain curves. The curves observed could be represented by two or three different curves.

The polyurethane (P1) is the lone example of the compression stress-stain curve fitted with two curves. Illustrated below in Figure 60, the P1 specimen starts in a linear region before entering a polynomial curve. The polynomial curve is fitted with the proper curve segment but is shown in the top right corner away from the curve. This was to not only show the curve through the software and get an equation but to give a visual reference of the magnitude of the curve when compared to the other infiltrate type’s graphs.

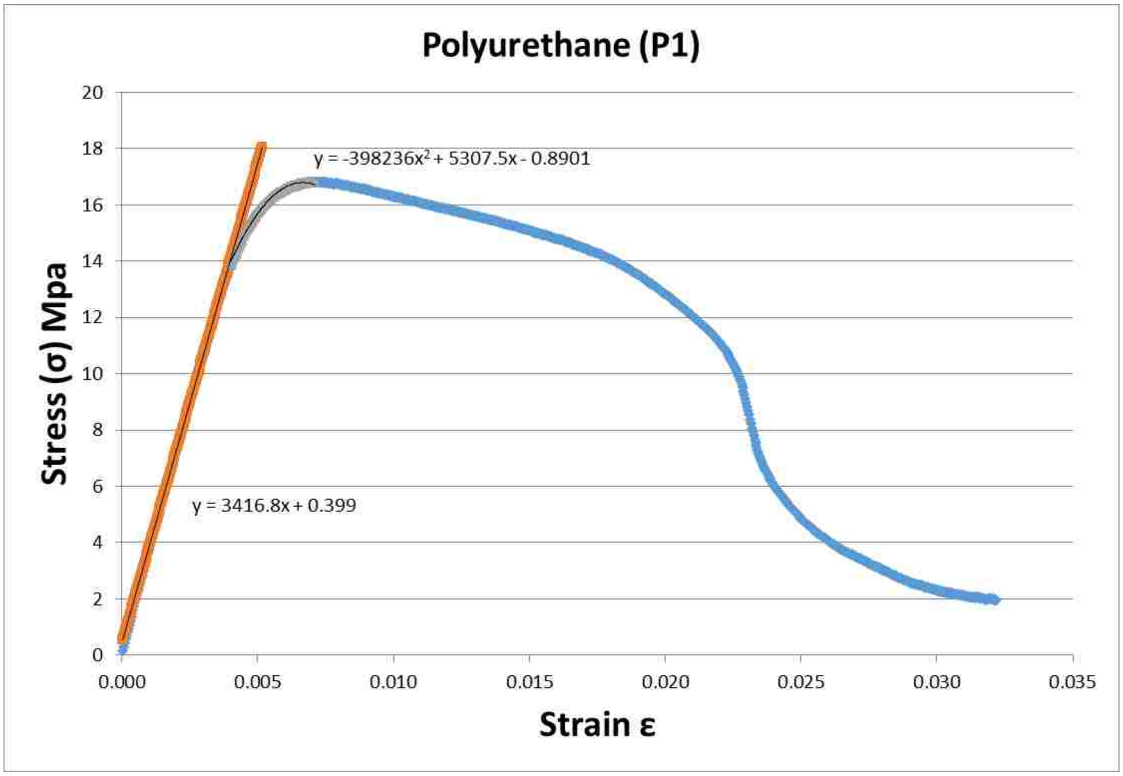

Figure 60 Compressive stress – strain curve for polyurethane (P1)

While this type of curve representation is expected from a brittle material, the other infiltration type specimens need three curves equations to fit their respected stress-strain curves. An example is illustrated in Figure 61 with the stress-strain curve of the epoxy (R2). This curve has an extra polynomial curve at the beginning of the test.

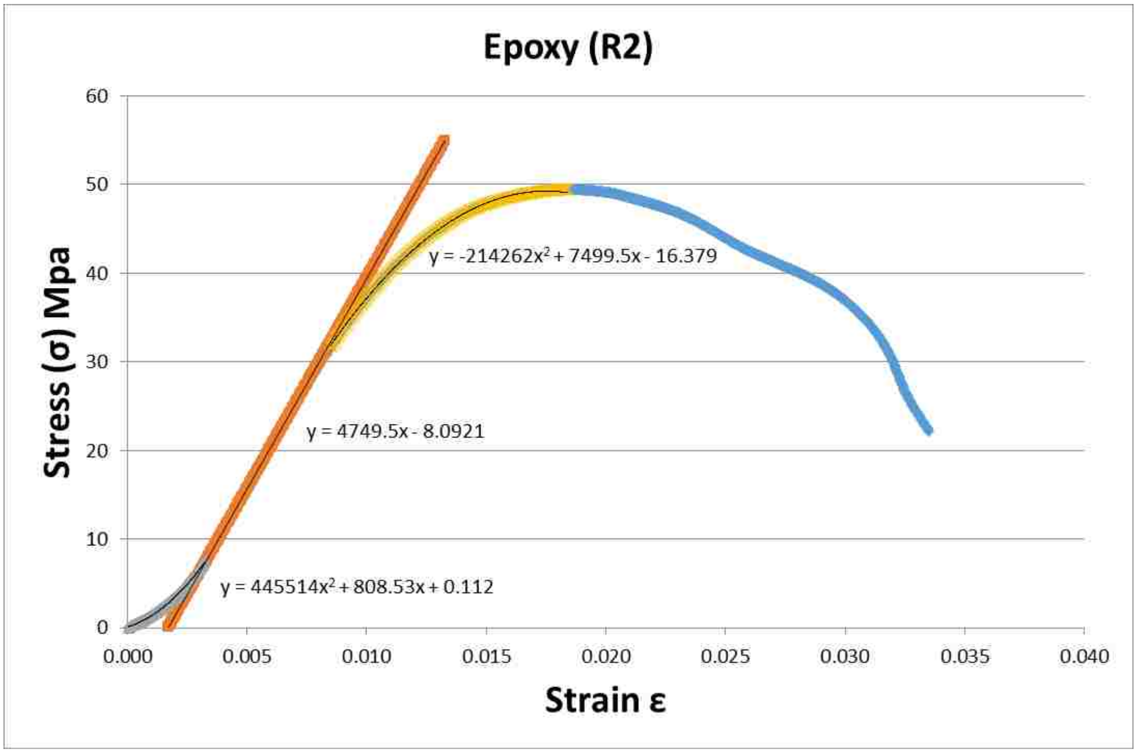

Figure 61 Compressive stress – strain curve for epoxy (R2)

This ramp up polynomial curve is also reflected in the polyurethane (P2), epoxy (R1), cyanoacrylate and the control specimens which can be seen in Appendix J.

Some of the infiltration type might have had the same type of curves to fit but each was at different magnitudes and was bounded in different areas. Table 36 gives a summary of the different curve types, equations and bounded sections. The region number is given along with the linear equation that is used as the specimen's modulus of elasticity (E).

Compression						
Infiltrate	Code	Run	Equation	Region #	Curve Shape	Bound
Control	C	49	y = 448961x2 + 352.86x + 0.1006	1	Polynomial	[0,.002]
			y = 2429.63x - 2.26178	2 (E)	Linear	[.002,.004]
			y = -741718x2 + 7975.6x - 12.583	3	Polynomial	[.004,.005]
Epoxy	R1	37	y = 700610x2 + 1051.6x + 0.124	1	Polynomial	[0,.002]
			y = 4507.36x - 4.266	2 (E)	Linear	[.002,.007]
			y = -217778x2 + 6725.2x - 9.5406	3	Polynomial	[.007,.005]
	R2	27	y = 445514x2 + 808.53x + 0.112	1	Polynomial	[0,.003]
			y = 4749.504x - 8.09208	2 (E)	Linear	[.003,.0085]
			y = -214262x2 + 7499.5x - 16.379	3	Polynomial	[.0085,.0184]
Cyanoacrylate	B	19	y = 452727x2 - 154.42x + 0.2059	1	Polynomial	[0,.003]
			y = 4351.22x - 9.34866	2 (E)	Linear	[.003,.0063]
			y = -406170x2 + 8605x - 20.331	3	Polynomial	[.0063,.0108]
Polyurethane	P1	22	y = 3416.786x + 0.399	1 (E)	Linear	[0,.004]
			y = -398236x2 + 5307.5x - 0.8901	2	Polynomial	[.004,.007]
	P2	89	y = 356186x2 + 755.89x + 0.0995	1	Polynomial	[0,.0014]
			y = 2385.85x - 1.564	2 (E)	Linear	[.0014,.0043]
			y = -157085x2 + 2726.9x - 0.0894	3	Polynomial	[.0043,.01]

Table 36 Summary of the different curve types, equations and bounded sections for compression

8.4 Flexural

The curves that were selected to examine more closely are the curves illustrated earlier in the paper. Below illustrated in Figure 62 are the curves selected for the measuring curve shape. These samples are selected from the highest performing test runs of each of the infiltrate types.

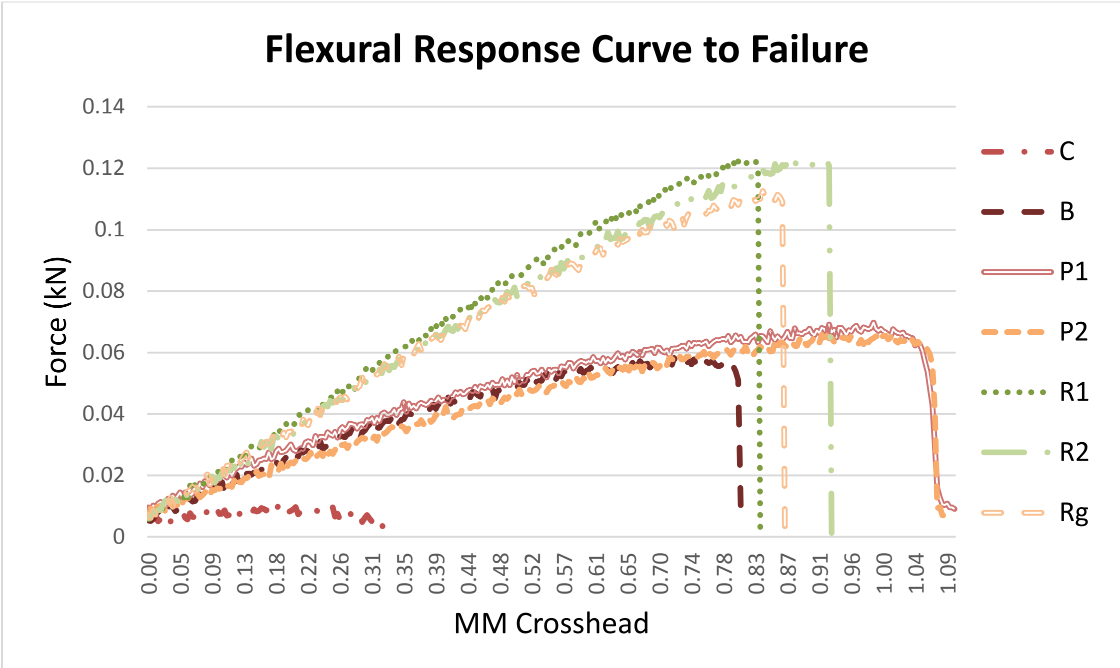

Figure 62 Select compressive response curves

Each of the curves were separated and graphed individually to examine the curves more closely. While each of the specimens was built using the same material, the infiltration type produced different stress-strain curves. Unlike the compression and tensile test, the flexural stress-strain curves are not smooth. This made is more difficult when fitting the curve and therefore, led to the curves being segmented into different linear regions. The curves observed could be represented by two or three different linear regions.

The control specimen, as illustrated in Figure 63, was particularly choppy and therefore, was only fitted with two linear regions. The graph shows the original curve along with the bounded areas for the linear regions.

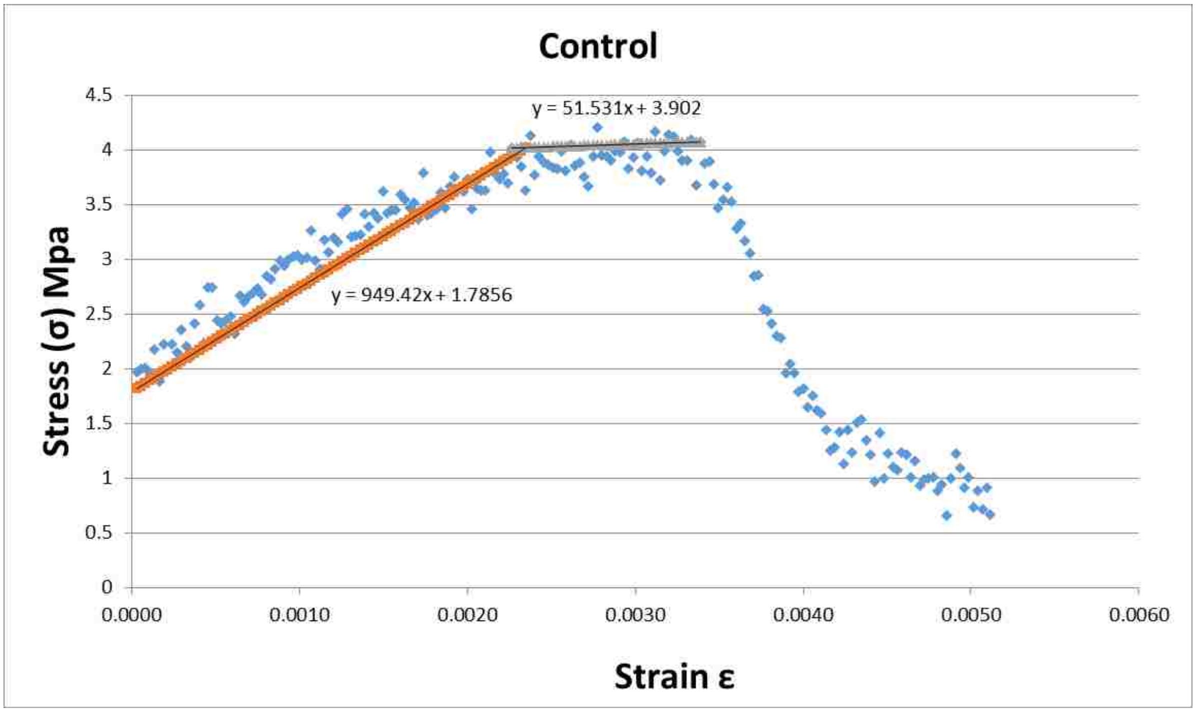

Figure 63 Flexural stress – strain curve for control

The other curves were a bit smoother and led to dividing them into 3 linear regions. An example of this separation can be seen in the stress-strain curve for polyurethane (P2), illustrated in Figure 64. Like the above graph, the bounded areas are marked and the linear regions are shown overlapping the original curve.

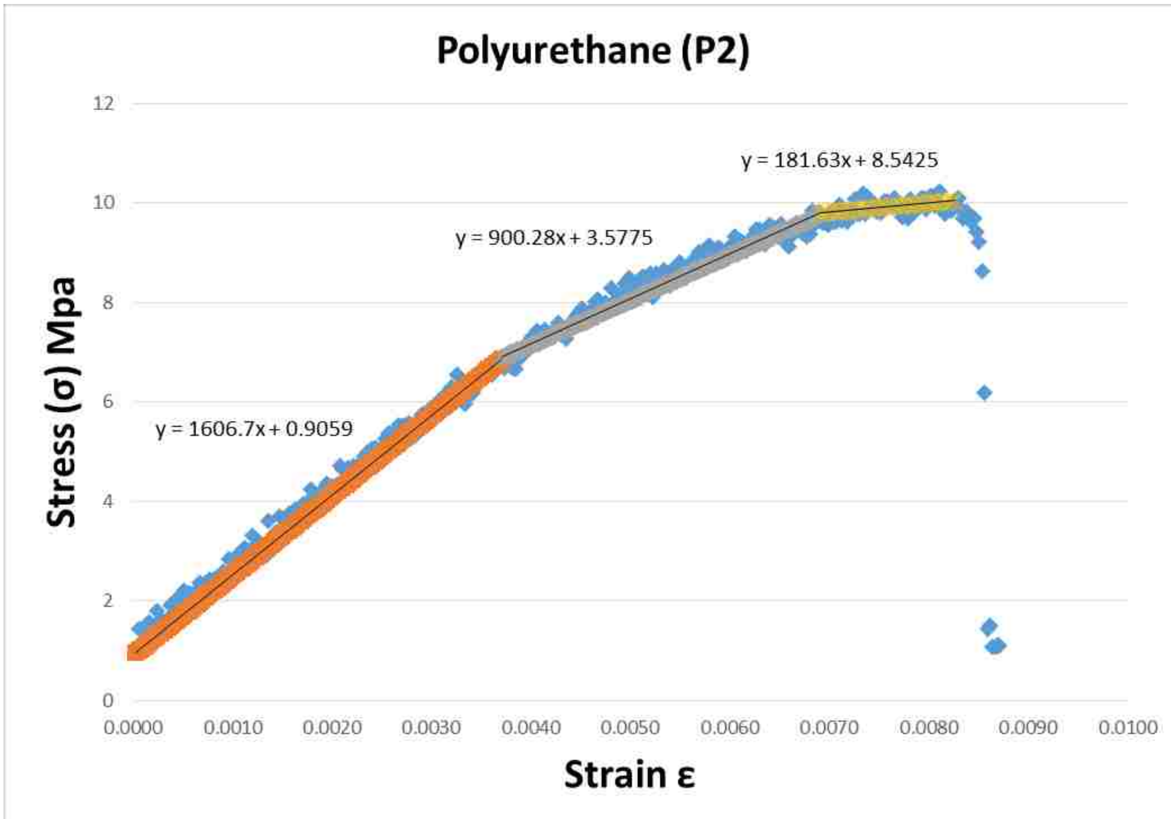

Figure 64 Flexural stress – strain curve for polyurethane (P2)

Other examples of this three linear region curve fit can be seen in the stress-strain curves of the cyanoacrylate, epoxy (R1, R2 & Rg), and polyurethane (P1), in Appendix K.

The other infiltration types had the same type of curves fit but each were at different slopes and were bounded in different areas. Table 37 gives a summary of the different curve types, equations and bounded sections. The region number is given along with the linear equation that is used as the specimen's modulus of elasticity (E).

Flexural						
Infiltrate	Code	Run	Equation	Region #	Curve Shape	Bound
Control	C	4	y = 949.41x + 1.7855	1 (E)	Linear	[0,.0023]
			y = 51.5309x + 3.902	2	Linear	[.0023, .0034]
Epoxy	R1	11	y = 3130.423x + .895189	1	Linear	[0,.0038]
			y = 2542.037x + 3.156562	2 (E)	Linear	[.0038,.0059]
			y = 1118.201x + 11.55107	3	Linear	[.0059,.0066]
	R2	10	y = 2781.91x +.09499	1	Linear	[0,.005]
			y = 1910.758x + 5.3448	2 (E)	Linear	[.005,.0068]
			y = 981.2559x + 11.71955	3	Linear	[.0068,.0074]
	Rg	27	y = 2745.512x + 1.1375	1	Linear	[0,.0044]
			y = 1887.03x + 4.9416	2 (E)	Linear	[.0044,.0063]
			y = 484.627x + 13.77	3	Linear	[.0063,.0069]
Cyanoacrylate	B	28	y = 1991.9x + .830699	1	Linear	[0,.0024]
			y = 1157.402x + 2.8602	2 (E)	Linear	[.0024,.0048]
			y = 189.611x + 7.56076	3	Linear	[.0048,.0063]
Polyurethane	P1	6	y = 1793.75x + 1.324	1	Linear	[0,.0029]
			y = 1047.79x + 3.472376	2 (E)	Linear	[.0029,.0056]
			y = 359.37x + 7.3275	3	Linear	[.0056,.0082]
	P2	20	y = 1606.7x + .9572	1	Linear	[0,.0037]
			y = 900.28x + 3.5786	2 (E)	Linear	[.0037,.0069]
			y = 181.6337x + 8.5437	3	Linear	[.0069,.0083]

Table 37 Summary of the different curve types, equations and bounded sections for flexural

8.5 Observations

The results from the test runs and curve fittings are subject to the specific machine-materials used in this experiment. While the outcome might be specific for this experiment, the changes that were made on the material with the different infiltrate type are quite dramatic. The material and specimens were brittle and there was no necking evident during tensile testing. The curves did resemble more toward that of curves from tests conducted on brittle material. Each of the curves for the in-depth study all were fitted with linear regions. The linear regions, with the resulting slopes for tension, compression and flexural, are summarized in Tables 38, 39, and 40.

Tensile				
Infiltrate	Code	Run	E= σ/ε Slope	Region #
Control	C	37	160.22	3 (E)
Epoxy	R1	72	1080.23	3 (E)
	R2	48	1387.62	2 (E)
Cyanoacrylate	B	19	753.52	(E)
Polyurethane	P1	22	808.57	2 (E)
	P2	89	591.67	2 (E)

Table 38 Linear regions, with the resulting slopes for tension.

Compression				
Infiltrate	Code	Run	E= σ/ε Slope	Region #
Control	C	49	2429.63	2 (E)
Epoxy	R1	37	4507.36	2 (E)
	R2	27	4749.5	2 (E)
Cyanoacrylate	B	90	4351.22	2 (E)
Polyurethane	P1	30	3416.79	1 (E)
	P2	19	2385.85	2 (E)

Table 39 Linear regions, with the resulting slopes for compression.

Flexural				
Infiltrate	Code	Run	E= σ/ε Slope	Region #
Control	C	4	949.42	1 (E)
Epoxy	R1	11	2542.037	2 (E)
	R2	10	1910.76	2 (E)
	Rg	27	1887.03	2 (E)
Cyanoacrylate	B	28	1157.4	2 (E)
Polyurethane	P1	6	1047.8	2 (E)
	P2	20	900.28	2 (E)

Table 40 Linear regions, with the resulting slopes for flexural.

For all of the tests, the hardest material with the largest slope was the epoxy specimens. By infiltrating these specimens with the epoxy, they not only became the strongest of the samples but became the most brittle. Other than the control specimens, and the cyanoacrylate tensile specimen, the polyurethane specimen sets produced the lowest slope. Of the set, the specimens with the longer application time had the lowest. This could show that the material, while getting strength from the infiltrate, the infiltrate itself might be more elastic increasing the materials elasticity with the more infiltrate absorbed.

The last observation refers to the opening remarks to the section. It stated that while the brittle material might have a larger compression strength compared to tensile, the linear regions for both are similar in slope. By comparing the above tables for tensile and compression, it is clear that the material does not act similar to documents brittle material. The magnitude difference between them is ranging from 3.5X (R2) to 15X (C) larger in compression that in tension. This results in a dramatically steeper slope in compression, as illustrated by Figure 65. By the fluctuations in slopes amongst the different infiltrate and the levels among the infiltrate set, for the 3D printed material, the reaction cannot be confidently predicted or assumed to react to forces similar to other brittle material. This material, with the different infiltrates could affect the designers' decision when selecting infiltrates, resources and/or AM technologies.

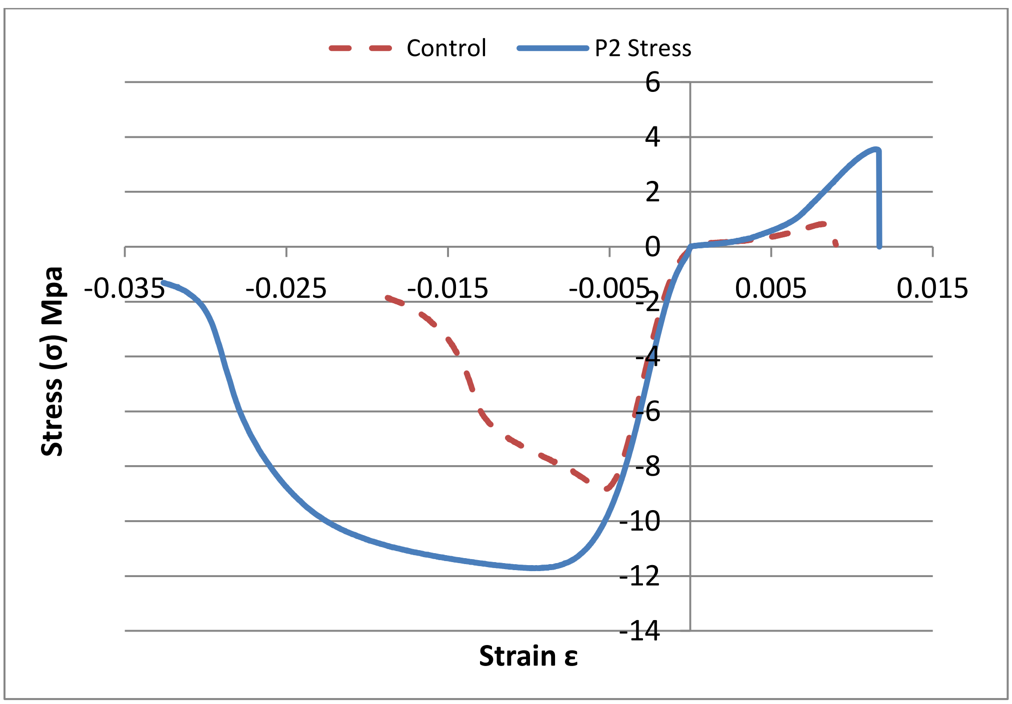

(a)

(b)
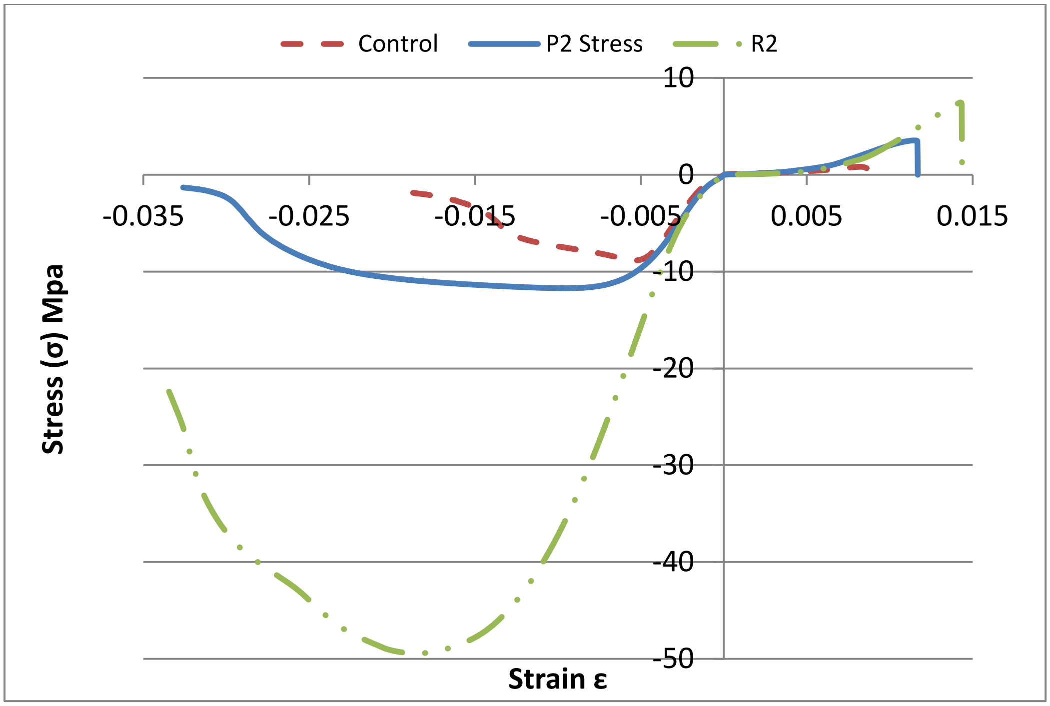

(c)
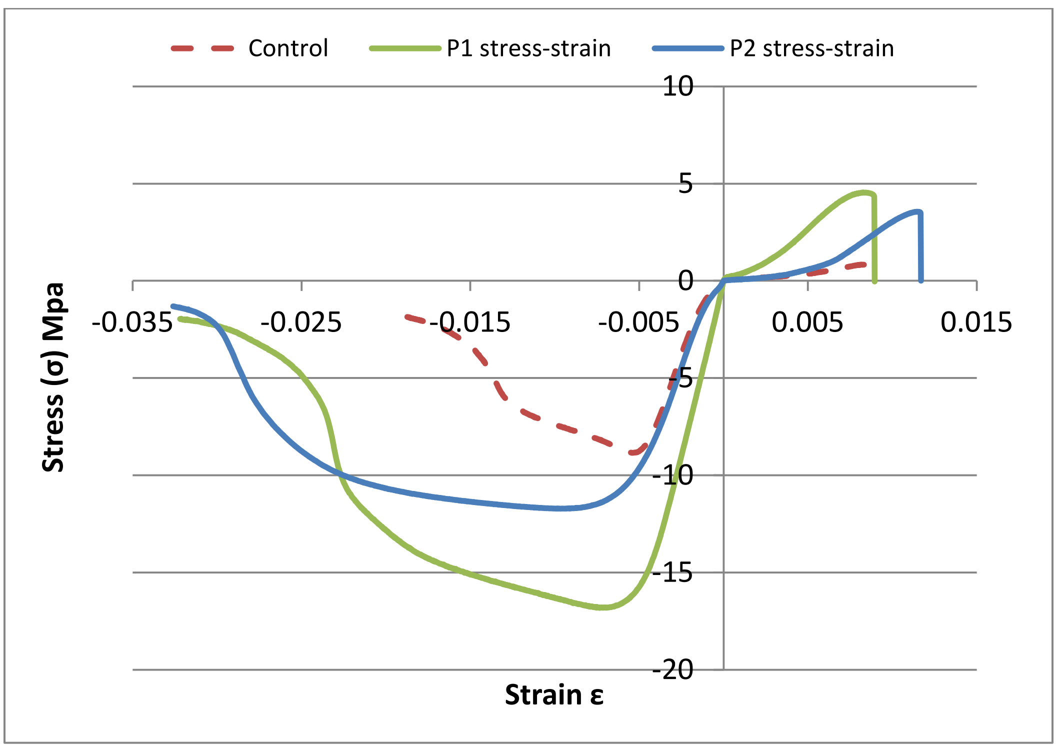

Figure 65 Stress strain curve for tensile and compression (a) Polyurethane glue infiltrate: P2 configuration (b) P2 with added Epoxy R2 configuration (c) Both Polyurethane configurations, P1 & P2

CHAPTER 9

CONCLUSIONS

Experimental work has been done to some mechanical characteristics for the 3DP process; however, the work published to date has been limited. This comprehensive study shows that infiltrates can significantly improve the mechanical characteristics, but performance degradation can also occur, which occurred with the Epsom salts infiltrate conditions (S1 and S1b in particular).

By conducting multiple test scenarios, it is now understood that this material does not react similar to other materials and cannot be easily predicted from just one study. It is also understood that the characteristics and strength of the parts cannot be confidently predicted by changing the build direction angle. The predictive curve for the strength of the parts for tensile and compression where built off the data for the 3 build angles and are illustrated in Figure 66 A&B.

(a)
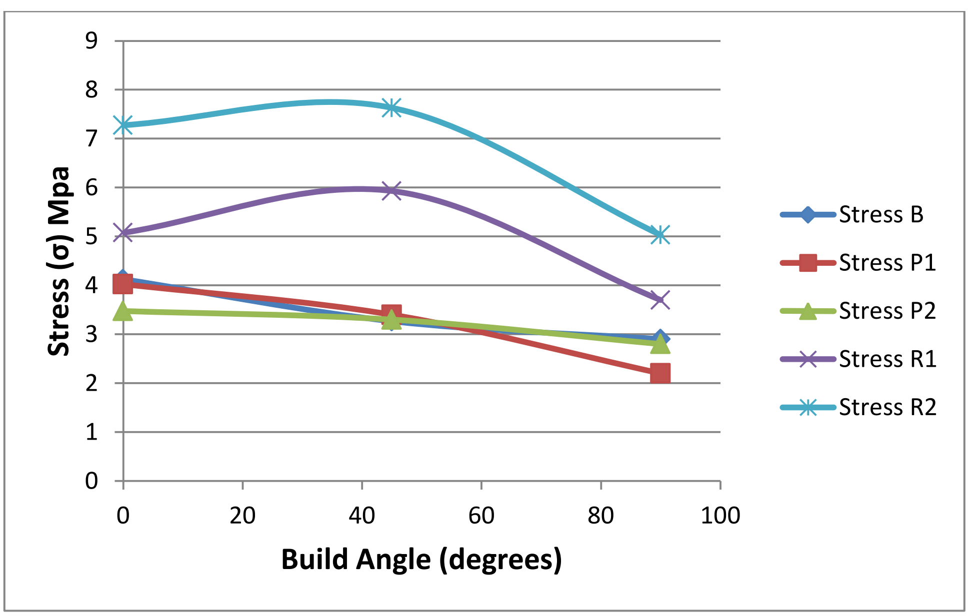

(b) 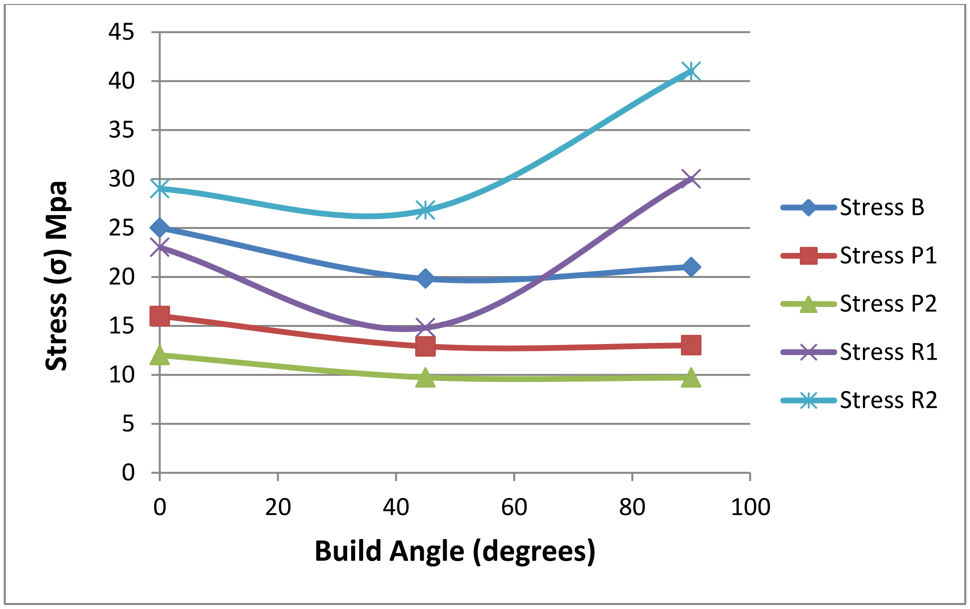

Figure 66 Predictive strength vs. Build angle (a) Tensile (b) Compression

To determine the performance characteristics for different base material and infiltrate options, and prior to performing optimization or virtual simulations, experimental work must be conducted to determine how the samples react to applied forces, as well as the failure points. The material-infiltrate performance characteristics vary per build orientation; hence, the necessity of determining the best and worst cases for designers. Ranked results from the study, illustrated in the Table 41, show that there are many of the build areas to view the variable and the outcome. Not one type and orientation is completely better than another as they all have their advantages. The ranked results summary can be used by designers as a decision matrix to understand the different resources, variable and how they interact with obtaining the results. It can be used in the planning stage to ensure that the correct resources are available to achieve the desired results or what types of results would be expected with the specific resources on hand. Immediately below the summary table, Table 42 is the legend and rational for ranking the items.

	Build Direction	Physical Strength			Absorption Depth *	Time			Materials			Safety	High Modulus			**Curve Fitting
		Tensile	Compressive	Flexural		Application	Cure	Extra	Build Needed	Binder used	Infiltrate cost		Tensile	Compressive	Flexural	
C	0															
	45															
	90															
B	0															
	45															
	90															
P1	0															
	45															
	90															
P2	0															
	45															
	90															
R1	0															
	45															
	90															
R2	0															
	45															
	90															
Rg***	0															
S1	0															
	45															
	90															
Sb	0															
	45															
	90															
S2	0															
	45															
	90															
S2b	0															
	45															
	90															

Table 41 Ranked Summary Table for Variables

RANK 1-5, 1=best	Physical Strength (Mpa)			Absorption Depth (mm)	Time			Materials		
	Tensile	Compressive	Flexural		Application (sec)	Cure	Extra (Mixing, safety setup)	Build Needed (High - Low)	Binder used (High -Low)	Infiltrate cost
1	7	29.6	15	4.62	28	10mins	Nothing	Min.	Min.	Nothing
2	5.25	22.2	12	3.78	51	1 hr	gloves			Common
3	3.5	14.8	9	2.94	74	8hrs	Gloves, smock			Store
4	1.75	7.4	6	2.10	97	1 day	PPE			Order
5	0	3	3	1.27	120	3 days	PPE and Mix	MAX	MAX	Rare

RANK 1-5, 1=best	Safety 1 =safest	High Modulus			Curve Fitting
		Tensile	Compressive	Flexural	
1	Nothing	1152	4317	2212	Linear
2	gloves	904	3834	1884	Mult. Linear
3	Gloves, smock	656	3351	1556	Linear/Poly
4	PPE	408	2868	1228	Mult. Poly
5	PPE, Hood	160	2385	900	More

*Absorption depth represents the different test specimens and not the build orientation, (0=Tensile, 45=Compression & 90=flexural)

**Curve fitting represents the different test specimens and not the build orientation, (0=Tensile, 45=Compression & 90=flexural)

*** Rg would always represent the 0 build orientation and the flexural test specimen

Table 42 Legend and rational for ranking of summary table

The table includes the ranking of each of the items, whether qualitative or quantitative. For all qualitative data, bounded levels were made to rank the observations. The lowest result of the category / column was subtracted from the highest recorded result. The resultant was then subdivided into 5 equal levels with the highest and lowest points being the ultimate bounds. By ranking them by this method, the table would reflect the possible large variation between the results. The grey squares in the chart are items that do not have data to allow them to be ranked. Also, in the table, there are some blacked out squares. These squares represent the results of the items that were observed to perform worse than the control specimen set. This is made to standout showing there is no benefit found by building a part at the particular build orientation, with the specific infiltrate for the type of testing.

The qualitative ranking was produced to understand the complexities within the choice of the level of effort need for the item. The curve fitting rankings reflect the types and amounts of stress-strain curves that can be observed while reacting to forces. Infiltrate cost is based more on the perceived availability and the speed at which the item can be replaced. The safety ranking is one of the most important items ranked and can be easily overlooked. For example, proper personal protective equipment (PPE) must be used, including a respirator when working with the two infiltrate type that raked as the strongest, cyanoacrylate and epoxy. If the proper PPE is not available, another infiltrate should be used or the post processing put on hold until the items can be obtained, as safety should always come first.

This experimental data related to the both the performance results and the resources needs to be collected to be able to develop a design-build optimization model. With respect to time and binder usage, for this experiment set, the horizontal build orientation is the most sensitive to design variants in the Z plane and overall had the least performance improvements. However, this would provide a conservative baseline. Specific testing is required for new machine-material-infiltrate combinations to calibrate a performance model and to develop a post-processing configuration database.

CHAPTER 10

FUTURE WORK

This study is only the beginning to help understand the reactions that some of the processing and post processing decision affecting the design decision. Short term future work include testing different intermittent angles, testing using double angles, and adding analysis under the stress statin curve. Testing the specimen built at intermittent angle will aid in better understanding and mapping the mechanical characteristics based on build orientation.

Currently, it is known that the three build orientations have an effect on the parts but the reaction of the material between the measured angles cannot be confidently predicted. As a supplement to this testing, double angles specimen can be integrated into the experiment to observe the reaction of multiplying the variable.

Reporting and analyzing the ultimate strengths are important but to add to the overall knowledge of this material, an area under the curve analysis should be done. The area under the stress strain curve is the strain energy density. This analysis shows insight on the toughness of the material to the amount of force absorbed, not just the acute force observed at failure.

Future work in general will include greater detail and focus toward standardizing specimen geometry for 3D printed or AM material, introducing and testing different infiltrates, and observing the curve reactions for more studies and physical tests.

Further understanding of the material and mechanical characteristics can be realized through different specimen geometry and testing methods. This study adapted standard geometry to help eliminate some of the bias and noise that could have been a factor with different geometry. The shape was used to reduce the number of specimens that needed to be built. While this was a way of limiting, the rectangular version could be made to see if the actual build rotation at the different directions could affect the parts. Also, the diameter of the specimen was chosen because that the deepest observed distance an infiltrate was observed. Similar results could be found using smaller specimens but tests must be conducted to ultimately understand the standard thickness that a standard test specimen must have for AM material. This would take into account for the optimum number of layers needed and distance between shells and support material. By having a standard, more technologies and material could be easily compared.

Along with different test geometry, additional physical testing should be performed to access the torsional, fatigue, notch strength and delamination characteristics for this infiltrate set. This complete test set should be conducted for the infiltrates covered and for all new infiltrates. To maximize the information and knowledge from the test runs, the use of stain gauges should be incorporated. With more data, trends might seem more evident among not only this technology but other AM technologies. With this added knowledge and trends, a robust package could be obtained to include simulation on how the materials and subsequent parts will react to forces. This simulation could lead to more development and usages for these printed parts. Scale models that could perform with scale failures could be used for demonstrations, testing and models. While this test is specific for this machine and material, other tests can be conducted and results can be calibrated with these. By using at least one of the mention infiltrates with the proper post processing, the results and ranking can be used any other subsequent tests conducted. Whether the tests were different infiltrates or application, the results could help to identify how they will react.

The curve fittings can help designers choose unique reactions that might mimic the reactions to force found in biomechanical testing. The curve fittings would help to produce items to scale or variants that could be used as testing with the advantage of predictive replication of the specimen. Combination of geometry and post processing would assist in altering reaction curves to the designers’ specifications.

APPENDIX A

ASTM tensile test specimens (adapted from ASTM std. B557-14)

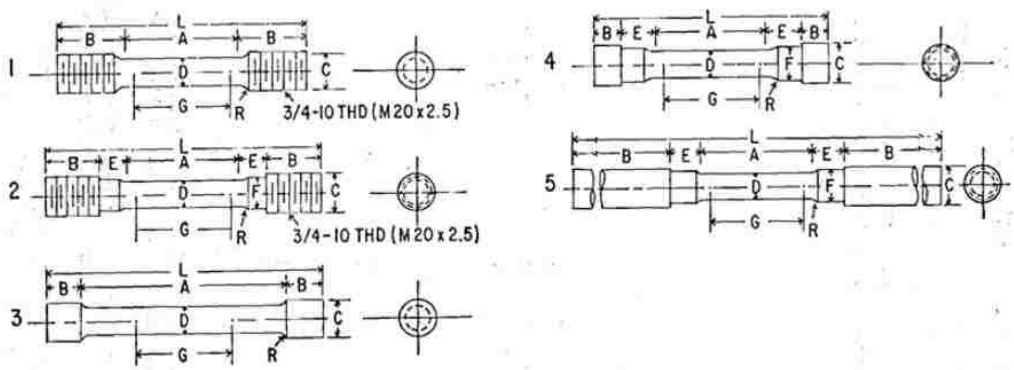

	Dimensions, in.				
	Specimen 1	Specimen 2	Specimen 3	Specimen 4	Specimen 5
G—Gage length	2.000 ± 0.005	2.000 ± 0.005	2.000 ± 0.005	2.000 ± 0.005	2.000 ± 0.005
D—Diameter (Note 1)	0.500 ± 0.010	0.500 ± 0.010	0.500 ± 0.010	0.500 ± 0.010	0.500 ± 0.010
R—Radius of fillet, min	⅜	⅜	1⁄16	⅜	⅜
A—Length of reduced section	2¼, min	2¼, min	4, approximately	2¼, min	2¼, min
L—Over-all length, approximate	5	5½	5½	4¾	9½
B—Length of end section (Note 2)	1⅜, approximately	1, approximately	¾, approximately	½, approximately	3, min
C—Diameter of end section	¾	¾	23⁄32	⅞	¾
E—Length of shoulder and fillet section, approximate	...	⅝	...	¾	⅝
F—Diameter of shoulder	...	⅝	...	⅝	19⁄32

APPENDIX B

Example of test run data –Tensile (B19)

File Path: C:\Users\Criterion C43 50 kN\Desktop\Dave\Test Run 19 10-14-2014 4 58 35 PM\DAQ- Crosshead, ... - (Timed).csv

	Crosshead	Load	Time		Crosshead	Load	Time		Crosshead	Load	Time
	mm	kN	msec		mm	kN	msec		mm	kN	msec
1	0.003752192	0.00101318	130	53	0.17706773	0.01867634	5330	105	0.35038326	0.034426	10530
2	0.007087473	0.00162827	230	54	0.18034344	0.01861809	5430	106	0.35371853	0.03631953	10630
3	0.010363197	0.00473826	330	55	0.18367873	0.02125138	5530	107	0.35705382	0.03492219	10730
4	0.013758037	0.00519123	430	56	0.18701401	0.01863573	5630	108	0.36032955	0.03666288	10830
5	0.017033759	0.00520642	530	57	0.1903493	0.01739647	5730	109	0.36372439	0.03646095	10930
6	0.020369042	0.00676695	630	58	0.19368457	0.01915232	5830	110	0.36700012	0.03754767	11030
7	0.023704324	0.00897065	730	59	0.19701985	0.01877871	5930	111	0.37039493	0.03853771	11130
8	0.027039605	0.00760741	830	60	0.20035513	0.01830355	6030	112	0.37367066	0.03666975	11230
9	0.030374886	0.00918722	930	61	0.2036904	0.01985636	6130	113	0.37700593	0.03778725	11330
10	0.033710166	0.00820953	1030	62	0.20702569	0.01983204	6230	114	0.38040077	0.03816357	11430
11	0.037105008	0.00967774	1130	63	0.21036097	0.02089233	6330	115	0.3836765	0.03865096	11530
12	0.040380732	0.0107704	1230	64	0.21369626	0.0205173	6430	116	0.38707134	0.0391391	11630
13	0.043716012	0.01060442	1330	65	0.21703154	0.01901438	6530	117	0.39034706	0.04015329	11730
14	0.047110851	0.01169472	1430	66	0.22030727	0.02150081	6630	118	0.39368236	0.03919995	11830
15	0.050386578	0.01063857	1530	67	0.2237021	0.02093406	6730	119	0.39701763	0.03865511	11930
16	0.053781416	0.01143457	1630	68	0.22709694	0.0216281	6830	120	0.40029336	0.03965521	12030
17	0.057057139	0.01182129	1730	69	0.23037267	0.02055265	6930	121	0.4036882	0.04046961	12130
18	0.06039242	0.01154707	1830	70	0.23376751	0.02266498	7030	122	0.4070235	0.04110439	12230
19	0.063727704	0.01096458	1930	71	0.23704323	0.02128342	7130	123	0.41035877	0.04193839	12330
20	0.067003428	0.01230492	2030	72	0.24043808	0.02243372	7230	124	0.41369404	0.04311137	12430
21	0.070398266	0.01170376	2130	73	0.24377335	0.02231107	7330	125	0.41702931	0.04721993	12530
22	0.073673989	0.01208103	2230	74	0.24704909	0.02280129	7430	126	0.42042416	0.04489644	12630
23	0.077068828	0.01292157	2330	75	0.25038436	0.02250477	7530	127	0.42369988	0.04600962	12730
24	0.080404112	0.01192752	2430	76	0.25371963	0.02350806	7630	128	0.42709472	0.04390149	12830
25	0.083679835	0.01620834	2530	77	0.25705493	0.02370358	7730	129	0.43042999	0.04383929	12930
26	0.087015113	0.01211127	2630	78	0.26033065	0.02663102	7830	130	0.43370575	0.04517888	13030
27	0.090350397	0.01188822	2730	79	0.26366592	0.02401885	7930	131	0.43710056	0.04282082	13130
28	0.093745242	0.01427194	2830	80	0.26706076	0.02459357	8030	132	0.44037629	0.04385277	13230
29	0.097020958	0.01272454	2930	81	0.27033649	0.0260377	8130	133	0.44377113	0.04700624	13330
30	0.100356243	0.01371866	3030	82	0.27373133	0.02666607	8230	134	0.44704686	0.04613032	13430
31	0.103691527	0.01394217	3130	83	0.27700706	0.02600813	8330	135	0.45038215	0.04804006	13530
32	0.106967251	0.01518462	3230	84	0.28034233	0.02593241	8430	136	0.45371742	0.04828118	13630
33	0.110362089	0.01240703	3330	85	0.2836776	0.0260748	8530	137	0.45699312	0.04769754	13730
34	0.113637812	0.01445238	3430	86	0.2870129	0.0269659	8630	138	0.46038796	0.04851096	13830
35	0.116973097	0.01442683	3530	87	0.29034817	0.02647046	8730	139	0.46366369	0.0470248	13930
36	0.120367928	0.01479278	3630	88	0.29368346	0.0267424	8830	140	0.46699899	0.0492749	14030
37	0.123703212	0.0141258	3730	89	0.29707831	0.02782667	8930	141	0.47039383	0.04821843	14130
38	0.127038496	0.01533743	3830	90	0.30035403	0.02840354	9030	142	0.47366956	0.04822215	14230
39	0.130373781	0.01440397	3930	91	0.3036893	0.02807267	9130	143	0.4770644	0.05120834	14330
40	0.133709065	0.01543226	4030	92	0.3070246	0.02892967	9230	144	0.48034012	0.05062099	14430
41	0.137103896	0.01491293	4130	93	0.31030033	0.03006729	9330	145	0.48367539	0.05074377	14530
42	0.14037962	0.01737046	4230	94	0.31369517	0.0296124	9430	146	0.48707024	0.05149483	14630
43	0.143774465	0.01522225	4330	95	0.31703044	0.02918105	9530	147	0.49034593	0.05011403	14730
44	0.147050188	0.01659821	4430	96	0.32036574	0.030268	9630	148	0.49374078	0.0516053	14830
45	0.150385473	0.01658739	4530	97	0.32376056	0.03044821	9730	149	0.49701653	0.05102567	14930
46	0.153720757	0.01643203	4630	98	0.32703628	0.03113382	9830	150	0.50041138	0.05283153	15030
47	0.156996481	0.01595969	4730	99	0.3304311	0.03398274	9930	151	0.50368707	0.05323508	15130
48	0.160391312	0.0168046	4830	100	0.33370685	0.03246453	10030	152	0.50702237	0.05431773	15230
49	0.163667035	0.01820715	4930	101	0.33710166	0.03253849	10130	153	0.51041722	0.05470368	15330
50	0.16706188	0.01806781	5030	102	0.34043696	0.033154	10230	154	0.51369291	0.05478062	15430
51	0.170337604	0.01759396	5130	103	0.34371269	0.03395935	10330	155	0.51708776	0.05520113	15530
52	0.173672888	0.01675931	5230	104	0.34710753	0.03390818	10430	156	0.52042305	0.0567812	15630

157	0.523758354	0.05600996	15730	212	0.70707971	0.09296342	21230	267	0.89034153	0.14411581	26730
158	0.527093594	0.05697728	15830	213	0.71035547	0.09448586	21330	268	0.89373637	0.14767406	26830
159	0.530369347	0.05992666	15930	214	0.71375031	0.09625106	21430	269	0.89701213	0.14991507	26930
160	0.533764192	0.05769509	16030	215	0.71702601	0.09893226	21530	270	0.90040697	0.15600291	27030
161	0.537099491	0.06016818	16130	216	0.72042085	0.09763876	21630	271	0.90368267	0.15179521	27130
162	0.540434732	0.05907352	16230	217	0.72375615	0.09861878	21730	272	0.90707751	0.15232556	27230
163	0.543770031	0.06044737	16330	218	0.72703185	0.09931184	21830	273	0.91041281	0.15330226	27330
164	0.547045784	0.05884256	16430	219	0.73042669	0.10009703	21930	274	0.91368851	0.15431354	27430
165	0.550381024	0.0593284	16530	220	0.73370244	0.1000657	22030	275	0.91708335	0.15594652	27530
166	0.553656777	0.06123115	16630	221	0.73709729	0.09693964	22130	276	0.9203591	0.15794603	27630
167	0.557051622	0.06066683	16730	222	0.74037298	0.10120142	22230	277	0.92375389	0.15866106	27730
168	0.560386921	0.06196057	16830	223	0.74370822	0.10343365	22330	278	0.92702959	0.15980026	27830
169	0.563662616	0.06149344	16930	224	0.74704352	0.10293253	22430	279	0.93036488	0.1652858	27930
170	0.567057403	0.06334956	17030	225	0.75031922	0.10355218	22530	280	0.93370018	0.16217534	28030
171	0.570333155	0.06255034	17130	226	0.75371406	0.10633538	22630	281	0.93703542	0.16461568	28130
172	0.573728001	0.06508153	17230	227	0.75698982	0.10634903	22730	282	0.94037072	0.16535655	28230
173	0.577003695	0.06592157	17330	228	0.76038466	0.10826172	22830	283	0.94364648	0.16672191	28330
174	0.580338994	0.06530428	17430	229	0.7637199	0.10839308	22930	284	0.94704132	0.16709279	28430
175	0.583733839	0.06976981	17530	230	0.7670552	0.10983884	23030	285	0.95037656	0.16884541	28530
176	0.587009534	0.06708337	17630	231	0.7703905	0.10897629	23130	286	0.95365231	0.17002255	28630
177	0.590404379	0.06780511	17730	232	0.77366619	0.11103897	23230	287	0.95704716	0.17236807	28730
178	0.593680132	0.06669272	17830	233	0.77706104	0.11159406	23330	288	0.96032285	0.17261438	28830
179	0.597015431	0.06966463	17930	234	0.78039634	0.11331219	23430	289	0.9637177	0.17528314	28930
180	0.600350671	0.07067652	18030	235	0.78367209	0.11465965	23530	290	0.967053	0.17549776	29030
181	0.60368597	0.07016448	18130	236	0.78706694	0.11509889	23630	291	0.97032875	0.17824756	29130
182	0.607080816	0.07145964	18230	237	0.79034263	0.11480672	23730	292	0.9737236	0.18124171	29230
183	0.610356568	0.07460025	18330	238	0.79367793	0.11730955	23830	293	0.97699929	0.17970615	29330
184	0.613751414	0.07361814	18430	239	0.79701323	0.11801692	23930	294	0.98039408	0.18230626	29430
185	0.617086655	0.07362254	18530	240	0.80034847	0.11962499	24030	295	0.98366989	0.18352509	29530
186	0.620421953	0.07399632	18630	241	0.80374331	0.11889058	24130	296	0.98700507	0.18476718	29630
187	0.623757252	0.07498947	18730	242	0.80701907	0.11588168	24230	297	0.99039997	0.18710638	29730
188	0.627092493	0.07533352	18830	243	0.81047346	0.12199992	24330	298	0.99367567	0.18639018	29830
189	0.630427792	0.07555605	18930	244	0.81374921	0.11901505	24430	299	0.99707057	0.18766396	29930
190	0.633763091	0.07710394	19030	245	0.81708445	0.12347284	24530	300	1.00034627	0.19016246	30030
191	0.637038785	0.07725038	19130	246	0.8203602	0.12557984	24630	301	1.00374117	0.19145239	30130
192	0.640374084	0.07619678	19230	247	0.8236955	0.12373577	24730	302	1.00707635	0.19257724	30230
193	0.643649837	0.07839259	19330	248	0.82709029	0.12794889	24830	303	1.01035216	0.19391118	30330
194	0.647044682	0.07978226	19430	249	0.83042553	0.12614741	24930	304	1.01374695	0.19367279	30430
195	0.650379923	0.0800598	19530	250	0.83376083	0.12772823	25030	305	1.01702276	0.19623656	30530
196	0.653715222	0.07988255	19630	251	0.83703652	0.12998747	25130	306	1.02035794	0.19832376	30630
197	0.657050463	0.08067049	19730	252	0.84037182	0.13144077	25230	307	1.02375285	0.19975883	30730
198	0.660326157	0.08081199	19830	253	0.84370712	0.13067519	25330	308	1.02702854	0.20010103	30830
199	0.663721003	0.08208691	19930	254	0.84698282	0.1286806	25430	309	1.03042345	0.20267085	30930
200	0.667056302	0.08282813	20030	255	0.85037766	0.13411754	25530	310	1.03369902	0.20306508	31030
201	0.670332054	0.08379333	20130	256	0.85371296	0.13886356	25630	311	1.03703444	0.20509613	31130
202	0.6737269	0.08480853	20230	257	0.85698871	0.13145622	25730	312	1.04036962	0.20592342	31230
203	0.677002594	0.08382052	20330	258	0.86038356	0.13577501	25830	313	1.04364543	0.21059689	31330
204	0.680397439	0.08698696	20430	259	0.86365925	0.13937485	25930	314	1.04704022	0.20943707	31430
205	0.683673192	0.08705204	20530	260	0.8670541	0.13864653	26030	315	1.05031603	0.21041449	31530
206	0.687068037	0.08773587	20630	261	0.8703894	0.14127867	26130	316	1.05371082	0.21130116	31630
207	0.690343732	0.09102708	20730	262	0.87366509	0.14229242	26230	317	1.057046	0.21245674	31730
208	0.693679031	0.09006732	20830	263	0.87705994	0.1423766	26330	318	1.06032181	0.21515782	31830
209	0.697073876	0.09091245	20930	264	0.88033569	0.14378918	26430	319	1.06365699	0.21624931	31930
210	0.70034957	0.09217523	21030	265	0.88373054	0.14466447	26530	320	1.06699229	0.21798065	32030
211	0.703744416	0.09234406	21130	266	0.88700623	0.14502995	26630	321	1.07038708	0.22007765	32130

322	1.073722495	0.21929672	32230	377	1.2570438	0.30133719	37730	432	1.44030561	0.39744882	43230
323	1.077057677	0.22169347	32330	378	1.26031961	0.30417813	37830	433	1.44364091	0.40066107	43330
324	1.080393093	0.22284198	32430	379	1.26365479	0.30447812	37930	434	1.44703581	0.40158679	43430
325	1.083668671	0.22382394	32530	380	1.26699009	0.30967355	38030	435	1.45031151	0.40444562	43530
326	1.087063574	0.2252077	32630	381	1.27032539	0.30875977	38130	436	1.45370641	0.40639865	43630
327	1.090339269	0.22416563	32730	382	1.27372029	0.31111066	38230	437	1.45698199	0.40755389	43730
328	1.093734172	0.22979468	32830	383	1.27699599	0.31115903	38330	438	1.46037689	0.40978519	43830
329	1.097069355	0.23186093	32930	384	1.28033129	0.31317648	38430	439	1.46371219	0.41120364	43930
330	1.100345165	0.233145	33030	385	1.28366647	0.31686353	38530	440	1.46698789	0.41389084	44030
331	1.103739953	0.23436186	33130	386	1.28700188	0.3177774	38630	441	1.47032319	0.41532272	44130
332	1.107015763	0.23475813	33230	387	1.29033707	0.32007327	38730	442	1.47365849	0.41737469	44230
333	1.110410551	0.24369283	33330	388	1.29367237	0.32039716	38830	443	1.47699378	0.41969879	44330
334	1.11374585	0.23810616	33430	389	1.29700766	0.32232083	38930	444	1.48032908	0.42173224	44430
335	1.117021544	0.23486421	33530	390	1.30034296	0.32264188	39030	445	1.48366427	0.42342038	44530
336	1.120416448	0.23968607	33630	391	1.30367826	0.32441071	39130	446	1.48699968	0.42294797	44630
337	1.123692142	0.24198123	33730	392	1.30701356	0.32905771	39230	447	1.49027526	0.42829346	44730
338	1.127027441	0.24259244	33830	393	1.31034874	0.32945273	39330	448	1.49372977	0.43110406	44830
339	1.130303135	0.2455231	33930	394	1.31374365	0.33109509	39430	449	1.49700546	0.43179346	44930
340	1.133638434	0.24810631	34030	395	1.31707895	0.3301091	39530	450	1.50034064	0.43419675	45030
341	1.137033221	0.24732088	34130	396	1.32035452	0.33380463	39630	451	1.50367606	0.43561429	45130
342	1.140309032	0.24509187	34230	397	1.32368994	0.33544226	39730	452	1.50701124	0.43704605	45230
343	1.143703819	0.25006952	34330	398	1.32696552	0.33621976	39830	453	1.51034654	0.4393046	45330
344	1.146979514	0.25137057	34430	399	1.33036042	0.33904199	39930	454	1.51368184	0.44147095	45430
345	1.150314813	0.25387566	34530	400	1.33363612	0.34125375	40030	455	1.51701714	0.44546152	45530
346	1.1537096	0.25411258	34630	401	1.33697153	0.34191513	40130	456	1.52035232	0.44575696	45630
347	1.15698541	0.25690552	34730	402	1.34036632	0.34501108	40230	457	1.52362813	0.44745871	45730
348	1.160380198	0.25463599	34830	403	1.34364201	0.34559875	40330	458	1.52702292	0.44956854	45830
349	1.163656008	0.25793338	34930	404	1.34697731	0.3473754	40430	459	1.53029873	0.45371808	45930
350	1.167050796	0.26235889	35030	405	1.35031261	0.35087134	40530	460	1.53369352	0.4547019	46030
351	1.170386095	0.26357303	35130	406	1.35364779	0.35161679	40630	461	1.53696933	0.45554971	46130
352	1.173661789	0.26399484	35230	407	1.3570427	0.35389655	40730	462	1.54030451	0.45747952	46230
353	1.177056693	0.26621756	35330	408	1.36031839	0.35985199	40830	463	1.54369941	0.46031094	46330
354	1.18033227	0.26680521	35430	409	1.36371329	0.35920856	40930	464	1.54697511	0.46136926	46430
355	1.183727174	0.26784491	35530	410	1.36698899	0.35963675	41030	465	1.55037001	0.46488806	46530
356	1.187062473	0.26980563	35630	411	1.37032429	0.35899918	41130	466	1.55364559	0.46577744	46630
357	1.190338284	0.27172369	35730	412	1.37365959	0.36105377	41230	467	1.55704049	0.4679808	46730
358	1.193733071	0.27081766	35830	413	1.37699489	0.36385187	41330	468	1.56037579	0.46968283	46830
359	1.197008765	0.27371417	35930	414	1.38038967	0.36590622	41430	469	1.5636516	0.47134464	46930
360	1.200403553	0.27601123	36030	415	1.38366548	0.36719278	41530	470	1.56704639	0.47498944	47030
361	1.203679363	0.27609839	36130	416	1.38700067	0.37005078	41630	471	1.57032209	0.4774245	47130
362	1.207014546	0.278302	36230	417	1.39033608	0.36887482	41730	472	1.57365738	0.47939059	47230
363	1.210349961	0.27928006	36330	418	1.39367126	0.37182541	41830	473	1.57699268	0.48097412	47330
364	1.213685144	0.28195639	36430	419	1.39700656	0.37459052	41930	474	1.58032787	0.48471805	47430
365	1.217080047	0.2831785	36530	420	1.40034186	0.37636371	42030	475	1.58366328	0.48578635	47530
366	1.220355742	0.28727399	36630	421	1.40373677	0.37868021	42130	476	1.58699846	0.4872005	47630
367	1.223691041	0.28694473	36730	422	1.40701234	0.37980844	42230	477	1.59033376	0.48910599	47730
368	1.22702634	0.28672748	36830	423	1.41034764	0.38180258	42330	478	1.59366906	0.49061493	47830
369	1.230361639	0.29091525	36930	424	1.41368294	0.38336313	42430	479	1.59700424	0.49447388	47930
370	1.233696821	0.2909288	37030	425	1.41701812	0.38509967	42530	480	1.60033966	0.49670355	48030
371	1.236972515	0.29238367	37130	426	1.42035354	0.38472568	42630	481	1.60367484	0.49784299	48130
372	1.240307814	0.29378647	37230	427	1.42368872	0.38846838	42730	482	1.60706975	0.50084872	48230
373	1.243643113	0.2967283	37330	428	1.42702414	0.39130063	42830	483	1.61034544	0.50192532	48330
374	1.246978412	0.30146875	37430	429	1.43035932	0.39284167	42930	484	1.61368074	0.50442496	48430
375	1.2503732	0.30255774	37530	430	1.43363513	0.39368057	43030	485	1.61701592	0.50686212	48530
376	1.25364901	0.29902414	37630	431	1.43702992	0.39708743	43130	486	1.62029173	0.50746143	48630

487	1.623686519	0.51069153	48730	542	1.80700794	0.63885223	54230
488	1.62696233	0.51320557	48830	543	1.81034324	0.64143573	54330
489	1.630297513	0.51455835	48930	544	1.81361905	0.64344757	54430
490	1.633632928	0.51747491	49030	545	1.81695423	0.64557507	54530
491	1.636968111	0.52031421	49130	546	1.82028953	0.65174152	54630
492	1.640363014	0.52214709	49230	547	1.82362483	0.65093829	54730
493	1.643638709	0.52481421	49330	548	1.82701973	0.65119391	54830
494	1.647033612	0.52749377	49430	549	1.83029531	0.65535895	54930
495	1.650368795	0.52934277	49530	550	1.83363073	0.65779248	55030
496	1.653644606	0.53074982	49630	551	1.83696591	0.6582179	55130
497	1.657039393	0.53381281	49730	552	1.84030121	0.66045612	55230
498	1.660315203	0.53789569	49830	553	1.84369599	0.66133667	55330
499	1.663709991	0.53594879	49930	554	1.84697181	0.66505579	55430
500	1.666985685	0.54049615	50030	555	1.8503071	0.66636774	55530
501	1.670320984	0.54247125	50130	556	1.85364229	0.66848395	55630
502	1.673656283	0.5470686	50230	557	1.85697759	0.6716983	55730
503	1.676931977	0.54674524	50330	558	1.86031288	0.67420911	55830
504	1.680326764	0.55034637	50430	559	1.86358858	0.6745885	55930
505	1.683662063	0.55254089	50530	560	1.86698337	0.67895984	56030
506	1.686997362	0.55430145	50630	561	1.87025918	0.67819958	56130
507	1.690332661	0.55750122	50730	562	1.87359448	0.6802348	56230
508	1.693667844	0.55983661	50830	563	1.87698938	0.68226416	56330
509	1.697003259	0.56031024	50930	564	1.88026496	0.68686578	56430
510	1.700278954	0.56447314	51030	565	1.88365986	0.68514691	56530
511	1.703673857	0.56544568	51130	566	1.88699516	0.68605933	56630
512	1.70700904	0.56979626	51230	567	1.89033046	0.68712384	56730
513	1.710344339	0.57029578	51330	568	1.89366564	0.6864707	56830
514	1.713679638	0.57288422	51430	569	1.89688196	-0.00735644	56940
515	1.716955332	0.57491608	51530				
516	1.720350119	0.57383264	51630				
517	1.72362593	0.58408844	51730				
518	1.726961113	0.58268127	51830				
519	1.730296528	0.58477722	51930				
520	1.733631711	0.58793628	52030				
521	1.736967126	0.58970459	52130				
522	1.740302308	0.59768872	52230				
523	1.743637607	0.59374774	52330				
524	1.747032395	0.59697607	52430				
525	1.750308205	0.59951886	52530				
526	1.753643388	0.60103375	52630				
527	1.756978803	0.60363354	52730				
528	1.760313986	0.60768567	52830				
529	1.763649401	0.6098631	52930				
530	1.766984584	0.61157257	53030				
531	1.770319766	0.61338116	53130				
532	1.773595577	0.61500885	53230				
533	1.776990364	0.61899597	53330				
534	1.780325663	0.62057153	53430				
535	1.783601358	0.62223737	53530				
536	1.786996261	0.62643121	53630				
537	1.790271956	0.62791351	53730				
538	1.793666859	0.6298985	53830				
539	1.797002042	0.63193365	53930				
540	1.800337457	0.63452789	54030				
541	1.80367264	0.63665442	54130				

APPENDIX C

Tensile Response Curve to Failure

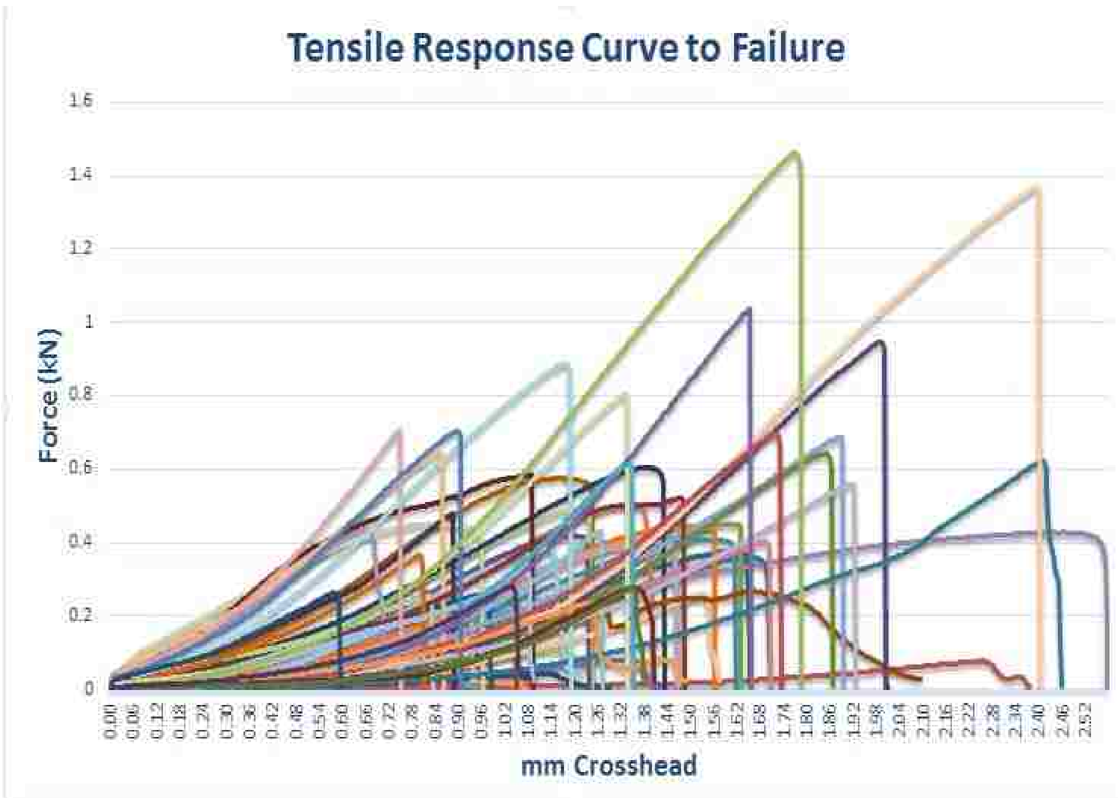

APPENDIX D

Example of test run data –Compression (B90)

File Path: C:\Users\Criterion C43 50 kN\Desktop\Dave\Test Run 90 9-30-2014 5 19 16 PM\DAQ- Crosshead, … - (Timed).txt

Test: Dave Compression

Test Run: Test Run 90

Date: 9/30/2014 5:17:38 PM

	Crosshead	Load	Time		Crosshead	Load	Time		Crosshead	Load	Time
	mm	kN	msec		mm	kN	msec		mm	kN	msec
1	0.002859	-0.000033	140	55	0.137759	0.186167	5540	109	0.272659	0.861111	10940
2	0.005360	0.003841	240	56	0.140320	0.193420	5640	110	0.275161	0.878473	11040
3	0.007802	0.007890	340	57	0.142822	0.200259	5740	111	0.277662	0.897233	11140
4	0.010363	0.012331	440	58	0.145323	0.206611	5840	112	0.280164	0.916007	11240
5	0.012865	0.014680	540	59	0.147824	0.212545	5940	113	0.282665	0.936080	11340
6	0.015307	0.017859	640	60	0.150326	0.220557	6040	114	0.285107	0.953982	11440
7	0.017808	0.020652	740	61	0.152768	0.227250	6140	115	0.287668	0.974075	11540
8	0.020369	0.023502	840	62	0.155210	0.235487	6240	116	0.290169	0.992946	11640
9	0.022811	0.024497	940	63	0.157771	0.242252	6340	117	0.292671	1.011830	11740
10	0.025312	0.027606	1040	64	0.160272	0.249850	6440	118	0.295172	1.032345	11840
11	0.027873	0.030545	1140	65	0.162714	0.257654	6540	119	0.297674	1.051236	11940
12	0.030315	0.032953	1240	66	0.165275	0.266539	6640	120	0.300116	1.070847	12040
13	0.032817	0.034343	1340	67	0.167777	0.274897	6740	121	0.302677	1.090771	12140
14	0.035378	0.035739	1440	68	0.170218	0.283289	6840	122	0.305178	1.110244	12240
15	0.037820	0.038585	1540	69	0.172720	0.292472	6940	123	0.307680	1.130257	12340
16	0.040321	0.040613	1640	70	0.175221	0.301885	7040	124	0.310181	1.149304	12440
17	0.042823	0.042237	1740	71	0.177723	0.310849	7140	125	0.312683	1.170156	12540
18	0.045384	0.044338	1840	72	0.180224	0.321333	7240	126	0.315125	1.188873	12640
19	0.047826	0.046949	1940	73	0.182785	0.330441	7340	127	0.317626	1.206727	12740
20	0.050327	0.049313	2040	74	0.185227	0.340901	7440	128	0.320187	1.227684	12840
21	0.052828	0.051123	2140	75	0.187729	0.350438	7540	129	0.322629	1.247179	12940
22	0.055270	0.053604	2240	76	0.190290	0.361707	7640	130	0.325130	1.266600	13040
23	0.057772	0.055992	2340	77	0.192791	0.373118	7740	131	0.327691	1.287263	13140
24	0.060333	0.058460	2440	78	0.195233	0.383757	7840	132	0.330133	1.306982	13240
25	0.062775	0.060460	2540	79	0.197794	0.395754	7940	133	0.332575	1.326397	13340
26	0.065276	0.063212	2640	80	0.200296	0.407625	8040	134	0.335136	1.346561	13440
27	0.067778	0.065773	2740	81	0.202737	0.420493	8140	135	0.337697	1.365863	13540
28	0.070279	0.068987	2840	82	0.205298	0.431952	8240	136	0.340139	1.384526	13640
29	0.072721	0.071423	2940	83	0.207800	0.445222	8340	137	0.342641	1.404511	13740
30	0.075282	0.074645	3040	84	0.210242	0.457101	8440	138	0.345142	1.423728	13840
31	0.077784	0.076929	3140	85	0.212803	0.471366	8540	139	0.347584	1.442464	13940
32	0.080285	0.079772	3240	86	0.215304	0.484951	8640	140	0.350085	1.462871	14040
33	0.082786	0.083872	3340	87	0.217746	0.499121	8740	141	0.352587	1.482333	14140
34	0.085347	0.087530	3440	88	0.220248	0.513261	8840	142	0.355088	1.502004	14240
35	0.087789	0.090710	3540	89	0.222809	0.526891	8940	143	0.357530	1.521309	14340
36	0.090291	0.093571	3640	90	0.225251	0.542332	9040	144	0.360091	1.540738	14440
37	0.092852	0.098616	3740	91	0.227752	0.557271	9140	145	0.362593	1.559610	14540
38	0.095294	0.102252	3840	92	0.230313	0.572745	9240	146	0.365035	1.579256	14640
39	0.097795	0.105724	3940	93	0.232815	0.587889	9340	147	0.367536	1.596853	14740
40	0.100356	0.109736	4040	94	0.235256	0.602610	9440	148	0.370097	1.616612	14840
41	0.102798	0.114530	4140	95	0.237758	0.619253	9540	149	0.372539	1.635354	14940
42	0.105300	0.117943	4240	96	0.240259	0.635155	9640	150	0.375041	1.654814	15040
43	0.107801	0.122710	4340	97	0.242701	0.650866	9740	151	0.377602	1.674347	15140
44	0.110303	0.128390	4440	98	0.245203	0.667190	9840	152	0.380043	1.692188	15240
45	0.112804	0.132009	4540	99	0.247764	0.684400	9940	153	0.382545	1.711208	15340
46	0.115305	0.136864	4640	100	0.250206	0.701164	10040	154	0.385106	1.730811	15440
47	0.117866	0.141512	4740	101	0.252707	0.716685	10140	155	0.387607	1.748585	15540
48	0.120308	0.146865	4840	102	0.255209	0.735528	10240	156	0.390049	1.766235	15640
49	0.122810	0.152172	4940	103	0.257710	0.751782	10340	157	0.392610	1.786662	15740
50	0.125311	0.157466	5040	104	0.260152	0.769281	10440	158	0.395112	1.803727	15840
51	0.127813	0.163127	5140	105	0.262653	0.788004	10540	159	0.397554	1.821404	15940
52	0.130255	0.168887	5240	106	0.265155	0.806078	10640	160	0.400055	1.840946	16040
53	0.132816	0.174590	5340	107	0.267597	0.823796	10740	161	0.402616	1.858020	16140
54	0.135317	0.180994	5440	108	0.270158	0.842341	10840	162	0.405058	1.873951	16240

163	0.407560	1.893095	16340	229	0.572418	2.812098	22940	295	0.737276	3.180698	29540
164	0.410121	1.911282	16440	230	0.574860	2.821435	23040	296	0.739718	3.182733	29640
165	0.412562	1.927921	16540	231	0.577361	2.831008	23140	297	0.742279	3.185416	29740
166	0.415004	1.945699	16640	232	0.579922	2.841785	23240	298	0.744780	3.186812	29840
167	0.417565	1.963454	16740	233	0.582424	2.850416	23340	299	0.747222	3.188167	29940
168	0.420067	1.981661	16840	234	0.584865	2.858592	23440	300	0.749783	3.191603	30040
169	0.422509	1.998225	16940	235	0.587426	2.867453	23540	301	0.752285	3.192717	30140
170	0.425070	2.015247	17040	236	0.589928	2.876789	23640	302	0.754727	3.192807	30240
171	0.427571	2.031777	17140	237	0.592370	2.884875	23740	303	0.757228	3.194410	30340
172	0.430013	2.048677	17240	238	0.594871	2.894066	23840	304	0.759789	3.196207	30440
173	0.432574	2.065435	17340	239	0.597432	2.902508	23940	305	0.762291	3.195557	30540
174	0.435076	2.082725	17440	240	0.599874	2.910476	24040	306	0.764792	3.198011	30640
175	0.437518	2.098883	17540	241	0.602376	2.918012	24140	307	0.767353	3.199715	30740
176	0.440019	2.115468	17640	242	0.604937	2.927081	24240	308	0.769795	3.200477	30840
177	0.442520	2.132984	17740	243	0.607379	2.934617	24340	309	0.772237	3.201074	30940
178	0.444962	2.148259	17840	244	0.609821	2.942178	24440	310	0.774798	3.201521	31040
179	0.447464	2.163217	17940	245	0.612381	2.949613	24540	311	0.777359	3.204081	31140
180	0.449965	2.180391	18040	246	0.614883	2.957948	24640	312	0.779801	3.202358	31240
181	0.452467	2.196344	18140	247	0.617325	2.965206	24740	313	0.782362	3.203795	31340
182	0.454968	2.210653	18240	248	0.619886	2.972869	24840	314	0.784863	3.203933	31440
183	0.457470	2.227769	18340	249	0.622387	2.979162	24940	315	0.787305	3.202683	31540
184	0.459971	2.243469	18440	250	0.624829	2.986805	25040	316	0.789807	3.203866	31640
185	0.462413	2.258267	18540	251	0.627331	2.993599	25140	317	0.792368	3.204220	31740
186	0.464914	2.274791	18640	252	0.629892	3.000434	25240	318	0.794810	3.204877	31840
187	0.467475	2.290147	18740	253	0.632334	3.006661	25340	319	0.797311	3.204417	31940
188	0.469977	2.304163	18840	254	0.634835	3.013807	25440	320	0.799812	3.204714	32040
189	0.472478	2.319640	18940	255	0.637337	3.020927	25540	321	0.802314	3.203886	32140
190	0.475039	2.334662	19040	256	0.639838	3.025889	25640	322	0.804756	3.203706	32240
191	0.477481	2.349258	19140	257	0.642220	3.031266	25740	323	0.807317	3.204333	32340
192	0.479923	2.362980	19240	258	0.644781	3.038737	25840	324	0.809818	3.204224	32440
193	0.482484	2.379417	19340	259	0.647283	3.044123	25940	325	0.812260	3.203382	32540
194	0.484986	2.393275	19440	260	0.649784	3.049032	26040	326	0.814762	3.203906	32640
195	0.487428	2.406729	19540	261	0.652286	3.055021	26140	327	0.817323	3.203653	32740
196	0.489989	2.420897	19640	262	0.654787	3.060661	26240	328	0.819765	3.203044	32840
197	0.492490	2.435949	19740	263	0.657229	3.065369	26340	329	0.822266	3.202461	32940
198	0.494932	2.448585	19840	264	0.659790	3.072397	26440	330	0.824827	3.202729	33040
199	0.497493	2.462771	19940	265	0.662292	3.077951	26540	331	0.827269	3.200794	33140
200	0.499994	2.476336	20040	266	0.664793	3.082211	26640	332	0.829770	3.200281	33240
201	0.502436	2.489557	20140	267	0.667295	3.086406	26740	333	0.832331	3.200957	33340
202	0.504938	2.503515	20240	268	0.669856	3.091955	26840	334	0.834773	3.200514	33440
203	0.507499	2.516943	20340	269	0.672357	3.096343	26940	335	0.837215	3.198942	33540
204	0.509941	2.529201	20440	270	0.674799	3.100790	27040	336	0.839717	3.198013	33640
205	0.512442	2.541783	20540	271	0.677360	3.106040	27140	337	0.842278	3.197792	33740
206	0.514944	2.556139	20640	272	0.679861	3.110436	27240	338	0.844720	3.196834	33840
207	0.517445	2.567447	20740	273	0.682303	3.114137	27340	339	0.847281	3.196256	33940
208	0.519947	2.580225	20840	274	0.684864	3.119081	27440	340	0.849782	3.195104	34040
209	0.522448	2.592609	20940	275	0.687366	3.123061	27540	341	0.852224	3.192889	34140
210	0.524950	2.605432	21040	276	0.689808	3.126814	27640	342	0.854725	3.192050	34240
211	0.527391	2.615547	21140	277	0.692309	3.129446	27740	343	0.857287	3.191939	34340
212	0.529893	2.628314	21240	278	0.694870	3.134348	27840	344	0.859788	3.190372	34440
213	0.532454	2.640234	21340	279	0.697312	3.136748	27940	345	0.862230	3.188983	34540
214	0.534896	2.652513	21440	280	0.699814	3.140225	28040	346	0.864791	3.189064	34640
215	0.537397	2.663248	21540	281	0.702375	3.145070	28140	347	0.867292	3.187525	34740
216	0.539958	2.674921	21640	282	0.704816	3.147756	28240	348	0.869794	3.185733	34840
217	0.542400	2.686793	21740	283	0.707258	3.150559	28340	349	0.872355	3.184984	34940
218	0.544842	2.696833	21840	284	0.709819	3.154391	28440	350	0.874856	3.183817	35040
219	0.547403	2.708232	21940	285	0.712321	3.156355	28540	351	0.877298	3.182254	35140
220	0.549905	2.719598	22040	286	0.714822	3.158975	28640	352	0.879859	3.181045	35240
221	0.552346	2.729782	22140	287	0.717324	3.162811	28740	353	0.882361	3.180082	35340
222	0.554848	2.740905	22240	288	0.719825	3.164955	28840	354	0.884743	3.176546	35440
223	0.557349	2.751076	22340	289	0.722267	3.167079	28940	355	0.887304	3.176446	35540
224	0.559851	2.761520	22440	290	0.724769	3.169897	29040	356	0.889865	3.174221	35640
225	0.562352	2.771231	22540	291	0.727330	3.173285	29140	357	0.892307	3.172386	35740
226	0.564913	2.782242	22640	292	0.729772	3.174420	29240	358	0.894749	3.170642	35840
227	0.567355	2.791635	22740	293	0.732273	3.175900	29340	359	0.897310	3.169665	35940
228	0.569857	2.801107	22840	294	0.734774	3.179628	29440	360	0.899811	3.167346	36040

361	0.902253	3.165999	36140	427	1.067350	3.025737	42740	493	1.232387	2.844154	49340
362	0.904814	3.165802	36240	428	1.069851	3.023326	42840	494	1.234828	2.840399	49440
363	0.907316	3.162883	36340	429	1.072353	3.019754	42940	495	1.237330	2.836833	49540
364	0.909758	3.160729	36440	430	1.074854	3.017183	43040	496	1.239891	2.834191	49640
365	0.912259	3.159392	36540	431	1.077355	3.015093	43140	497	1.242333	2.830753	49740
366	0.914820	3.157942	36640	432	1.079857	3.012209	43240	498	1.244834	2.827551	49840
367	0.917262	3.155272	36740	433	1.082299	3.009625	43340	499	1.247395	2.823628	49940
368	0.919763	3.153460	36840	434	1.084860	3.008592	43440	500	1.249897	2.820651	50040
369	0.922324	3.152576	36940	435	1.087302	3.005310	43540	501	1.252339	2.816823	50140
370	0.924766	3.150537	37040	436	1.089803	3.003260	43640	502	1.254900	2.813654	50240
371	0.927268	3.148763	37140	437	1.092364	3.000733	43740	503	1.257342	2.811174	50340
372	0.929769	3.147276	37240	438	1.094866	2.998023	43840	504	1.259843	2.807327	50440
373	0.932271	3.143886	37340	439	1.097308	2.995365	43940	505	1.262404	2.803646	50540
374	0.934713	3.142265	37440	440	1.099809	2.993107	44040	506	1.264906	2.800439	50640
375	0.937274	3.140544	37540	441	1.102310	2.990937	44140	507	1.267407	2.796339	50740
376	0.939775	3.138961	37640	442	1.104812	2.988501	44240	508	1.269909	2.791970	50840
377	0.942217	3.136181	37740	443	1.107314	2.986252	44340	509	1.272410	2.789432	50940
378	0.944778	3.134926	37840	444	1.109874	2.983293	44440	510	1.274852	2.785137	51040
379	0.947280	3.133860	37940	445	1.112317	2.980947	44540	511	1.277353	2.780679	51140
380	0.949721	3.131487	38040	446	1.114818	2.977524	44640	512	1.279914	2.778438	51240
381	0.952283	3.128773	38140	447	1.117379	2.975440	44740	513	1.282356	2.773139	51340
382	0.954784	3.127818	38240	448	1.119821	2.972195	44840	514	1.284858	2.768626	51440
383	0.957285	3.124685	38340	449	1.122322	2.969562	44940	515	1.287419	2.766842	51540
384	0.959787	3.122516	38440	450	1.124883	2.968022	45040	516	1.289861	2.762114	51640
385	0.962348	3.120646	38540	451	1.127325	2.965664	45140	517	1.292362	2.757186	51740
386	0.964849	3.118276	38640	452	1.129767	2.962768	45240	518	1.294923	2.754153	51840
387	0.967291	3.116327	38740	453	1.132328	2.959837	45340	519	1.297365	2.750373	51940
388	0.969852	3.114774	38840	454	1.134830	2.956332	45440	520	1.299866	2.746563	52040
389	0.972354	3.112992	38940	455	1.137331	2.953866	45540	521	1.302368	2.739630	52140
390	0.974796	3.110149	39040	456	1.139833	2.950790	45640	522	1.304869	2.738894	52240
391	0.977297	3.108286	39140	457	1.142334	2.948260	45740	523	1.307371	2.734885	52340
392	0.979858	3.105070	39240	458	1.144835	2.945409	45840	524	1.309872	2.730346	52440
393	0.982300	3.103532	39340	459	1.147277	2.942971	45940	525	1.312433	2.727033	52540
394	0.984801	3.101407	39440	460	1.149838	2.940800	46040	526	1.314875	2.721625	52640
395	0.987362	3.099382	39540	461	1.152340	2.937669	46140	527	1.317377	2.717620	52740
396	0.989804	3.096978	39640	462	1.154841	2.933881	46240	528	1.319938	2.712158	52840
397	0.992306	3.094884	39740	463	1.157343	2.931063	46340	529	1.322380	2.708614	52940
398	0.994867	3.093865	39840	464	1.159844	2.928679	46440	530	1.324881	2.703679	53040
399	0.997309	3.090429	39940	465	1.162346	2.925961	46540	531	1.327383	2.699941	53140
400	0.999751	3.087844	40040	466	1.164907	2.923758	46640	532	1.329884	2.695063	53240
401	1.002312	3.085797	40140	467	1.167408	2.921186	46740	533	1.332385	2.689969	53340
402	1.004813	3.082657	40240	468	1.169850	2.917907	46840	534	1.334887	2.685601	53440
403	1.007315	3.080845	40340	469	1.172352	2.915561	46940	535	1.337448	2.681678	53540
404	1.009816	3.078339	40440	470	1.174913	2.913391	47040	536	1.339890	2.675562	53640
405	1.012317	3.077113	40540	471	1.177354	2.910336	47140	537	1.342391	2.672115	53740
406	1.014759	3.074060	40640	472	1.179796	2.906938	47240	538	1.344893	2.666899	53840
407	1.017261	3.072251	40740	473	1.182357	2.904169	47340	539	1.347394	2.662544	53940
408	1.019822	3.069855	40840	474	1.184859	2.900717	47440	540	1.349896	2.657753	54040
409	1.022323	3.068051	40940	475	1.187360	2.897192	47540	541	1.352397	2.653052	54140
410	1.024765	3.064584	41040	476	1.189862	2.895674	47640	542	1.354899	2.647867	54240
411	1.027326	3.062908	41140	477	1.192363	2.892861	47740	543	1.357400	2.642235	54340
412	1.029828	3.060539	41240	478	1.194805	2.889587	47840	544	1.359961	2.638454	54440
413	1.032270	3.058155	41340	479	1.197366	2.886197	47940	545	1.362463	2.633400	54540
414	1.034771	3.055947	41440	480	1.199868	2.883850	48040	546	1.364964	2.628006	54640
415	1.037332	3.054589	41540	481	1.202310	2.880558	48140	547	1.367465	2.622588	54740
416	1.039774	3.052166	41640	482	1.204870	2.877497	48240	548	1.369967	2.617604	54840
417	1.042276	3.049389	41740	483	1.207372	2.874948	48340	549	1.372409	2.611502	54940
418	1.044836	3.048091	41840	484	1.209814	2.871688	48440	550	1.374910	2.606151	55040
419	1.047278	3.044083	41940	485	1.212315	2.868389	48540	551	1.377412	2.601080	55140
420	1.049780	3.042136	42040	486	1.214876	2.866574	48640	552	1.379913	2.595499	55240
421	1.052341	3.040388	42140	487	1.217318	2.862885	48740	553	1.382415	2.589646	55340
422	1.054842	3.037289	42240	488	1.219820	2.859002	48840	554	1.384916	2.583944	55440
423	1.057284	3.035431	42340	489	1.222381	2.855860	48940	555	1.387418	2.577356	55540
424	1.059845	3.032111	42440	490	1.224882	2.852804	49040	556	1.389860	2.571998	55640
425	1.062347	3.031108	42540	491	1.227324	2.849318	49140	557	1.392420	2.566844	55740
426	1.064789	3.028398	42640	492	1.229885	2.846392	49240	558	1.394922	2.561017	55840

559	1.397364	2.554599	55940	625	1.562520	2.061719	62540	691	1.727557	1.507545	69140
560	1.399925	2.549141	56040	626	1.565021	2.054289	62640	692	1.730058	1.499641	69240
561	1.402426	2.543212	56140	627	1.567523	2.045057	62740	693	1.732560	1.491411	69340
562	1.404928	2.535076	56240	628	1.569965	2.036621	62840	694	1.735061	1.483449	69440
563	1.407429	2.529671	56340	629	1.572526	2.029163	62940	695	1.737563	1.475181	69540
564	1.409990	2.524958	56440	630	1.574968	2.020951	63040	696	1.740064	1.466183	69640
565	1.412432	2.518249	56540	631	1.577469	2.012876	63140	697	1.742566	1.458898	69740
566	1.414934	2.511114	56640	632	1.579971	2.005102	63240	698	1.745067	1.450857	69840
567	1.417435	2.505324	56740	633	1.582472	1.996160	63340	699	1.747509	1.441488	69940
568	1.419937	2.498414	56840	634	1.584973	1.986675	63440	700	1.750070	1.434772	70040
569	1.422379	2.491414	56940	635	1.587475	1.979893	63540	701	1.752631	1.426119	70140
570	1.424939	2.485443	57040	636	1.590036	1.972894	63640	702	1.755073	1.418188	70240
571	1.427441	2.477783	57140	637	1.592478	1.963906	63740	703	1.757574	1.408810	70340
572	1.429942	2.471227	57240	638	1.594979	1.956208	63840	704	1.760135	1.401732	70440
573	1.432444	2.464031	57340	639	1.597540	1.947171	63940	705	1.762577	1.392439	70540
574	1.434945	2.458105	57440	640	1.599982	1.939397	64040	706	1.765079	1.384530	70640
575	1.437447	2.450386	57540	641	1.602484	1.930542	64140	707	1.767580	1.377049	70740
576	1.439889	2.443953	57640	642	1.605045	1.923031	64240	708	1.770082	1.368472	70840
577	1.442450	2.436813	57740	643	1.607546	1.914894	64340	709	1.772583	1.360039	70940
578	1.444951	2.429360	57840	644	1.609988	1.905564	64440	710	1.775085	1.351546	71040
579	1.447393	2.422490	57940	645	1.612549	1.897133	64540	711	1.777586	1.344715	71140
580	1.449954	2.414243	58040	646	1.615051	1.889559	64640	712	1.780028	1.335414	71240
581	1.452456	2.408337	58140	647	1.617492	1.880225	64740	713	1.782589	1.327764	71340
582	1.454898	2.400223	58240	648	1.619994	1.872526	64840	714	1.785090	1.320285	71440
583	1.457458	2.393162	58340	649	1.622555	1.863598	64940	715	1.787592	1.311630	71540
584	1.460020	2.386463	58440	650	1.624997	1.854704	65040	716	1.790093	1.303283	71640
585	1.462461	2.377867	58540	651	1.627498	1.846374	65140	717	1.792654	1.296831	71740
586	1.464963	2.370313	58640	652	1.630059	1.837126	65240	718	1.795096	1.289201	71840
587	1.467464	2.363992	58740	653	1.632501	1.828778	65340	719	1.797598	1.281532	71940
588	1.469966	2.356039	58840	654	1.635003	1.819904	65440	720	1.800159	1.273919	72040
589	1.472467	2.347037	58940	655	1.637564	1.812162	65540	721	1.802660	1.265374	72140
590	1.474969	2.341913	59040	656	1.640006	1.802307	65640	722	1.805162	1.257682	72240
591	1.477470	2.334508	59140	657	1.642507	1.794292	65740	723	1.807663	1.249820	72340
592	1.479912	2.327433	59240	658	1.645068	1.784663	65840	724	1.810165	1.242790	72440
593	1.482473	2.320134	59340	659	1.647570	1.775655	65940	725	1.812606	1.234856	72540
594	1.484975	2.312014	59440	660	1.650012	1.766758	66040	726	1.815108	1.228064	72640
595	1.487416	2.304483	59540	661	1.652573	1.756986	66140	727	1.817669	1.219095	72740
596	1.489918	2.296947	59640	662	1.655074	1.748779	66240	728	1.820111	1.211138	72840
597	1.492479	2.290053	59740	663	1.657516	1.740534	66340	729	1.822612	1.202016	72940
598	1.494921	2.281530	59840	664	1.660077	1.731884	66440	730	1.825173	1.195567	73040
599	1.497482	2.273770	59940	665	1.662578	1.723091	66540	731	1.827615	1.185932	73140
600	1.499983	2.266672	60040	666	1.665020	1.712908	66640	732	1.830057	1.179349	73240
601	1.502485	2.258865	60140	667	1.667522	1.704443	66740	733	1.832618	1.172096	73340
602	1.504927	2.250485	60240	668	1.670083	1.695996	66840	734	1.835120	1.164125	73440
603	1.507488	2.243194	60340	669	1.672584	1.686858	66940	735	1.837621	1.156536	73540
604	1.509989	2.235571	60440	670	1.675026	1.679147	67040	736	1.840123	1.150502	73640
605	1.512491	2.227071	60540	671	1.677528	1.669792	67140	737	1.842624	1.142759	73740
606	1.514992	2.220613	60640	672	1.680088	1.661449	67240	738	1.845066	1.134232	73840
607	1.517494	2.211595	60740	673	1.682531	1.652901	67340	739	1.847627	1.127742	73940
608	1.519935	2.203272	60840	674	1.685032	1.644740	67440	740	1.850188	1.120699	74040
609	1.522496	2.196375	60940	675	1.687593	1.636526	67540	741	1.852630	1.113136	74140
610	1.524998	2.187505	61040	676	1.690035	1.629004	67640	742	1.855131	1.106181	74240
611	1.527440	2.179627	61140	677	1.692596	1.619927	67740	743	1.857692	1.099128	74340
612	1.529941	2.171097	61240	678	1.695097	1.611823	67840	744	1.860134	1.091294	74440
613	1.532502	2.163317	61340	679	1.697539	1.603673	67940	745	1.862576	1.084206	74540
614	1.534944	2.154663	61440	680	1.700041	1.595859	68040	746	1.865137	1.077231	74640
615	1.537446	2.146116	61540	681	1.702602	1.588585	68140	747	1.867639	1.069994	74740
616	1.540007	2.138171	61640	682	1.705103	1.580129	68240	748	1.870080	1.062551	74840
617	1.542449	2.129361	61740	683	1.707545	1.571432	68340	749	1.872642	1.056333	74940
618	1.544950	2.121074	61840	684	1.710106	1.563740	68440	750	1.875143	1.049244	75040
619	1.547511	2.113236	61940	685	1.712608	1.555791	68540	751	1.877644	1.041041	75140
620	1.550013	2.104575	62040	686	1.715049	1.547507	68640	752	1.880146	1.035152	75240
621	1.552454	2.096186	62140	687	1.717611	1.539567	68740	753	1.882707	1.028949	75340
622	1.555016	2.087821	62240	688	1.720112	1.531626	68840	754	1.885149	1.021118	75440
623	1.557517	2.079393	62340	689	1.722554	1.522722	68940	755	1.887650	1.014575	75540
624	1.560018	2.070760	62440	690	1.725055	1.515366	69040	756	1.890211	1.008738	75640

757	1.892653	1.002645	75740	823	2.057631	0.764298	82340
758	1.895155	0.995781	75840	824	2.060192	0.762905	82440
759	1.897716	0.990827	75940	825	2.062693	0.760763	82540
760	1.900217	0.985533	76040	826	2.065135	0.758646	82640
761	1.902659	0.978519	76140	827	2.067696	0.756704	82740
762	1.905220	0.973048	76240	828	2.070197	0.755264	82840
763	1.907722	0.967171	76340	829	2.072699	0.752478	82940
764	1.910104	0.963393	76440	830	2.075200	0.751156	83040
765	1.912665	0.957178	76540	831	2.077702	0.749903	83140
766	1.915166	0.952690	76640	832	2.080203	0.747740	83240
767	1.917668	0.947324	76740	833	2.082705	0.745480	83340
768	1.920169	0.942208	76840	834	2.085206	0.744567	83440
769	1.922671	0.938313	76940	835	2.087708	0.742250	83540
770	1.925113	0.933299	77040	836	2.090209	0.740096	83640
771	1.927614	0.928303	77140	837	2.092770	0.738746	83740
772	1.930175	0.924545	77240	838	2.095272	0.736922	83840
773	1.932677	0.919371	77340	839	2.097714	0.735359	83940
774	1.935119	0.915543	77440	840	2.100215	0.733022	84040
775	1.937679	0.911189	77540	841	2.102716	0.731923	84140
776	1.940181	0.906122	77640	842	2.105158	0.729924	84240
777	1.942623	0.901516	77740	843	2.107660	0.728231	84340
778	1.945184	0.897778	77840	844	2.110221	0.726579	84440
779	1.947685	0.893264	77940	845	2.112663	0.724872	84540
780	1.950127	0.888071	78040	846	2.115164	0.723098	84640
781	1.952629	0.884899	78140	847	2.117725	0.722407	84740
782	1.955190	0.880827	78240	848	2.120167	0.721012	84840
783	1.957632	0.876564	78340	849	2.122669	0.719468	84940
784	1.960133	0.872757	78440	850	2.124932	0.716961	85040
785	1.962694	0.870826	78540				
786	1.965196	0.866832	78640				
787	1.967638	0.863150	78740				
788	1.970139	0.858838	78840				
789	1.972700	0.856266	78940				
790	1.975142	0.852324	79040				
791	1.977643	0.849619	79140				
792	1.980204	0.846010	79240				
793	1.982646	0.842451	79340				
794	1.985148	0.838088	79440				
795	1.987709	0.836051	79540				
796	1.990210	0.833885	79640				
797	1.992652	0.829931	79740				
798	1.995213	0.826736	79840				
799	1.997715	0.824344	79940				
800	2.000216	0.820806	80040				
801	2.002717	0.818155	80140				
802	2.005219	0.815367	80240				
803	2.007661	0.812984	80340				
804	2.010162	0.809853	80440				
805	2.012723	0.807458	80540				
806	2.015165	0.804555	80640				
807	2.017667	0.802033	80740				
808	2.020168	0.798808	80840				
809	2.022670	0.796638	80940				
810	2.025111	0.793521	81040				
811	2.027672	0.791123	81140				
812	2.030174	0.788049	81240				
813	2.032616	0.786248	81340				
814	2.035177	0.783516	81440				
815	2.037678	0.781980	81540				
816	2.040120	0.778883	81640				
817	2.042681	0.777750	81740				
818	2.045183	0.775310	81840				
819	2.047684	0.773146	81940				
820	2.050186	0.771241	82040				
821	2.052747	0.768404	82140				
822	2.055189	0.767036	82240				

APPENDIX E

Compression Response Curve to Failure

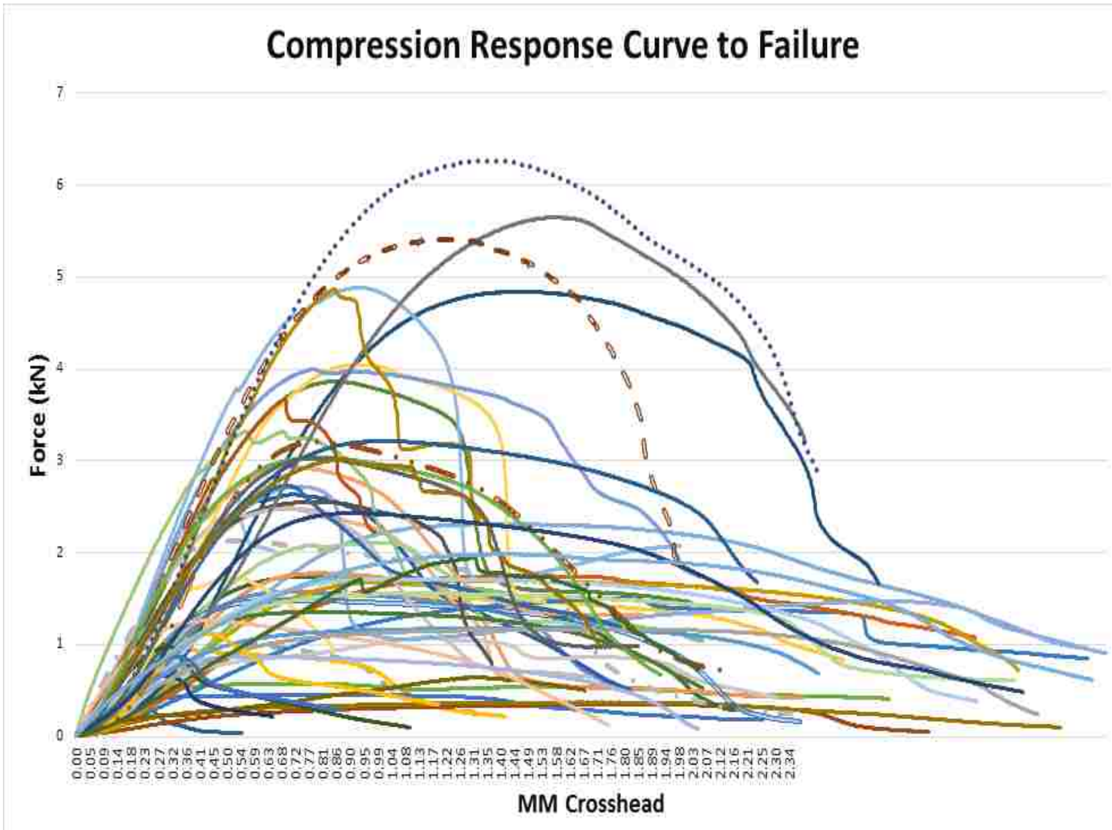

APPENDIX F

Example of test run data –Flexural (B19)

File Path: C:\Users\Criterion 150kn-2\Desktop\dave\Test Run 28 10-15-2014 12 30 12 AM\DAQ-Crosshead, … - (Timed).csv

	Crosshead	Load	Time		Crosshead	Load	Time		Crosshead	Load	Time
	mm	kN	sec		mm	kN	sec		mm	kN	sec
1	0.0041992	0.0053713	0.14	63	0.2107910	0.0282101	6.34	125	0.4175293	0.0446069	12.54
2	0.0075195	0.0051343	0.24	64	0.2140625	0.0274278	6.44	126	0.4207520	0.0435411	12.64
3	0.0109863	0.0058117	0.34	65	0.2174805	0.0282151	6.54	127	0.4241699	0.0441549	12.74
4	0.0142090	0.0073430	0.44	66	0.2207520	0.0278697	6.64	128	0.4273926	0.0442463	12.84
5	0.0176758	0.0080386	0.54	67	0.2241699	0.0264368	6.74	129	0.4307617	0.0452166	12.94
6	0.0208984	0.0087841	0.64	68	0.2273926	0.0286916	6.84	130	0.4339844	0.0438594	13.04
7	0.0243164	0.0102312	0.74	69	0.2307617	0.0285943	6.94	131	0.4374023	0.0441914	13.14
8	0.0275391	0.0074017	0.84	70	0.2340332	0.0278357	7.04	132	0.4406250	0.0455406	13.24
9	0.0308594	0.0082849	0.94	71	0.2374512	0.0310737	7.14	133	0.4440918	0.0471777	13.34
10	0.0340820	0.0115427	1.04	72	0.2406738	0.0285938	7.24	134	0.4473144	0.0469226	13.44
11	0.0375000	0.0096419	1.14	73	0.2441406	0.0294018	7.34	135	0.4507813	0.0461832	13.54
12	0.0407715	0.0083819	1.24	74	0.2474121	0.0294385	7.44	136	0.4540528	0.0456692	13.64
13	0.0441895	0.0088451	1.34	75	0.2508301	0.0306499	7.54	137	0.4574707	0.0479656	13.74
14	0.0474609	0.0098318	1.44	76	0.2541016	0.0306398	7.64	138	0.4606934	0.0484970	13.84
15	0.0508789	0.0119190	1.54	77	0.2575683	0.0297508	7.74	139	0.4640625	0.0478435	13.94
16	0.0541504	0.0117864	1.64	78	0.2607422	0.0315557	7.84	140	0.4672852	0.0467281	14.04
17	0.0576172	0.0108320	1.74	79	0.2641114	0.0327113	7.94	141	0.4707031	0.0482650	14.14
18	0.0607910	0.0124828	1.84	80	0.2673340	0.0327788	8.04	142	0.4739258	0.0451612	14.24
19	0.0641602	0.0114850	1.94	81	0.2707519	0.0324134	8.14	143	0.4773926	0.0474585	14.34
20	0.0673828	0.0116739	2.04	82	0.2739746	0.0334898	8.24	144	0.4806641	0.0478715	14.44
21	0.0708008	0.0131793	2.14	83	0.2774414	0.0337138	8.34	145	0.4841309	0.0480717	14.54
22	0.0740723	0.0130143	2.24	84	0.2806641	0.0354556	8.44	146	0.4873535	0.0476264	14.64
23	0.0774902	0.0153750	2.34	85	0.2841309	0.0342473	8.54	147	0.4908203	0.0485546	14.74
24	0.0807617	0.0157354	2.44	86	0.2873535	0.0352708	8.64	148	0.4940429	0.0492120	14.84
25	0.0841797	0.0163306	2.54	87	0.2908203	0.0313832	8.74	149	0.4974121	0.0488467	14.94
26	0.0874512	0.0147115	2.64	88	0.2940430	0.0341043	8.84	150	0.5006348	0.0491084	15.04
27	0.0908691	0.0142717	2.74	89	0.2974121	0.0346407	8.94	151	0.5040527	0.0484643	15.14
28	0.0940918	0.0160649	2.84	90	0.3006348	0.0357686	9.04	152	0.5073242	0.0502141	15.24
29	0.0975098	0.0163560	2.94	91	0.3040528	0.0366940	9.14	153	0.5107422	0.0494866	15.34
30	0.1006836	0.0167843	3.04	92	0.3073242	0.0345401	9.24	154	0.5140136	0.0495292	15.44
31	0.1041016	0.0178503	3.14	93	0.3107910	0.0373464	9.34	155	0.5174316	0.0513015	15.54
32	0.1073242	0.0149430	3.24	94	0.3140137	0.0355603	9.44	156	0.5207031	0.0501440	15.64
33	0.1107910	0.0187252	3.34	95	0.3174805	0.0355011	9.54	157	0.5241211	0.0520560	15.74
34	0.1140625	0.0171618	3.44	96	0.3207520	0.0366375	9.64	158	0.5273438	0.0493294	15.84
35	0.1174805	0.0171291	3.54	97	0.3241699	0.0376631	9.74	159	0.5307129	0.0505287	15.94
36	0.1207520	0.0180240	3.64	98	0.3273926	0.0376865	9.84	160	0.5339844	0.0506954	16.04
37	0.1241699	0.0202564	3.74	99	0.3308106	0.0376461	9.94	161	0.5374023	0.0508388	16.14
38	0.1273926	0.0160860	3.84	100	0.3340332	0.0387115	10.04	162	0.5406250	0.0523884	16.24
39	0.1307617	0.0162441	3.94	101	0.3374512	0.0371156	10.14	163	0.5440918	0.0533870	16.34
40	0.1339844	0.0187548	4.04	102	0.3406738	0.0395572	10.24	164	0.5473633	0.0508813	16.44
41	0.1374023	0.0205311	4.14	103	0.3441406	0.0370262	10.34	165	0.5507813	0.0530461	16.54
42	0.1406738	0.0206704	4.24	104	0.3474121	0.0381811	10.44	166	0.5540527	0.0507537	16.64
43	0.1440918	0.0202077	4.34	105	0.3508301	0.0383728	10.54	167	0.5574707	0.0515267	16.74
44	0.1473633	0.0209293	4.44	106	0.3541016	0.0398709	10.64	168	0.5606934	0.0533762	16.84
45	0.1508301	0.0208913	4.54	107	0.3575195	0.0401765	10.74	169	0.5640625	0.0521692	16.94
46	0.1541016	0.0210461	4.64	108	0.3607422	0.0399517	10.84	170	0.5672852	0.0539049	17.04
47	0.1575195	0.0218221	4.74	109	0.3641113	0.0401561	10.94	171	0.5707520	0.0536091	17.14
48	0.1607422	0.0232997	4.84	110	0.3673340	0.0412595	11.04	172	0.5740234	0.0533297	17.24
49	0.1641113	0.0230123	4.94	111	0.3707519	0.0409530	11.14	173	0.5774414	0.0521228	17.34
50	0.1673828	0.0248593	5.04	112	0.3740234	0.0407383	11.24	174	0.5806640	0.0525923	17.44
51	0.1707520	0.0240698	5.14	113	0.3774414	0.0405879	11.34	175	0.5841309	0.0544152	17.54
52	0.1740234	0.0247234	5.24	114	0.3807129	0.0412226	11.44	176	0.5874023	0.0535085	17.64
53	0.1774902	0.0243806	5.34	115	0.3841309	0.0409725	11.54	177	0.5908203	0.0546460	17.74
54	0.1807129	0.0235192	5.44	116	0.3874024	0.0422546	11.64	178	0.5939942	0.0533794	17.84
55	0.1841797	0.0226079	5.54	117	0.3908203	0.0431599	11.74	179	0.5973633	0.0539308	17.94
56	0.1874512	0.0249641	5.64	118	0.3940430	0.0417260	11.84	180	0.6006347	0.0544260	18.04
57	0.1908691	0.0259038	5.74	119	0.3974609	0.0433906	11.94	181	0.6040039	0.0550897	18.14
58	0.1940918	0.0255202	5.84	120	0.4006836	0.0419362	12.04	182	0.6072266	0.0543143	18.24
59	0.1974609	0.0234949	5.94	121	0.4041016	0.0436583	12.14	183	0.6106934	0.0552054	18.34
60	0.2006836	0.0262823	6.04	122	0.4073242	0.0420729	12.24	184	0.6139649	0.0544591	18.44
61	0.2041016	0.0260220	6.14	123	0.4107910	0.0453943	12.34	185	0.6174317	0.0546812	18.54
62	0.2073242	0.0261558	6.24	124	0.4140625	0.0433457	12.44	186	0.6207031	0.0560421	18.64

187	0.6241211	0.0547477	18.74
188	0.6272949	0.0544224	18.84
189	0.6307129	0.0539197	18.94
190	0.6339356	0.0533129	19.04
191	0.6373535	0.0547450	19.14
192	0.6406250	0.0553581	19.24
193	0.6440918	0.0542854	19.34
194	0.6473144	0.0560639	19.44
195	0.6507813	0.0548866	19.54
196	0.6540527	0.0561290	19.64
197	0.6574707	0.0556352	19.74
198	0.6606933	0.0566226	19.84
199	0.6641113	0.0555110	19.94
200	0.6673340	0.0557097	20.04
201	0.6707031	0.0571447	20.14
202	0.6739746	0.0563973	20.24
203	0.6774414	0.0560035	20.34
204	0.6806641	0.0564840	20.44
205	0.6841308	0.0551496	20.54
206	0.6873535	0.0558770	20.64
207	0.6908203	0.0574038	20.74
208	0.6940430	0.0573760	20.84
209	0.6974121	0.0561545	20.94
210	0.7006348	0.0568981	21.04
211	0.7040527	0.0565414	21.14
212	0.7073242	0.0561349	21.24
213	0.7107910	0.0576673	21.34
214	0.7140137	0.0560428	21.44
215	0.7174805	0.0582342	21.54
216	0.7207519	0.0560908	21.64
217	0.7241699	0.0560131	21.74
218	0.7273926	0.0568271	21.84
219	0.7307617	0.0553284	21.94
220	0.7340332	0.0561539	22.04
221	0.7374512	0.0578513	22.14
222	0.7406739	0.0561371	22.24
223	0.7441406	0.0578060	22.34
224	0.7473633	0.0560003	22.44
225	0.7507812	0.0588175	22.54
226	0.7540528	0.0572730	22.64
227	0.7574707	0.0572030	22.74
228	0.7606934	0.0571226	22.84
229	0.7640625	0.0565527	22.94
230	0.7672852	0.0569776	23.04
231	0.7707031	0.0568634	23.14
232	0.7739746	0.0558387	23.24
233	0.7774414	0.0554999	23.34
234	0.7806641	0.0558459	23.44
235	0.7840820	0.0566101	23.54
236	0.7873535	0.0555485	23.64
237	0.7907715	0.0561995	23.74
238	0.7939941	0.0540175	23.84
239	0.7973633	0.0554689	23.94
240	0.8006347	0.0538553	24.04
241	0.8040527	0.0510306	24.14
242	0.8072754	0.0094436	24.24
243	0.8107422	0.0073550	24.34
244	0.8130859	0.0083519	24.42

APPENDIX G

Flexural Response Curve to Failure

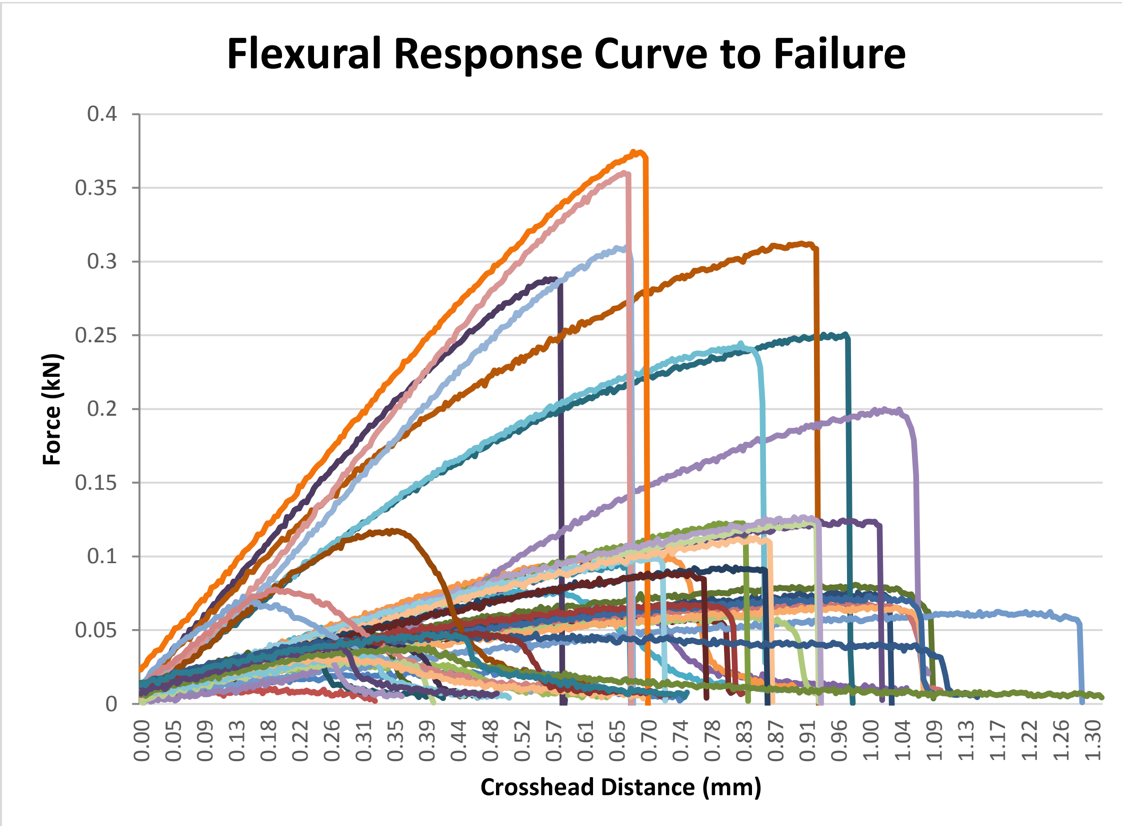

APPENDIX H

Polyurethane (P2) – Tensile Stress-Strain Curve

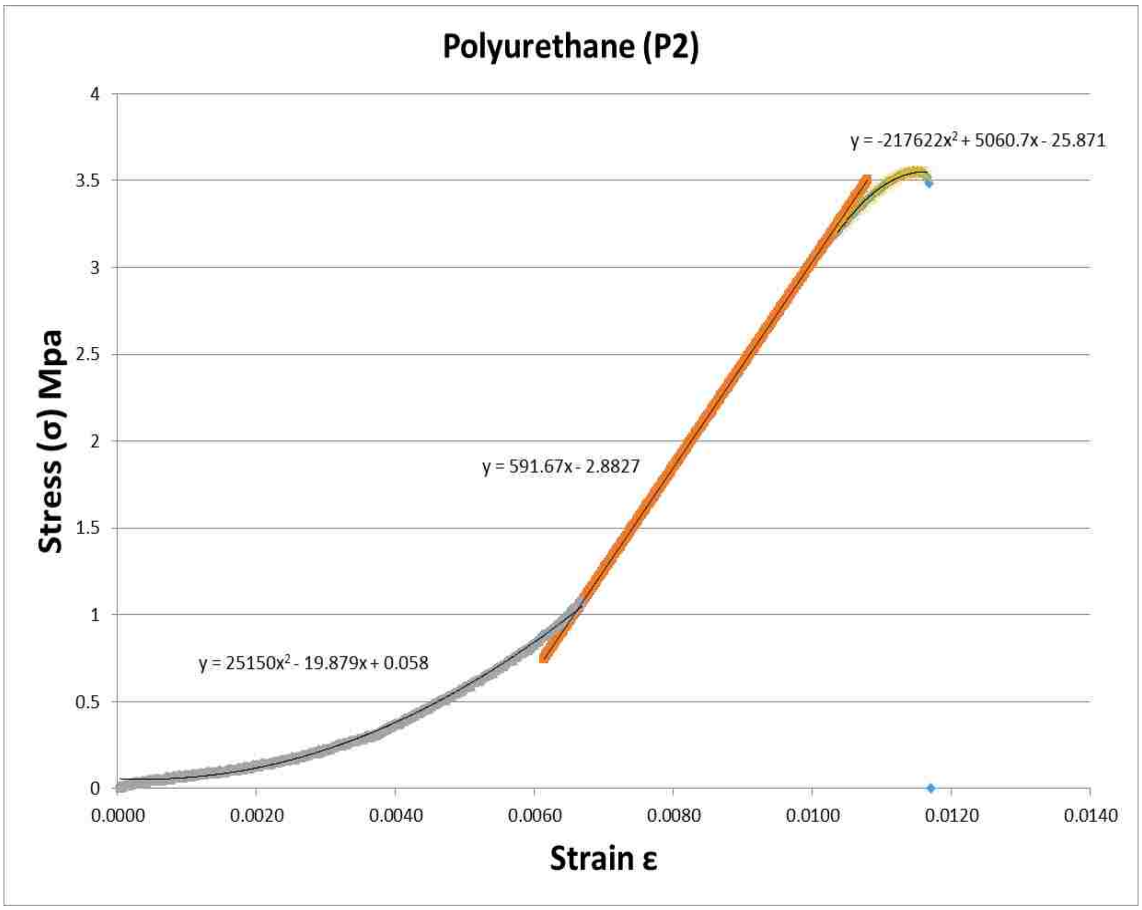

APPENDIX I

Control and Epoxy (R1) – Tensile Stress-Strain Curve

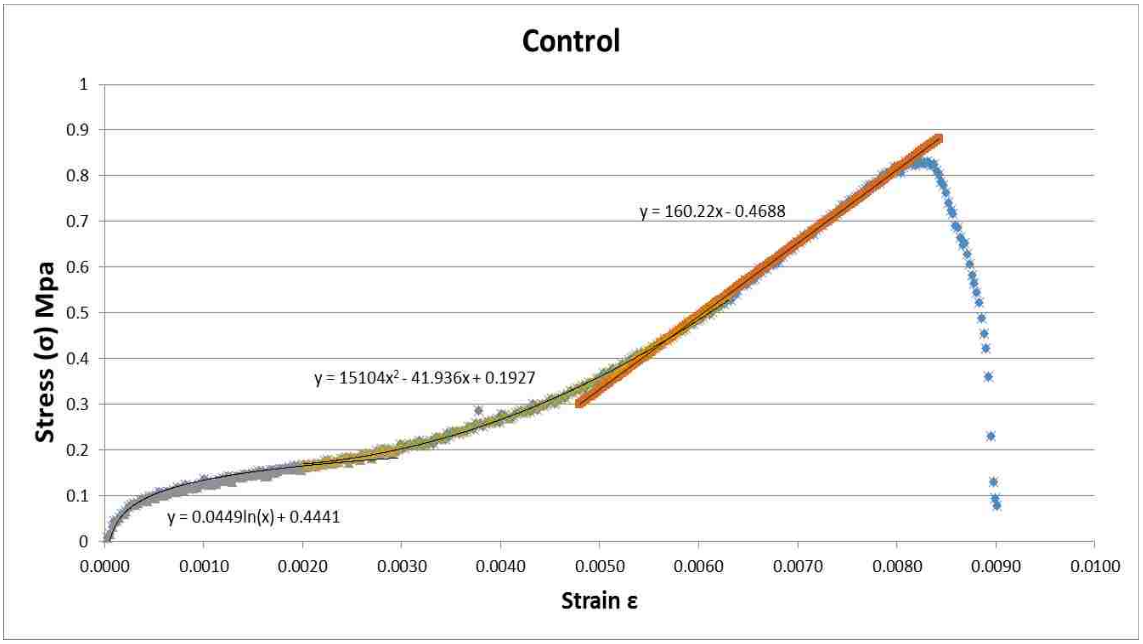

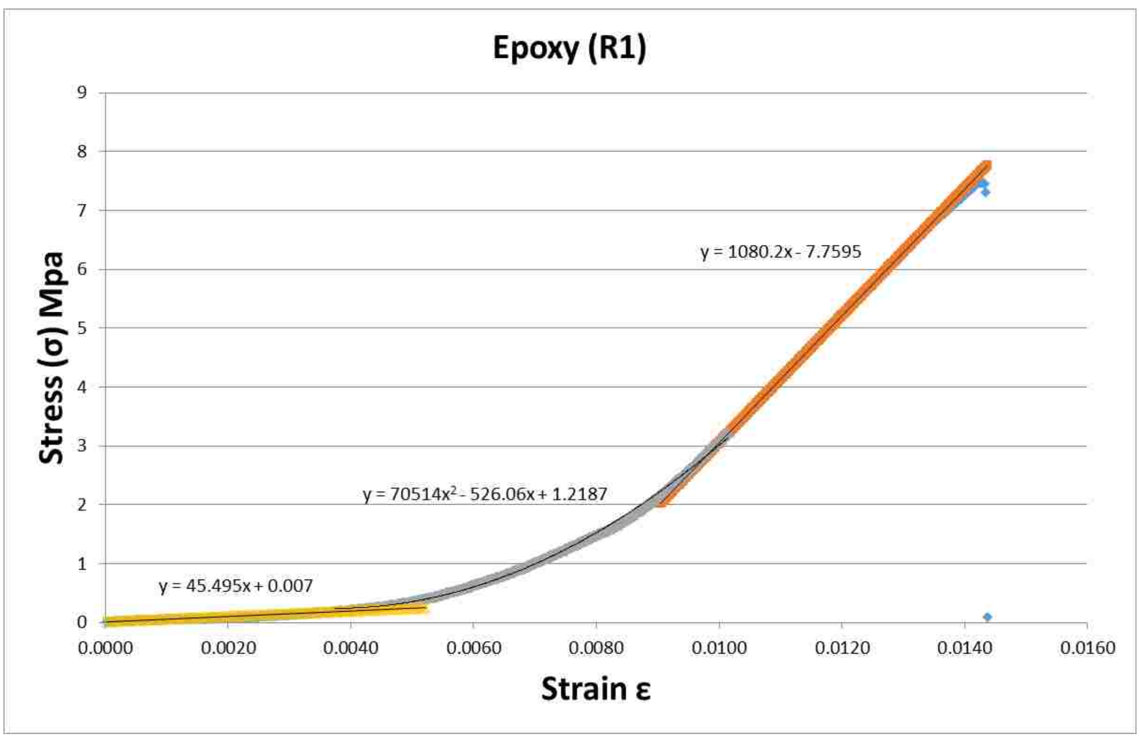

APPENDIX J

(P2) (R1) Cyanoacrylate and Control - Compressive Stress-Strain Curves

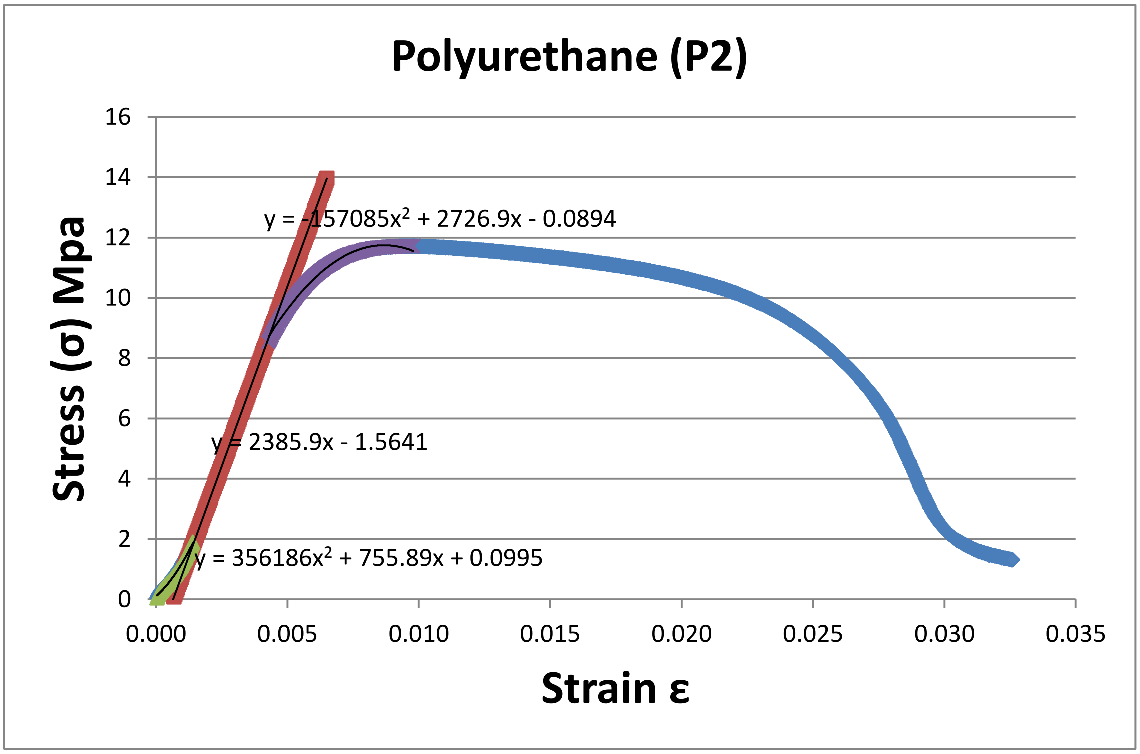

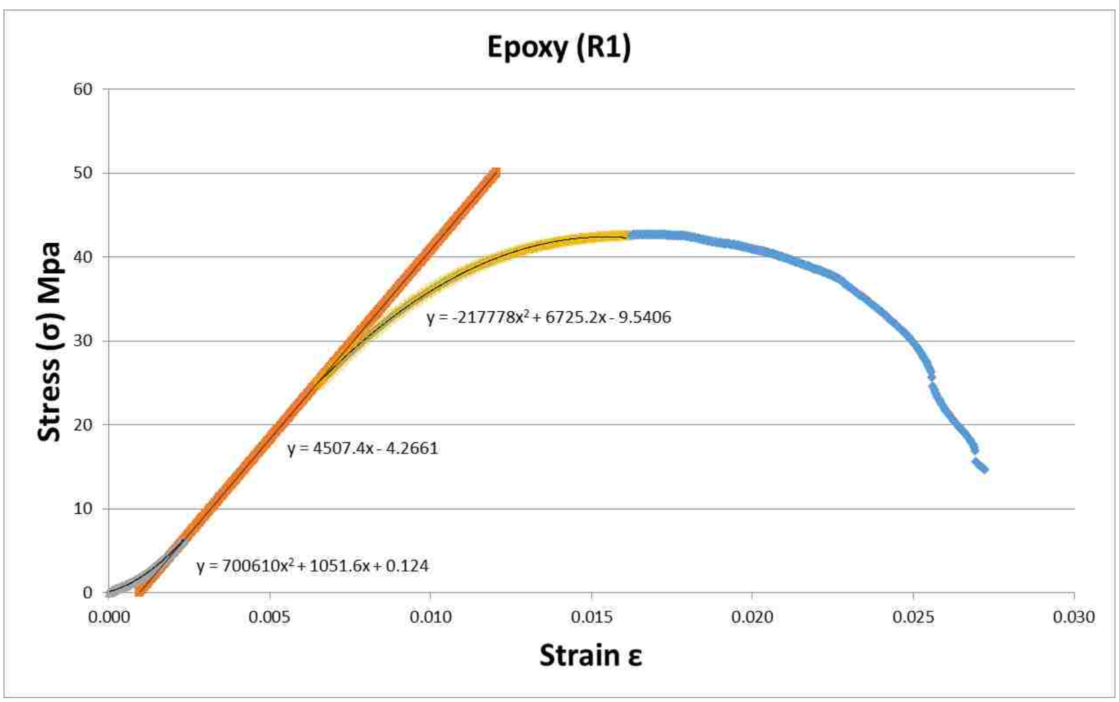

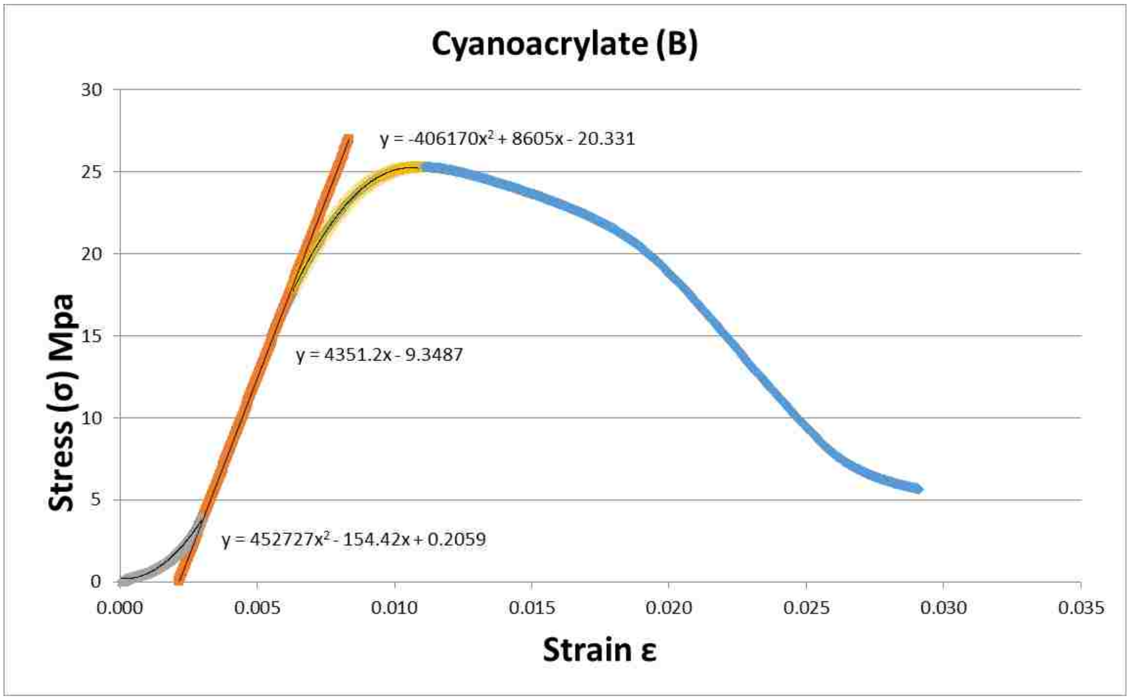

Cyanoacrylate (B)
y = -406170x2 + 8605x - 20.331
y = 4351.2x - 9.3487
y = 452727x2 - 154.42x + 0.2059
Stress (σ) Mpa
Strain ε
0
5
10
15
20
25
30
0.000
0.005
0.010
0.015
0.020
0.025
0.030
0.035

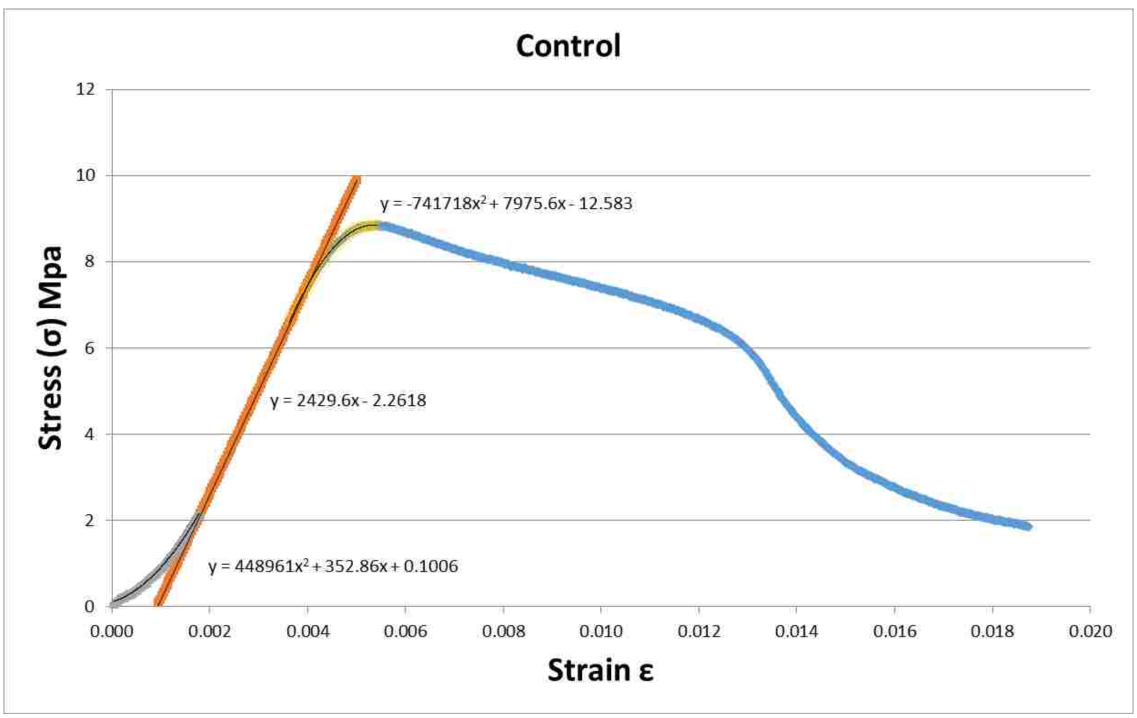

Control
y = -741718x2 + 7975.6x - 12.583
y = 2429.6x - 2.2618
y = 448961x2 + 352.86x + 0.1006
Stress (σ) Mpa
Strain ε
0
2
4
6
8
10
12
0.000
0.002
0.004
0.006
0.008
0.010
0.012
0.014
0.016
0.018
0.020

APPENDIX K

Cyanoacrylate, Epoxy sets and (P1) - Flexural Stress-Strain Curves

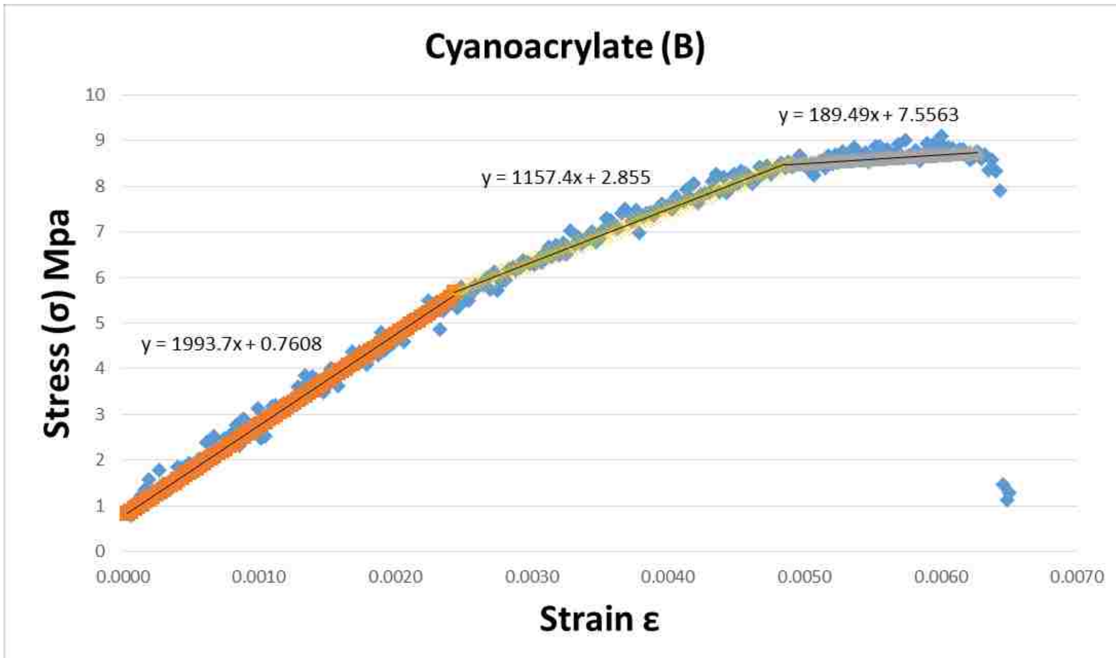

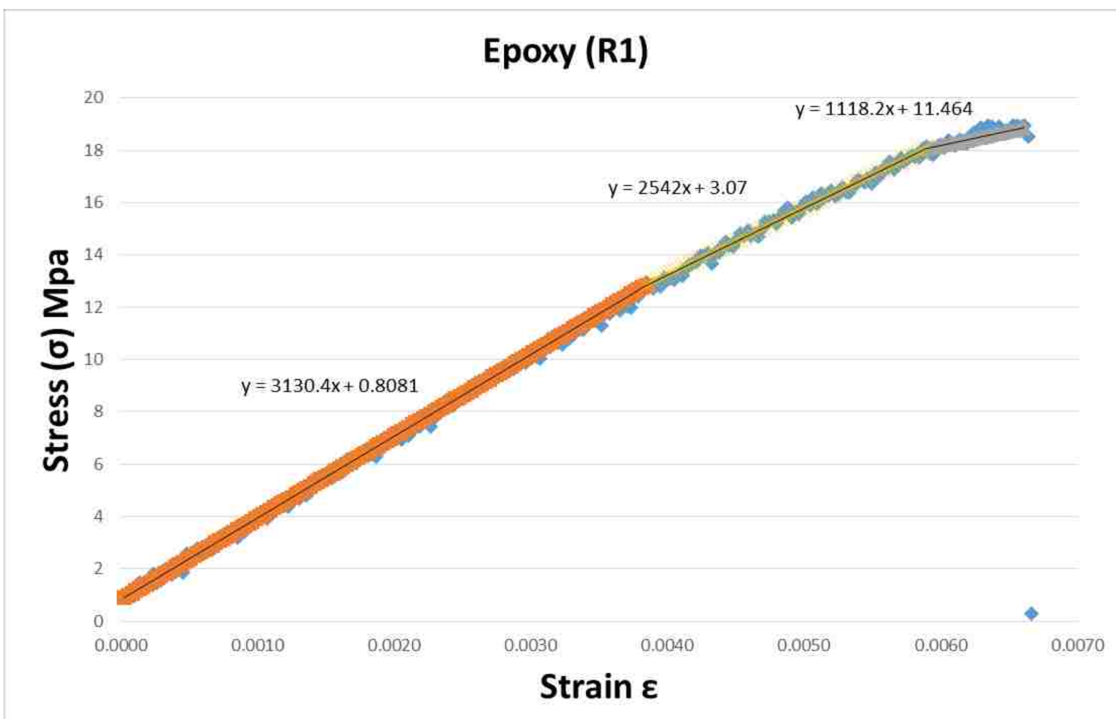

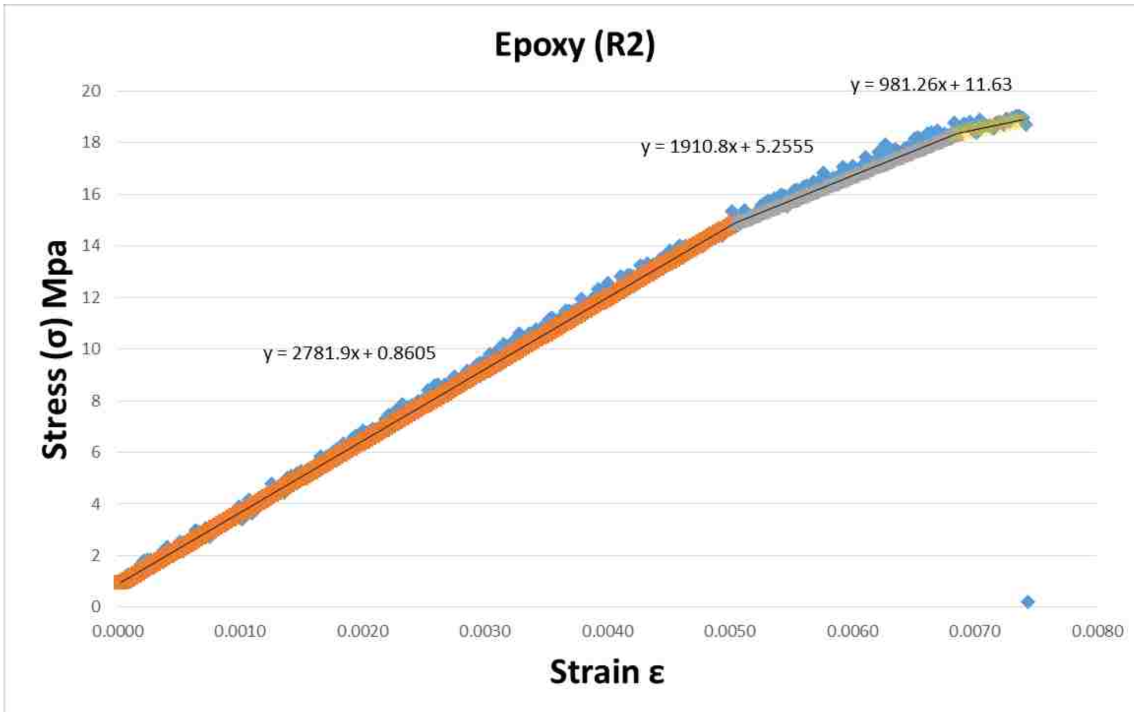
Epoxy (R2)
y = 981.26x + 11.63
y = 1910.8x + 5.2555
y = 2781.9x + 0.8605
Stress (σ) Mpa
Strain ε
20
18
16
14
12
10
8
6
4
2
0
0.0000
0.0010
0.0020
0.0030
0.0040
0.0050
0.0060
0.0070
0.0080

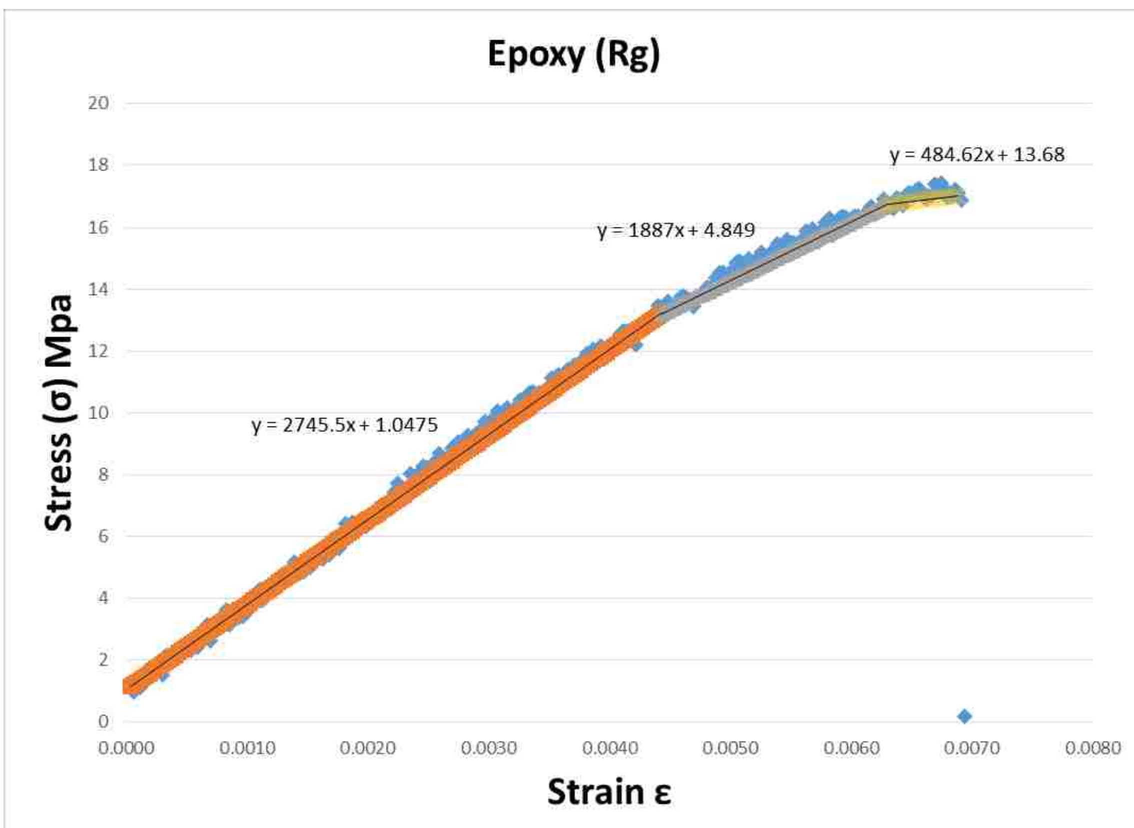
Epoxy (Rg)
y = 484.62x + 13.68
y = 1887x + 4.849
y = 2745.5x + 1.0475
Stress (σ) Mpa
Strain ε
20
18
16
14
12
10
8
6
4
2
0
0.0000
0.0010
0.0020
0.0030
0.0040
0.0050
0.0060
0.0070
0.0080

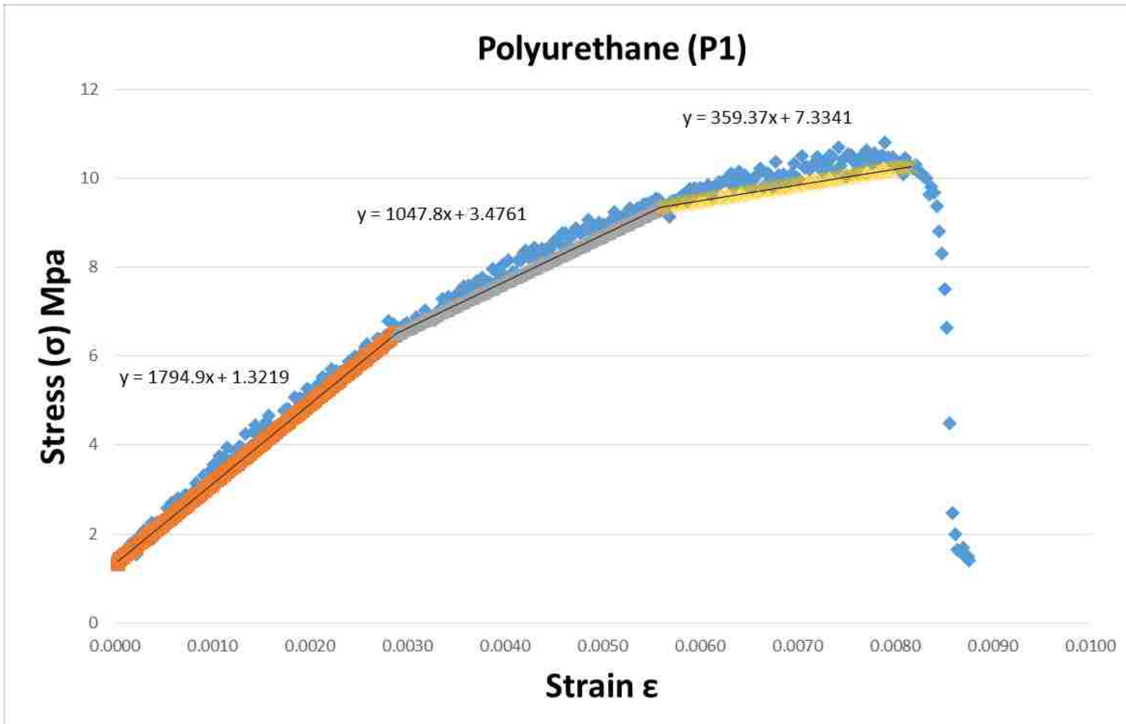
Polyurethane (P1)
12
10
8
6
4
2
0
y = 359.37x + 7.3341
y = 1047.8x + 3.4761
y = 1794.9x + 1.3219
Stress (σ) Mpa
0.0000
0.0010
0.0020
0.0030
0.0040
0.0050
0.0060
0.0070
0.0080
0.0090
0.0100
Strain ε

APPENDIX L

Copyright Permission

University of Windsor

Permission to use our combined work is granted for your thesis

1 message

Jill Urbanic <jurbanic@uwindsor.ca>
To: impensd@uwingmail.uwindsor.ca
Cc: Jill Urbanic <jurbanic@uwindsor.ca>

Dear Dave:

Permission is hereby granted to use our combined work, submitted to the INCOM 2015 conference (ID 424), and Rapid Prototyping Journal (RPJ-02-2015-0018), is granted for your thesis.

Best regards,

RJU

R. Jill Urbanic, Ph.D., P.Eng.
Associate Professor | 2013 Wighton Fellow | FEF Key Professor
Faculty of Engineering
Department of Mechanical, Automotive, and Materials Engineering
rm 3029 CEI
University of Windsor | Windsor, ON, Canada N9B 3P4
Tel: (519) 253-3000 Ext. 2633
E-mail: jurbanic at uwindsor dot ca

REFERENCES

Beer, F., Johnston, R., DeWolf, J., & Mazurek, D. (2008). *Mechanics of Materials* (Fifth ed.). New York: McGraw-Hill.

Caulfield,B., McHugh,P.E.,& Lohfeld,S.(2007) Dependence of mechanical properties of polyamide components on build parameters in the SLS process, *Journal of Materials Processing Technology, Volume 182, Issues 1–3,* 2 February 2007, Pages 477-488, ISSN 0924-0136, http://dx.doi.org/10.1016/j.jmatprotec.2006.09.007.

Duann (2012). Sealing Shapeways 3D Prints with Super Glue and Acetone, Retrieved from: http://www.shapeways.com/blog/archives/1823-sealing-shapeways-3d-prints-with-super-glue-and-acetone-video.html Viewed on: February 11th, 2014

Frascati, J. (2007). *EFFECTS OF POSITION, ORIENTATION, AND INFILTRATING MATERIAL ON THREE DIMENSIONAL PRINTING MODELS*. University of Central Florida Orlando, Florida. Retrieved from http://purl.fcla.edu/fcla/etd/CFE0001920

Galeta T., Kladaric I., Karakasic M., (2013). Influence of Processing Factors on the Tensile Strength of 3D-Printed Models. Materiali in tehnologije / Materials and technology 47 (2013) 6, 781–788. ISSN 1580-2949

Gharaie, S. H., Morsi, Y., & Masood, S. H. (2013). Tensile Properties of Processed 3D Printer ZP150 Powder Material. *Advanced Materials Research*, *699*, 813–816. doi:10.4028/www.scientific.net/AMR.699.813

Hsu, T. (2010). Manufacturing parts optimization in the three-dimensional printing process by the Taguchi method. *Journal of the Chinese Institute of Engineers.*, *33*(1), 121.

Lipson, H., & Kurma, M. (2013). *Fabricated: The New World of 3D Printing* . Indianapolis: John Wileys & Sons, Inc.

Lu, L., Zheng, J., and Mishra, S., (2014), "A Model-Based Layer-to-Layer Control Algorithm for Ink-Jet 3D Printing", ASME 2014 Dynamic Systems and Control Conference, Paper No. DSCC2014-5914.

Montgomery, Douglas C. (2009). Design and Analysis of Experiments, 7^{th} Edition, Published by: John Willey & Sons

MTS (2010) Series 642 Bend Fixtures Product Information, Manual 015-207-701 F Received from: www.MTS.com Viewed on: October 8^{th}, 2014

Pilipović, A., Raos, P., & Šercer, M. (2009). Experimental analysis of properties of materials for rapid prototyping. *The International Journal of Advanced Manufacturing Technology*, *40*(1-2), 105–115. doi:10.1007/s00170-007-1310-7

Suwanprateeb, J. (2006). Improvement in mechanical properties of three-dimensional printing parts made from natural polymers reinforced by acrylate resin for biomedical applications: a double infiltration approach. *Polymer International*, *55*(1), 57–62. doi:10.1002/pi.1918

Upcraft, S., & Fletcher, R. (2003). The rapid prototyping technologies. *Assembly Automation*, *23*(4), 318–330.

Vaezi, M., & Chua, C. K. (2011). Effects of layer thickness and binder saturation level parameters on 3D printing process. *The International Journal of Advanced Manufacturing Technology*, *53*(1-4), 275–284. doi:10.1007/s00170-010-2821-1

Yao, A. W. L., & Tseng, Y. C. (2002). A robust process optimization for a powder type rapid prototyper. *Rapid Prototyping Journal*, *8*(3), 180–189. doi:10.1108/13552540210431004

Z Corporation (2005). Z Corporation 3D Printing Technology, Company Brochure. Retrieved from:http://www.zcorp.com/documents/108_3D%20Printing%20White%20Paper%20FINAL.pdf Viewed on: September 19, 2013

Zañartu-Apara, G., & Ramos-Grez, J. (2010). Characterization of the mechanical properties of samples fabricated by an experimental SGM device. *Rapid Prototyping Journal*, *16*(5), 356–364.

ASTM B557-14, Standard Test Methods for Tension Testing Wrought and Cast Aluminum- and Magnesium-Alloy Products, ASTM International, West Conshohocken, PA, 2014, www.astm.org

ASTM C1424-10, Standard Test Method for Monotonic Compressive Strength of Advanced Ceramics at Ambient Temperature, ASTM International, West Conshohocken, PA, 2014, www.astm.org

ASTM C1684-13, Standard Test Method for Flexural Strength of Advanced Ceramics at Ambient Temperature—Cylindrical Rod Strength, ASTM International, West Conshohocken, PA, 2014, www.astm.org

ASTM C1424-10, Standard Test Method for Tensile Strength of Monolithic Advanced Ceramics at Ambient Temperature, ASTM International, West Conshohocken, PA, 2014, www.astm.org

VITA AUCTORIS

NAME:	David Impens
PLACE OF BIRTH:	Leamington, ON
YEAR OF BIRTH:	1977
EDUCATION:	University of Windsor, BASc. Industrial Engineering, Windsor, ON, 2012
	University of Windsor, MASc. Mechanical Engineering, Windsor, ON, 2015